## Title page

# Inhibition of *Hepatitis B* virus with adeno-associated virus vectors expressing primary microRNA-122/5



*Njabulo Mnyandu (1233650)*

*A dissertation submitted to the Faculty of Health Sciences, University of the Witwatersrand, Johannesburg, in fulfilment of the requirements for the degree of Masters of Science in Medicine.*

2018

## Declaration

I, *Njabulo Ziphezinhle Mnyandu* declare that this Dissertation is my own, unaided work. It is being submitted for the Degree of Masters in Medicine at the University of the Witwatersrand, Johannesburg. It has not been submitted before for any degree or examination at any other institution.

Signature of candidate

____day of _____20____in _____

## Dedication

This work is dedicated to my family, more especially my parents, *Zwelini and Jabulisiwe ka Ngcobo Mnyandu* whose unfailing love and support has seen me through my studies. I also dedicate this work to the memory of my dearly departed friend; *Charles Gumede* whose tragic passing due to chronic viral Hepatitis B induced liver cancer strengthens my belief in the importance of the work we do.

## Abstract

Chronic hepatitis B virus (HBV) infection is a global pandemic affecting approximately 240 million people world-wide. The shortcomings with nucleoside/nucleotide-analogues or interferon-α based drug therapy begs for alternative approaches such as gene therapy to treat chronic viral hepatitis. The highly conserved and compact HBV genomic structure makes it vulnerable to disruption therefore viral protein expression interruption. Recently, long-term RNA interference (RNAi) mediated inhibition of HBV replication was demonstrated using adeno-associated virus serotype 8 (AAV8) vector. However, prevalence of anti-AAV8 broadly neutralising antibodies in human population remains a challenge to effective therapeutic gene transfer. This study investigated transfer and liver-specific gene expression of primary-microRNA (pri-miR) mimic (pri-miR 122/5) using an in-silico constructed ancestral viral vector (Anc80L65) to activate RNAi against HBV. Anti-HBV Anc80L65 vector (Anc80L65-122/5) was produced and characterized in liver-derived Huh7 cells and in HBV transgenic mouse model. For assessment of transduction efficiency and long term transgene expression by Anc80L65 *in vivo*, a nano-luciferase expressing vector (Anc80L65-NLuc) was also produced. Significant expression of nano-luciferase from Anc80L65-NLuc was observed *in vitro*. A high and sustained nano-luciferase expression was also observed *in vivo*. Following a single dose of Anc80L65-122/5 in mice, an impressive and sustained HBV gene expression knockdown of up to 70% was observed over four months. Safety of Anc80L65 was demonstrated by absence of harmful immune-stimulatory effects and resultant liver toxicity, a fact supported by normal levels of serum alanine transaminase enzyme. There were no mice fatalities related to Anc80L65 mediated RNAi stimulation. The safety, high efficiency and the prolonged HBV inhibition by Anc80L65 makes it a

useful therapeutic delivery tool and will significantly contribute to the progression of anti-HBV RNAi based therapy in clinical applications.

# Acknowledgements

My unending thanks go to Dr. Betty Maepa for her outstanding guidance and support throughout my studies since I joined AGTRU family.

My appreciation also my co-supervisor, and head of AGTRU unit, Professor Patrick Arbuthnot for the way he makes all of us feel that we matter, and have something to contribute.

My gratitude goes to Professor Abdullah Ely for the invaluable assistance offered during the course of the study.

My appreciation goes to Ms Gladys Glagliardi, for her friendly demeanour, and superior administrative competence that makes our lives in the unit so much easier.

To the AGTRU family, thank you for all the support, advices, fun-times we have shared.

To my family members, Zwelini, Jabuliswe, Gugulethu, Jabulile, Sbongokuhle, Sibusisile, Cebo and Zipho, thank you for being there.

To my funders, SA-MRC, NRF, PRF and AGTRU, my thanks go to you, for without your financial support; my studies would not have been possible.

# TABLE OF CONTENTS

## Table of Figures

## LIST OF TABLES

# CHAPTER 1: INTRODUCTION

Despite the availability of an effective vaccine against HBV infection, about 240 million people world-wide are chronic sufferers and ~700 000 people die annually from viral chronic hepatitis induced liver complications including cirrhosis and hepatocellular carcinoma (Naghavi et al., 2015). The acute form of infection elicits a robust immune response, displayed by sustained T-cell activation and inflammatory response resulting in viral clearance. However, chronic infection is characterised by a supressed immune response, with T cell exhaustion and is often lethal (Fisicaro et al., 2017). The detection of persisting HBV surface antigen (HBsAg) in the blood suggests HBV infection chronicity. Clinically, elevated serum alanine amino transferase (ALT) and aspartate amino transferase (AST) levels above normal range indicate onset of liver injury [reviewed in (Ganem and Prince, 2004)]. Chronic hepatitis is most prevalent in sub-Saharan African countries, East and South-east parts of Asia, Western Pacific Islands, Greenland, Brazil and Saudi Arabia, (Naghavi et al., 2015). The current therapeutic interventions using interferon based drugs are inadequate, only effective in a subsection of chronic HBV sufferers i.e. HBV e-antigen positive carriers, even then with low efficacy [reviewed in (Arbuthnot et al., 2005)]. The use of nucleos(t)ide analogues disrupt HBV replicative competence because they target the viral polymerase and are well tolerated, but in most cases, they do not clear the virus. In the absence of an effective treatment to chronic HBV, understanding HBV genomic structure and how at a molecular level it causes chronic viral hepatitis may help in identifying drug targets for a cure.

## 1.1 HBV Biology

HBV is a small, 40-42 nm, lipid enveloped, hepatotropic virus belonging to Hepadnaviridae family, [reviewed in (Glebe and Bremer, 2013)]. Embedded in the viral envelope are glycoproteins or surface antigens. Inside the envelope is the capsid that encases the partially double stranded DNA genome, [**Figure 1.1,** (Molnar-Kimber et al., 1984)]. The negative DNA strand is base-paired to a partially synthesised positive strand resulting in an ~ 3-kb relaxed circular DNA [rc-DNA, (Landers et al., 1977)]. To the 5' end of a minus DNA strand is a covalently linked DNA polymerase. Both strands overlap each other by 240-bp at their 5' ends, and contain ~ 12-bp direct repeat sequences near each end (Molnar-Kimber et al., 1984). The positive strand carries a 5' capped, 19-bp pregenomic messenger RNA fragment (pg-mRNA) serving a primer function during positive DNA strand synthesis (Lien et al., 1986).

To be productive, HBV enters host cell through sodium taurocholate cotransporting polypeptide receptor (NTCP), uncoats the bi-layered lipid, and the naked nucleocapsid is transported to the nucleus (Yan et al., 2012). After release in the nucleus, the relaxed DNA conformation is repaired by intracellular machinery resulting in stable covalently closed circular DNA (cccDNA). Formation of cccDNA from a rc-DNA involves the removal of reverse transcriptase molecule attached at the 5' end of HBV minus DNA strand, removal of the short RNA primer from the plus strand, and completion of the plus-strand and ligation of both DNA strands [reviewed in (Seeger and Mason, 2000)]. The cccDNA locates episomally and serves as a template for transcription of all pregenomic RNA and sub-genomic RNAs from its

open reading frames (ORFs). Glucocorticoid response element (GRE) in the HBV genome enhances liver-specific expression of viral proteins from its four overlapping open-reading frames [ORFs, **Figure 1.1**, (Ruiz-Opazo et al., 1982)]. *Polymerase (pol)* ORF encodes a viral polymerase bearing reverse transcriptase (RT), RNase H and terminal protein domain. Once encapsidated in cytoplasm with polymerase protein, pregenomic RNA is reverse transcribed into negative DNA strand. The rc-DA is synthesised from negative DNA strand, and the nucleocapsid is either imported back into the nucleus to increase cccDNA levels or released to infect other cells.

The *Pre-core/core (pre-C/C)* ORF encodes hepatitis B e-antigen (HBeAg) intermediate and core proteins (HBcAg). The truncated surface proteins pre-S1, pre-S2 and the full surface protein are encoded by *pre-surface/surface (pre-S/S)* ORF. *HBx* ORF encodes an X protein required for viral replication and overlaps with the 3' end of the polymerase ORF necessary for virus reverse transcription, and regions important for transcription control (basic core promoter and negative regulatory elements).

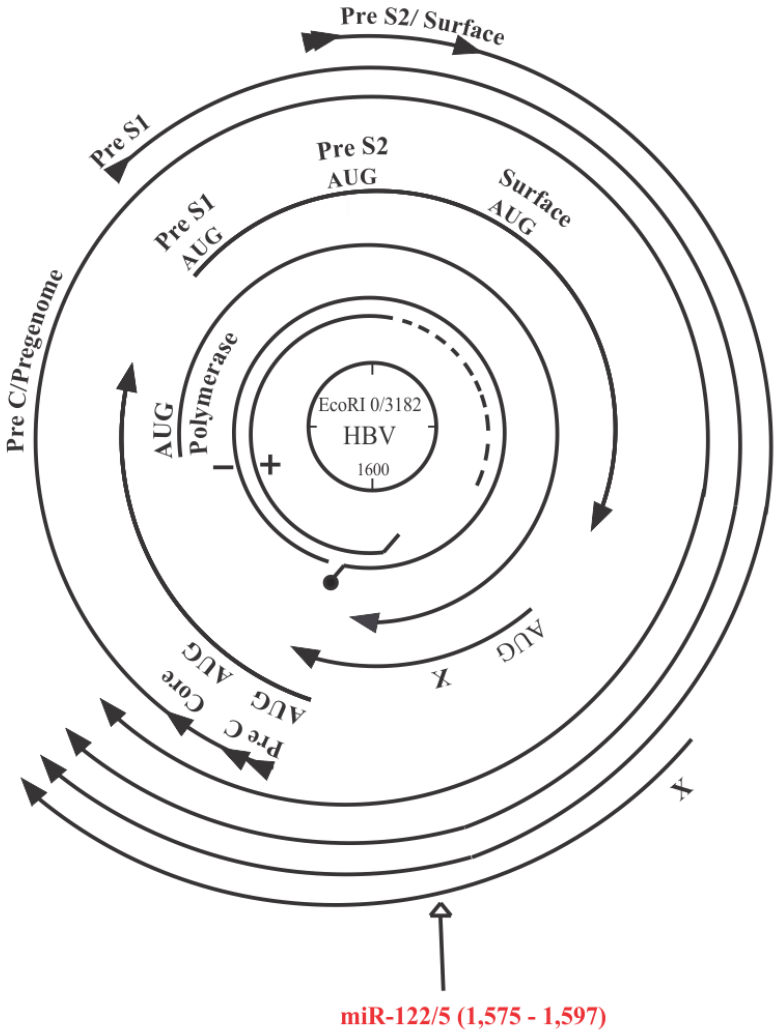


**Figure 1.1 Schematic representation of HBV genome.** At the center is circular, relaxed, partially duplex, and overlapping viral DNA consisting of inner + and outer – strands, with pregenomic mRNA fragment, and DNA polymerase attachments at 5' ends, respectively. The unique *EcoRI* site marks a clockwise nucleotide coordinates start point. The innermost, overlapping arrows immediately surrounding the HBV genome show HBV ORFs, core, polymerase, surface and X. Whereas the outermost overlapping arrows depict HBV transcripts, preC/pregenomic, preS1, preS2/S and X. The axial arrows in the ORF X framed within nucleotide coordinates in parenthesis show a pri-miR 122/5 mimic target site discussed later [Adapted from (Maepa et al., 2017)].

The current therapeutic interventions target different stages of the HBV replication cycle or host factors. Using interferon based anti-HBV drugs (like Roferon-A, Intron-Alferon-N, or Extavia) to activate the host immune response and effect HBV clearance have shown inadequacy, only effective in a subsection of chronic sufferers

i.e. HBV e-antigen positive carriers, even then with low efficacy [as reviewed (Arbuthnot et al., 2005)]. The use of nucleos(t)ide analogues (like amivudine, telbivudine, adefovir, entecavir, or tenofovir) inhibit HBV polymerase, but do not destabilise cccDNA [as reviewed (Nassal, 2015). Treatment discontinuation resulting in HBV reactivation and drug resistance following long-term use remains a problem [reviewed in (Kwon and Lok, 2011)]. Since traditional methods of treating chronic viral hepatitis have not been a success, alternative therapy is required. Gene therapy has shown remarkable success in treating certain cancers and other monogenic disorders in both pre-clinical and clinical studies. Hence it may be a suitable alternative for HBV infection treatment.

## 1.2. Gene therapy

Gene therapy approach involves treating a disease condition by introducing nucleic acid to cells. The potential of gene therapy has been demonstrated by recent progression of several gene therapeutics in to clinic (Cideciyan et al., 2008, Maguire et al., 2008, Rafii et al., 2014). A lipoprotein lipase deficiency leading to dysfunctional triglycerides metabolism or a cancer resulting from tumour suppressor gene dysregulation is now treatable using commercially available gene therapeutics [reviewed in (Ma et al., 2009, Ferreira et al., 2014)].

In August 30, 2017, the US Food and Drug Administration (FDA) agency announced its approval of a gene therapy to treat acute lymphoblastic leukaemia (ALL), a malignant blood disorder wherein white blood cells become cancerous (FDA, 2017).

Amongst others, novel gene therapeutic approaches have used strategies such as reprogramming of RNA interference (RNAi) pathway (Ivacik et al., 2015, Maepa et al., 2017) and applied modern molecular editing instruments such as clustered regulatory interspaced short palindromic repeats (CRISPR)/ CRISPR associated (Cas) systems (Scott et al., 2017, Wang et al., 2016), Zinc-finger nucleases (Holt et al., 2010, Yuan et al., 2012), and transcription activator-like effector nucleases [TALENs, (Bloom et al., 2013, Dreyer et al., 2016)] for rational drug design.

## 1.2.1 Gene Therapy Tools

### 1.2.1.1 Gene editing tools

Gene editing or reprogrammable nucleases (CRISPR/Cas systems, Zinc-finger nucleases and TALENs) have in common a sequence-specific DNA binding domain for gene sequence targeting, and nuclease domain for cleaving the DNA. The DNA binding domains and nucleases bind and effect DNA double stranded breaks (DSBs), respectively, thereby inducing the organism's DNA repair mechanism [reviewed in (Gaj et al., 2013, Kim and Kim, 2014).

These gene therapeutic approaches have taken advantage of organism's repair mechanisms [homology directed repair (HDR) or non-homologous end joining (NHEJ)] to correct genetic disorders underlying disease. HDR repairs a DNA strand double break, through a series of events involving a strand invasion to base-pair with a nearby homologous strand, one after the other, followed by branch migration, Holliday junction formation and strand resolution to achieve repair. Non-homologous end joining (NHEJ) is an error-prone repair pathway that introduces mutation-causing insertions or deletions (indels) [reviewed in (Gaj et al., 2013, Kim and Kim, 2014)].

Recently CRISPR/Cas mutagenic targeting of HBV surface ORF *in vitro* has shown over 95% gene knockdown over 27 days (Scott et al., 2017). Also, using TALENs to target multiple sites in the *Surface* and *Core* ORFs of HBV resulted in disabling HBV replication *in vitro* and *in vivo (*Bloom et al., 2013). The *CCR5,* a receptor for HIV-1 entry was mutated following CD4+ cells being treated with TALENs leading to HIV-1 entry inhibition (Sather et al., 2015). In separate studies, CRISPR/Cas mediated gene modification was used to induce suicide genes' integration to cancerous cells causing cells death (Nelson et al., 2016). The major disadvantages of using reprogrammable nucleases are the probability to introduce unintended adverse mutations in the genome that inactivates essential genes and a possible immune stimulation by the delivered nucleases that can lead to clearance of the transduced cells as well as toxicity. Recent reports also indicate presence of pre-existing immunity in the human population to CRISPR/Cas (Zhang, 2018). Hence the scope of the current study will focus on RNA interference (RNAi)-based therapy in treating HBV.

#### 1.2.1.2 RNAi mediated gene therapy

RNAi is a double stranded RNA (dsRNA) induced post-transcriptional gene silencing pathway present in most eukaryotic cells (Hamilton and Baulcombe, 1999, Elbashir et al., 2001a). The well understood and most explored RNAi pathway for gene therapy is the microRNA pathway. It is initiated in the nucleus whereby the microRNA expressing gene is transcribed in to a long stem-loop or multi stem-loop primary microRNA (pri-miR) that carries a sequence homologous to the target mRNA. The pri-miR is then processed to an ~70 nucleotide (nt) long precursor microRNA (pre-miR) by an RNase III enzyme Drosha with its RNA binding partner DiGeorge

syndrome critical region 8 - DGCRG8 (Zeng et al., 2005). After Ran-GTP dependent exportin-5 mediated transport through the nuclear pore in to the cytoplasm (Bohnsack et al., 2004), pre-miR is further processed in to an ~22 nt microRNA (miR) duplex by another RNA III enzyme Dicer (Han et al., 2004, Knight and Bass, 2001, Yi et al., 2003, Ketting et al., 2001). The microRNA duplex is then incorporated into a cytoplasmic RNA-induced silencing complex (RISC) for guide strand selection to allow for target binding. Once full or partial hybridisation between the guided complex and the target mRNA is achieved, the target mRNA is degraded or translation is inhibited, respectively [**Figure 1.2,** (Hutvagner and Zamore, 2002, Song et al., 2004, Yekta et al., 2004)].

RNAi pathway can be manipulated for therapeutic purposes by introducing expressed or synthetic mimics of the pathway intermediates. This has been done by introducing a promoter driven self-complementary DNA (scDNA) or dsDNA sequence into the nucleus (Wang et al., 2003, Mowa et al., 2012) or synthetic short interfering RNA (siRNA) that enters and bind to the cytoplasmic RISC complex (Giladi et al., 2003) and these mimic the miR duplex. The scDNA or dsDNA is transcribed into a pri-miR mimic or pre-miR mimic (short hairpin RNA, shRNA). Synthetic mimics produce transient expression (Elbashir et al., 2001b), while expressed mimics yields long-term expression (Maepa et al., 2017), which makes the latter suitable for targeting chronic conditions like HBV infection.

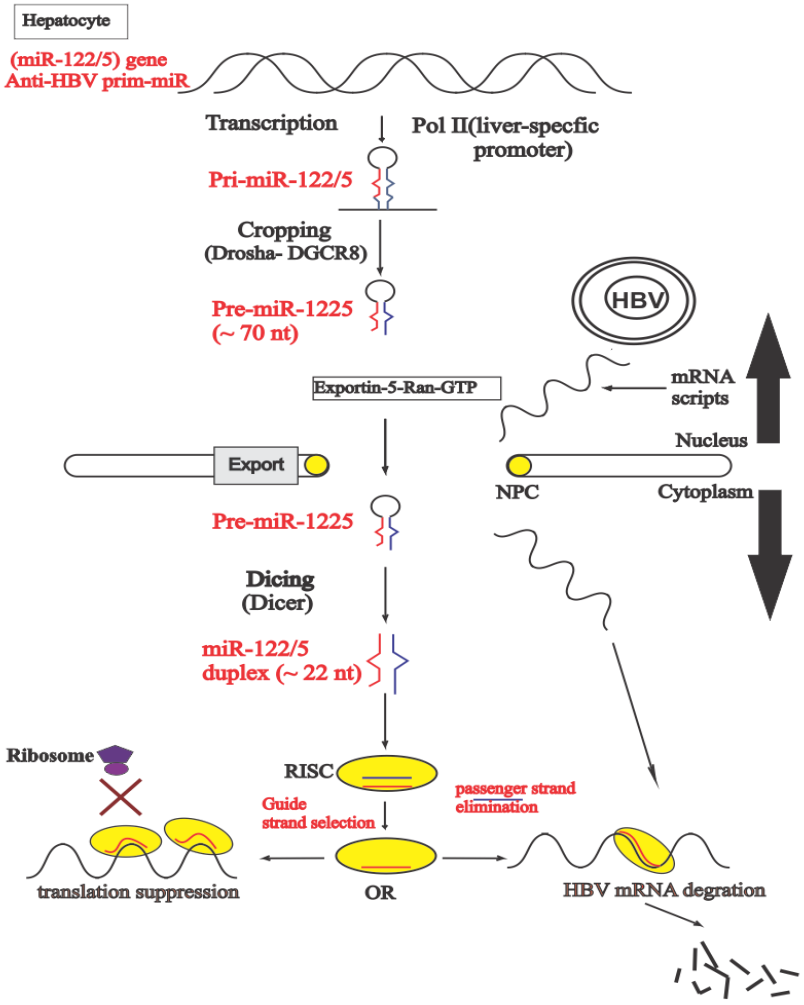


**Figure 1.2 Illustration of RNAi pathway model used to inhibit HBV replication in an infected hepatocyte.** The top half is nucleus; miR-122/5 gene is transcribed to pri-miR-122/5, cropped by DCGR8 bound Drosha protein producing pre-miR-122/5 which relies on Ran-GTP dependent exportin-5 interactions for export to cytoplasm through a nuclear pore complex (NPC). On the right; the stable HBV cccDNA transcribes mRNA transcripts which are then transported into the cytoplasm. Bottom half is cytoplasm; Dicer processes pre-miR-122/5 resulting in a miR-122/5 duplex that incorporates into RISC, where guide and passenger strand is selected and eliminated, respectively. Guide strand targets RISC to hybridise to HBV mRNA. Full or partial hybridisation leads to mRNA degradation or translation suppression, respectively.

### 1.2.1.3 Antiviral RNAi therapy

RNAi based therapeutic approaches have been used in preclinical studies to treat diseased conditions caused by amongst others, infections from HIV-1 implicated in acquired immune deficiency syndrome (Novina et al., 2002), human cytomegalovirus

(HCMV) associated with harmful pneumonitis and retinitis especially in immunocompromised individuals (Xiaofei et al., 2012), deadly influenza viruses H5N1 and H1N1(Tompkins et al., 2004) and human papilloma virus (HPV) associated with cervical cancer (Butz et al., 2003, von Knebel Doeberitz et al., 1992). Various studies have been conducted in exploring of RNAi based therapeutics against chronic viral hepatitis B infection (Grimm et al., 2006; Giering et al., 2008; Ely et al., 2008; Ely et al., 2009; Mowa et al., 2012; Ivacik et al., 2015; Maepa et al., 2017).

#### 1.2.1.4 RNAi based therapy against HBV infection

The compact nature of the HBV genome makes it a good target for RNAi based therapies. Cationic liposomes carrying anti-HBV siRNA targeting *HBx* ORF were hydrodynamically injected in HBV transgenic mice and effecting a HBsAg level reduction of ~ 85% three days post-injection, but after 21 days these levels had rebounded (Marimani et al., 2015). Synthetic siRNA was also used to target *HBx* ORF in an acute HBV mouse model. In three to five days, up to ~50% HBsAg level reduction in relation to controls was observed, which quickly rebounded to higher levels like that of controls after day 5 (Shin et al., 2006). In a study by Shlomai and Shaul, anti-HBV siRNAs were co-transfected with 1.3 × HBV genome to allow ORF *pre-C/C* or *HBx* targeting in two different cell lines, Huh7 and HepG2.2.15. Targeting *PreC/C* or *HBx* in Huh7 cells yielded 13% or 68% level reduction in the 3.5 kb pregenomic RNA, respectively. When using HepG2.2.15 cells, there was about 63% pregenomic RNA reduction or no effect when *HBx* or *pre-C/C* was targeted, respectively. These siRNA sequences were highly specific as introduction of four silent point mutations in the target abrogated the siRNA's effect on viral gene expression (Shlomai and Shaul, 2003).

Anti-HBV RNAi based therapy using synthetic siRNA (ARC-520) is currently in Phase II human clinical trial, and was administered intravenously to chronic Hepatitis patients. Significant and sustained HBsAg level reduction by 50% for up to 43 – 57 days compared to placebo control was observed. The treatment was well tolerated up to a dose of 3 mg/kg, and its anti-HBV effects were found to be dose dependent. No toxic and undesirable inflammatory response were observed [reviewed in (Manzoor et al., 2015)]. These findings, especially from Phase II human clinical trials are encouraging, however, the main shortcoming of this approach is the use of synthetic siRNA for chronic HBV which by their mode of action have transient effect, requiring the chronic HBV suffers to take regular medication to sustain the HBV antigen suppressive effect.

McCaffrey and team were the first to demonstrate HBV viral replication inhibition *in vivo* using expressed RNAi therapeutics. They introduced shRNAs expressing plasmids by transfection methods in liver-derived cell line and hydrodynamic injection in immunosuppressed mice. They also used immunocompetent mice to distinguish the effects of RNAi from immune modulation. The shRNA targeted multiple regions of HBV ORFs encoding core, pregenomic RNA, polymerase and surface proteins. After 7 and 8 days, up to 88% and 94% Hepatitis surface antigen (HBsAg) level reductions were observed during *in vivo* and *in vitro* studies, respectively. Moreover, Hepatitis core antigen (HBcAg) and viral replication intermediates (minus DNA strand, rcDNA, and pregenomic RNA) required for replication were not detectable from mice liver samples (McCaffrey et al., 2003).

A study by another group using shRNAs showed markedly improved results also targeting the *HBx* region in an HBV transgenic murine model, thus confirming the potency of RNAi activators targeting this region (Carmona et al., 2006). Collectively these findings identified *HBx* as a potent RNAi target to effect HBV replication cycle interruption, moreover this ORF overlaps with *preC/C*, *preS/S* and *Polymerase* ORFs. Therefore, the RNAi activator used in the study targets a site in the *HBx* ORF.

The compatibility of RNA polymerase III (pol III) to drive anti-HBV shRNA, and their efficiency to inhibit HBV has been extensively demonstrated (Carmona et al., 2006, Chen et al., 2012, Uprichard et al., 2005). Adenoviral vector mediated delivery of pol III (H1) driven anti-HBV shRNA targeting multiple sites in the p *pre-S/S* ORF of HBV transgenic mice led to HBsAg decline by ~ 50 % four days post treatment which was undetectable by the 17$^{th}$ day. The use of cytokine deficient (tumour necrosis factor (TNF), interferon-γ, or interferon-α/β), HBV transgenic mice eliminated the notion that the HBV knockdown effect seen resulted from immune mediated clearance of Adenoviral infected hepatocytes (Uprichard et al., 2005). Using pol III (U6) driven anti-HBV shRNA hydrodynamically injected in HBV transgenic mice or cotransfected with HBV-antigen producing plasmid in Huh7 cells yielded significant HBsAg reduction of ~90% which was not detectable four days post injection (Carmona et al., 2006).

However, the use of RNA polymerase III (pol III) promoters to drive shRNAs was implicated in overloading the endogenous silencing pathway machinery with microRNA intermediates resulting in toxicity and mice fatalities (Grimm et al., 2006). Hence, in 2008 and 2009 Ely and others designed pol II driven anti-HBV pri-miR mimics, namely, pri-miR 31/5, pri-miR 31/5, pri-

miR 122/5 and pri-miR 31/5-8-9, targeting single or multiple sites within the *HBx* ORF. These sequences were made within the background of naturally occurring, ubiquitously expressed miR-31 and a liver-specific miR-122. Using these potent anti-HBV sequences, a significant but short-term HBsAg expression knockdown of ~ 95% was observed during *in vitro* and *in vivo* studies. There was no toxicity or fatalities as observed in previous studies resulting from oversaturation of the endogenous RNAi pathway (Ely et al., 2009, Ely et al., 2008). Hence, our study expressed pri-miR-122/5 from a Pol II liver specific mouse transthyretin (mTTR) promoter to inhibit HBV replication. The pri-miR-122/5 RNAi activator is preferentially expressed in the liver, and has not been assessed with any AAV vector before.

To be useful, RNAi activators need to flow in blood circulation, enter interstitium, pass through vesicular walls, taken up by cells and incorporated in to the RNAi pathway to effect a target specific mRNA cleavage or translation inhibition. However, after intravenous injection, RNAi effectors in blood circulation become targets of degradation by nucleases in the serum (Water et al., 2006). Naked RNAi activator's immunogenicity and susceptibility to nuclease or lysosomal degradation leading to diluted and transient gene silencing effects has been a barrier to advancing RNAi-based anti-HBV therapy to the clinic. Also, the treatment of viral chronic hepatitis requires sustained therapeutic intervention. Hence there is a need for an efficient delivery systems for this highly effective anti-HBV gene therapy.

## 1.3 Anti-HBV RNAi activator gene delivery systems

Gene therapy transfer systems can be classified into three major types: physical, non-viral and viral vectors [reviewed in (Jin et al., 2014, Gebbing et al., 2015, Khan et al., 2017). Most commonly used physical method for anti-HBV targeted gene delivery is hydrodynamic injection, which uses hydrodynamic pressure to permeabilise endothelial and parenchymal cells to allow gene transfer. This type of delivery can be invasive and lead to cellular damage (Rossmanith et al., 2002).

Cationic liposomes have been used for non-viral vector mediated liver targeted gene transfer. They are synthetic lipid spheres with an aqueous core, where a therapeutic nucleic acid can be contained. The core is surrounded by one or more bi-layered membrane bearing fatty acids. Liposomes have shown many advantages namely: low immunogenicity, bigger DNA-shuttle size, protection against DNA enzymatic degradation, and once inside cell facilitates endosomal escape (Marimani et al., 2015). However, their positively charged surfaces promote non-specific interaction with intracellular components which have resulted in lessening cellular adhesion, haemolysis and low transfection efficiency (Escriou et al., 1998, Zelphati et al., 1998). Other non-viral vectors that have been used for anti-HBV gene transfer are polymer based. They are defined as a synthetic polymer tethered to a targeted gene or other biomolecule to facilitate gene transfer (Dewangan et al., 2018). However, their small size makes them not amenable to carrying larger RNAi activating expression cassettes.

Viruses offer an alternative way to deliver gene therapeutics. They have evolved advanced mechanisms of cell transduction, which makes them efficient at delivery of transgenes *in vivo*. They can interact with cell surface molecules to facilitate endocytosis, activate host signalling pathways, and effect a cascade of events terminating with transgene delivery and expression in the cell (Sanlioglu et al., 2000, Asokan et al., 2006, Kaminsky et al., 2012, Pillay et al., 2016). Recombinant Lentiviral Vectors (LVs), Adenoviral vectors and Adeno-associated viral vectors (AAV) vectors have shown excellent transduction efficiency of the liver, hence their consideration to deliver for anti-HBV therapeutics (Chen et al., 2009, Wang et al., 2011, Ivacik et al., 2015, Poling et al., 2017).

However, Adenoviral and Lentiviral vectors show high immunogenicity, with Adenoviral vectors displaying relatively short-term transgene gene expression (Mowa et al., 2014). Lentiviral vector chromosomal integration carries oncogenic risks and which makes them unsuitable therapeutic vectors for chronic HBV therapeutics (Ivacik et al., 2015). We have identified AAVs as potential candidates for RNAi based therapy delivery because of their biosafety profile demonstrated in various studies (Chen et al., 2009, Maepa et al., 2017, Nathwani et al., 2011).

### 1.3.1 AAV Biology

AAVs are small, non-enveloped, *Parvoviridae* family members assigned under *Dependovirus* genus due to reliance on other viruses such as Adenovirus or Herpes simplex for replication [as reviewed (Daya and Berns, 2008)]. Continuous AAV isolation has uncovered twelve AAV serotypes identified as AAV1 up to AAV12, with

AAV2, 3, 5, 6, and 9 originating from humans, and AAV1, 4, 7, and 8 from non-human primates [reviewed in (Drouin and Agbandje-McKenna, 2013, Grimm and Kay, 2003)]. AAV2 serotype is well studied and has given insights into AAV particle structure, function, replication cycle as well as its suitability for therapeutic gene delivery vector.

The AAV particle's defining feature is its icosahedral-shaped capsid with 12 five-fold symmetry pore bearing axes required for infectivity and genome packaging (Bleker et al., 2005, Kronenberg et al., 2001). The AAV capsid bears a conserved core structure (eight-stranded β-barrel motif and the αA helix) with nine variable regions (VR-I to VR-IX) conferring diversity (DiMattia et al., 2012, Xie et al., 2002). The catalogue of traits exhibited by the AAV capsid defines the T-cell epitopes (Mingozzi et al., 2007), immunogenic motifs (Vandenberghe et al., 2006) and monoclonal antibody docking sites (DiMattia et al., 2012) found on AAV surface as well as attributes such as receptor-binding (Bell et al., 2012, Kern et al., 2003, Wu et al., 2000), phospholipase activity and infectivity (Girod et al., 2002, Grieger et al., 2006).

#### 1.3.1.1 AAV genome structure and gene expression

AAV has a single stranded 4.7 kb size genome with inverted terminal repeats (ITRs) flanking *cap* and *rep* genes [**Figure 1.3,** (Srivastava et al., 1983, Berns and Parrish, 2007)]. The 145-bp long gene flanking ITRs consisting of six complementary palindromic regions, A-A', B-B', C-C and one non-palindromic D region conform the single-stranded DNA to a 3'OH-bearing T-shaped/hairpin structure with either 'flip' or 'flop' configuration [**Figure 1.4**,(Koczot et al., 1973)]. ITRs also contains Rep protein binding element (RBE), terminal resolution site (TRS) and are important for viral gene

expression, replication, and encapsidation (Koczot et al., 1973). Once the genome adopts a double stranded conformation it is able to express its *cap* and *rep* ORFs (Ferrari et al., 1996) . Located adjacent to left-hand ITR, p40 promoter driven *Cap* gene expresses four overlapping polypeptides, namely, Viral protein (VP) 1, VP2, VP3, and AAP [assembly-activating protein, (Becerra et al., 1988, Cassinotti et al., 1988, Trempe and Carter, 1988, Sonntag et al., 2010)]. The *cap* proteins (VP1, VP2, and VP3) make-up the ~ 22 nm, T=1 icosahedral capsid architecture having 60 VP subunits in a 1:1:10 ratio, respectively (Buller and Rose, 1978, Kronenberg et al., 2001, Xie et al., 2002).

The dual promoter (p5 and p15) driven *Rep* gene also expresses a quartet of overlapping polypeptides named by size, Rep78, Rep68, Rep52 and Rep40 which are essential for viral genome replication [reviewed in (Daya and Berns, 2008)]. This Rep protein quartet has helicase and ATPase activities. The large Rep proteins (Rep78 and Rep68) exercises a site-specific binding activity within AAV genome ITR's terminal resolution site (trs) and site-specific endonuclease activity at the RBE position. [**Figure 1.4**., reviewed inn (Daya and Berns, 2008)].

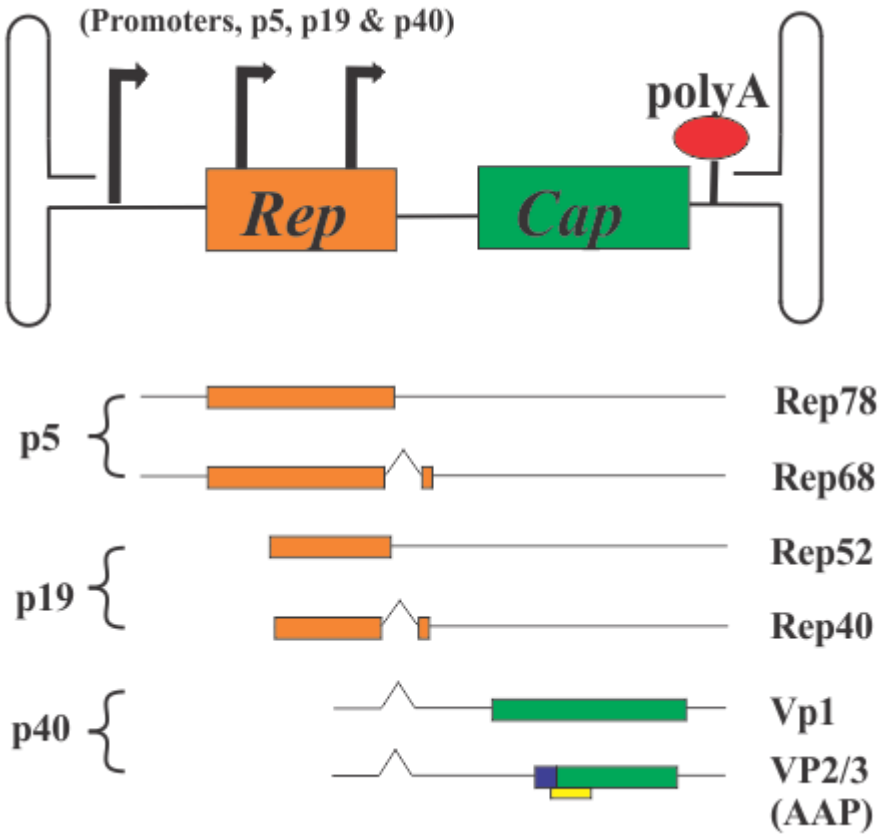


**Figure 1.3 Wild-type AAV2 genome structure, RNA transcripts, and protein names indicated.** *Rep* and *cap* genes are flanked by ITRs, and a polyA signal is indicated downstream of *cap* gene. Promoters p5, p19 and p40 drive the production of transcripts and related structural [VP1, VP2, VP3 and assembly activating protein (AAP)] and non-structural (Rep78, Rep68, Rep52 and Rep40) proteins. At the end of the blue segment an alternative ACG start codon for VP3 is found. The yellow segment indicates alternative start codon for AAP from within VP2-VP3 mRNA [Adapted from (Daya and Berns, 2008)].

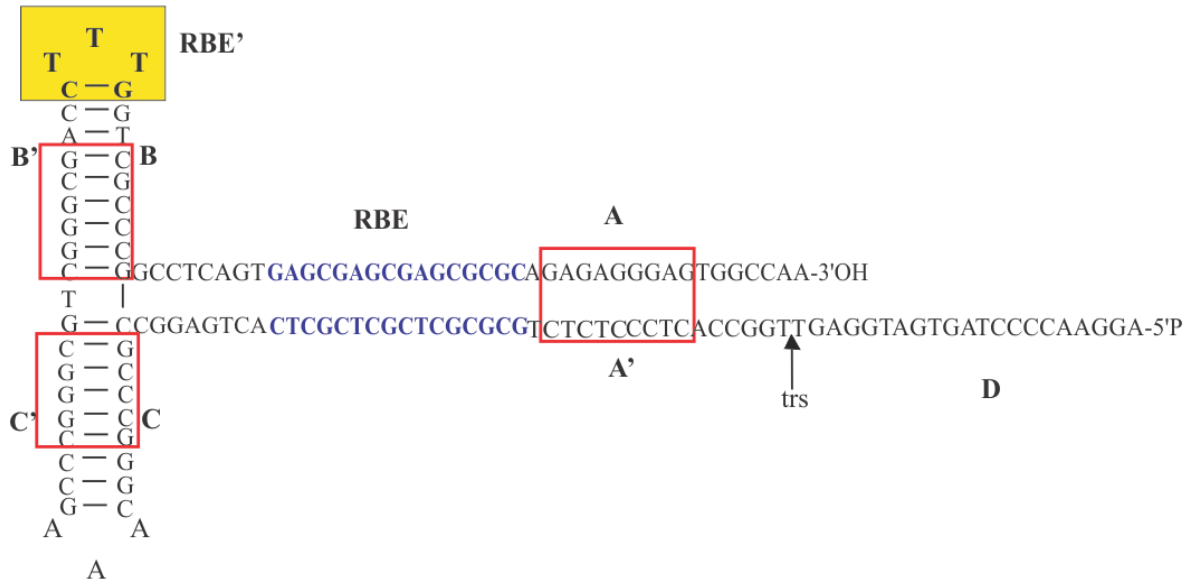


**Figure 1.4 Secondary structure of AAV2 ITR.** The ITR serves as origin of replication, has a T-structure whose configuration – flip (shown) or flop - is defined by the arrangement of its palindromic sequence in relation to the 3'OH. B'-B and C'-C or B-B' and C-C' palindromic arrangement denotes flip and flop configuration, respectively. The Rep binding element (RBE) is where Rep78 and Rep68 binds to and through their helicase and endonuclease activity also interact with terminal resolution site (trs). The yellow coloured area at the apex of the T-structure represents an RBE' whose role is to stabilise large Rep protein interaction with the ITR [Adapted from (Goncalves, 2005)].

### 1.3.1.2 AAV replication-cycle

AAV replication cycle is biphasic, either latent/lysogenic (dormant) or lytic (productive) phase promoting viral persistence or propagation, respectively [**Figure 1.5,** [reviewed in (Daya and Berns, 2008)]. In the absence of helper virus or UV radiation induced cellular stress to promote lytic phase, AAVs enters the lysogenic phase (Samulski et al., 1982, Yakobson et al., 1989, Yakobson et al., 1987).

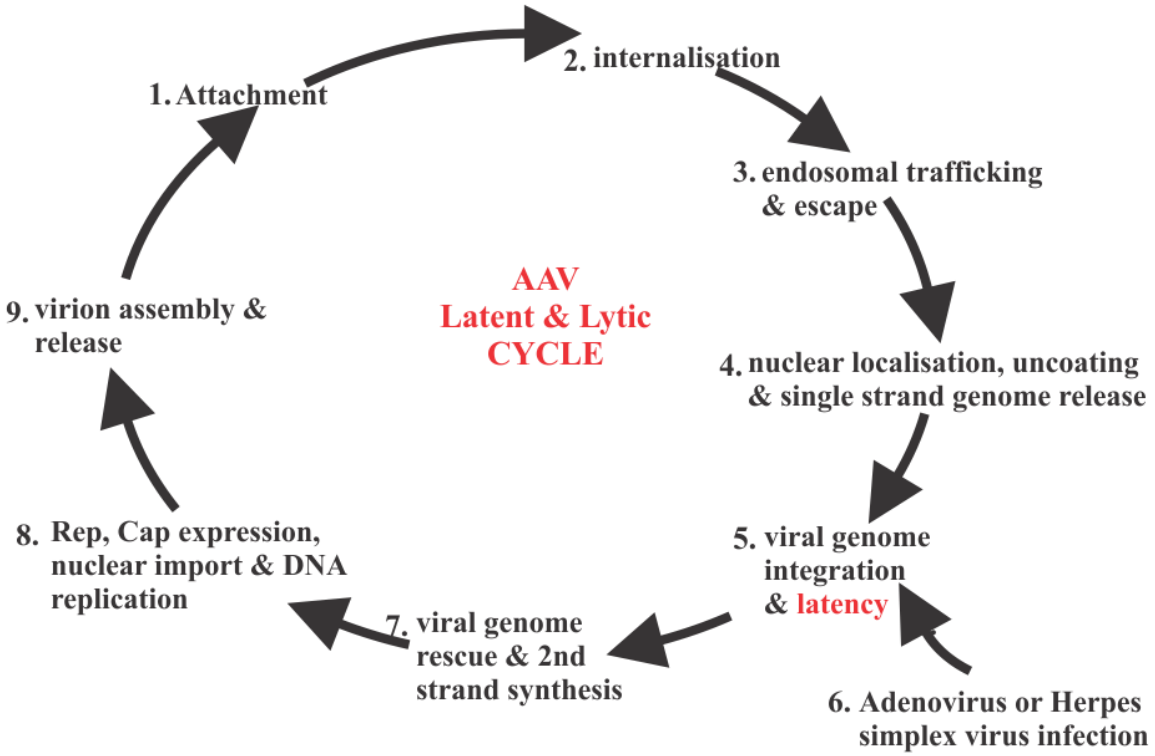


**Figure 1.5 Replication cycle of AAV.** (1) For cell entry AAV first attaches to the cell surface via heparin sulfate proteoglycans, (2) then binds to integrins (co-receptors, α5β1 and αVβ5), which allows for internalisation by clathrin dependent endocytosis, (3) followed by endosomal trafficking and escape leading up to (4) nuclear localisation, uncoating and single strand release. (5) Large Rep proteins mediate viral genome integration and latent state. (6) The production cycle can be triggered by Adenovirus or Herpes simplex virus infection or cellular stress leading to (7) viral genome rescue, second strand synthesis which allows for (8) *Rep* and *Cap* ORFs expression, and viral protein production in the cytoplasm, followed by protein nuclear import, (9) virion assembly, and release by budding.

Both phases, the latent and lytic are initiated by attachment to the cell membrane associated heparin proteoglycan receptors (Summerford and Samulski, 1998). In a clathrin-dependent endocytosis AAV capsid is internalized following cell surface binding to co-receptors, α5β1 and αVβ5 integrins (Asokan et al., 2006, Summerford et al., 1999). Intracellular events characterising AAV trafficking to the nucleus have not been fully elucidated, however some findings have been made. For AAV endosomal trafficking to the nucleus using microtubules certain signaling events

occur. The cellular signaling involves Rac1 activation and focal activation kinase (FAK) stimulation leading to phosphatidylinositol 3-kinase (PI3K) pathway activation. (Sanlioglu et al., 2000, Kaminsky et al., 2012). Pre-nuclear viral endosomal escape event is mediated by AAV capsid phospholipase $A_2$ motif with [reviewed in (Daya and Berns, 2008)]. Finally, AAV enters the nucleus by a mechanism still to be clarified.

**Latent/dormant phase**

The latent phase is characterised by negative regulation of large Rep proteins expression and this is associated with viral genome integration into unique gene locus 19q13.3-qter referred to as AAVS1 (Beaton et al., 1989, Kotin et al., 1990, Kyostio et al., 1995, Samulski et al., 1991). Supplied *in trans* is either of the large Rep proteins that mediates AAV integration by a poorly understood mechanism involving deletion, insertion and non-homologous recombination at the AAVS1 site (Dyall and Berns, 1998, Dyall et al., 1999, Linden et al., 1996a, Linden et al., 1996b, Surosky et al., 1997). Other elements needed for successful AAV integration at AAVS1 are the 6-bp RBE in *cis*, a spacer (4 to 6-bp), and TRS (6-bp). The spacer separating RBE and TRS must comply to a specific mandatory size and location for viral integration to occur (Meneses et al., 2000). Also required in the AAV genome for AAV specific site integration are the RBE and TRS found in ITRs or p5 TRS and p5 promoter integration efficiency element (p5IEE), both acting *in cis* (Philpott et al., 2002a, Philpott et al., 2002b).

**Productive/infectious phase**

Co-infection with helper virus such as Adenovirus virus transitions AAV to the lytic phase (Beaton et al., 1989, Samulski et al., 1982). In this productive cycle de-repression of p5 driven *rep* expression leads to increased *rep*-encoded protein levels (Beaton et al., 1989). In turn, large Rep proteins mediate AAV genome rescue (i.e. provirus DNA excision from AAVS1). Then the AAV infectious cycle proceeds which is characterised by host cell entry, genome replication, capsid formation, genome encapsidation, helper-virus induced lysis, virion release, and cell invasion [reviewed in (Goncalves, 2005)].

The AAV genome replication process requires host-derived proteins, AAV *rep*-encoded proteins, as well as helper-virus supplied proteins (Ni et al., 1998, Ward et al., 1998). The host-derived proteins include DNA polymerase δ complex, and partners like replication factor A and C (RFA and RFC), proliferation cell nuclear antigen (PCNA) and minichromosome maintenance complex (MCM). AAV genome replication occurs by a rolling hairpin mechanism (Berns and Parrish, 2007, Nash et al., 2008)]. Cycle of replication initiates at the AAV's hairpin 3'OH end which serves as a primer for second strand synthesis and DNA polymerase catalyses the daughter strand extension. The second strand synthesis results in a linear dsDNA molecule with one covalently closed hairpin end. The large Rep proteins facilitate nicking of the parental strand at the TRS leading to hairpin structure resolution, and formation of a ssDNA overhang. DNA polymerase catalyses the duplex strand creation from the ssDNA overhang. The DNA-duplex intermediate is followed by ITR maturation, isomerisation and finally single-strand displacement with all these processes

regulated by MCM, RFC, RFA, PCNA. Viral DNA is then packaged into assembled capsids. [**Figure 1.6,** reviewed in (Goncalves, 2005)].

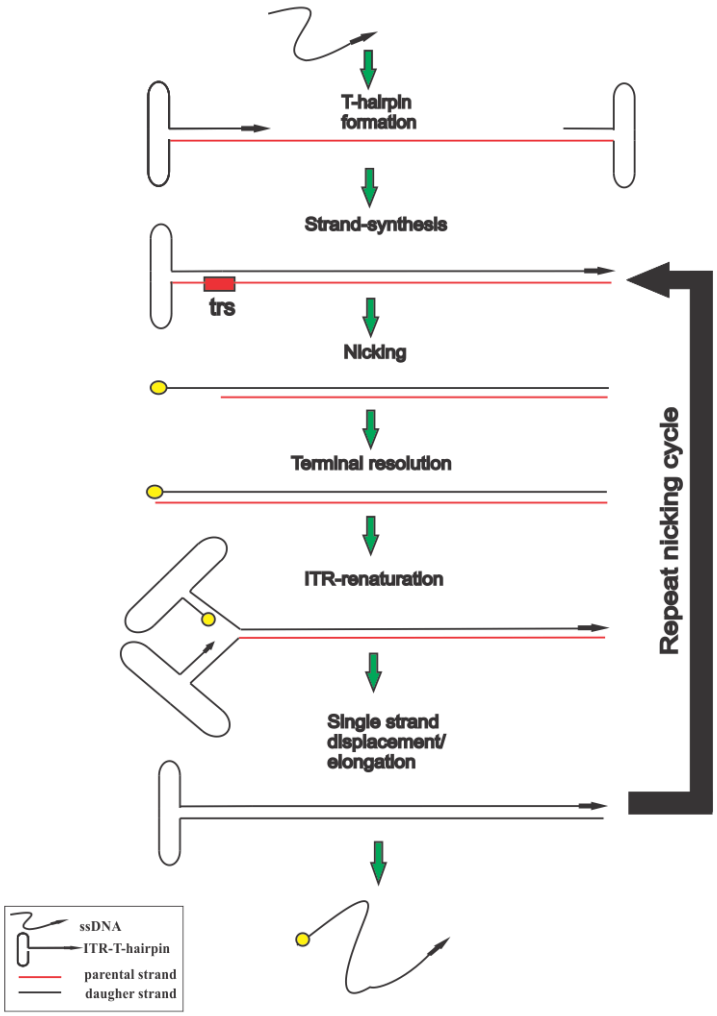


**Figure 1.6 AAV genome replication.** The T-hairpin 3' OH serves as a primer and it is where DNA polymerisation initiates. This result in duplex monomer (DM) covalently closed on one end maintaining a hairpin structure. The interaction of large Rep proteins with RBE leads to site-specific nicking at TRS causing the unravelling of the hairpin structure with resultant double stranded overhang. The exposed 3'OH allows parental strand extension. As the ITR matures, both parent and daughter palindromic strands develop terminal T-hairpin structures. This once again positions the 3'OH at terminal end for second strand synthesis. The DM forms, and the cycle repeats, while single stranded genomes are released [Adapted from (Goncalves, 2005)].

For capsid assembly, *cap* proteins are imported to the site of capsid assembly, the nucleus (Popa-Wagner et al., 2012). VP1 and VP2 possess properties that enable nuclear protein import [reviewed in (Daya and Berns, 2008)]. The co-expression of VP3 with VP1 or VP2 facilitates VP3 nuclear import and capsid assembly at correct *cap* protein stoichiometry (Popa-Wagner et al., 2012, Ruffing et al., 1992). The ITR

*cis*-acting elements, and Rep protein quartet facilitate genome packaging through capsid pores [reviewed in (Samulski and Muzyczka, 2014). The large Rep proteins tethers viral genome to capsid by binding to each other, and to both capsid and genome, while the small Rep proteins (Rep52 and Rep40) uses helicase activity as a motor to load genome to the capsid. Adenovirus infection promotes cell lysis and AAV is released following viral genome encapsidation to infect another cell (Jing et al., 2001). The understanding of the AAV biology and its well-recognised bio-safety profile has made this virus a popular recombinant vector for therapeutic gene transfer.

### 1.3.2. Engineering AAV for therapeutic application

AAV2 is a well-studied serotype, efficient in transducing cultured cells and has been used in clinical trials [reviewed in (Daya and Berns, 2008)]. AAV8 on the other hand transduces well *in vivo*, and exhibited 3 to 6-fold higher hepatocyte transduction efficiency than either AAV7 or AAV9 (Zincarelli et al., 2008). These properties make AAV8 useful for treating chronic cases of HBV, where virtually all hepatocytes are infected (Chen et al., 2007). In a clinical setting, safety is important, and therapeutic gene-transfer by viral vectors should not elicit immune response and cause toxicity. To counteract the cytotoxicity associated with *rep and cap* gene expression, the recombinant AAV (rAAV) vector constructs replaces the *cap* and *rep* ORFs with a therapeutic sequence [**Figure 1.7**, (Berns and Linden, 1995)]. The ITRs are retained as these are required in cis for genome packaging and replication during rAAV production (Markakis et al., 2010, Zincarelli et al., 2008). Also the *cis*-p5IEE required for viral chromosome integration is discarded to limit AAV integration (Philpott et al., 2002b, Grimm et al., 2003). However, rAAVs tend to integrate at low rate but

randomly in chromosomes but often favour transcriptionally active parts of the genome (Huser et al., 2014, Huser et al., 2010, Nakai et al., 2003, Nakai et al., 2005, Nakai et al., 2001).

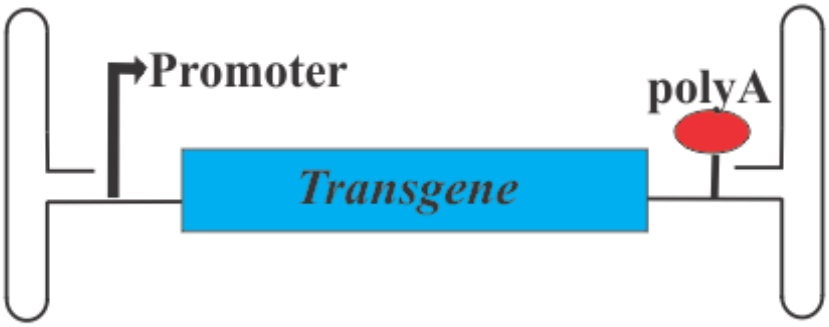


**Figure 1.7 Recombinant single-stranded AAV (ssAAV) genome.** The 145 bp ITRs flank the promoter driven gene or sequence of interest, and polyA signal added to terminate transcription. *Rep* and *Cap* ORFs have been removed.

The AAV2 ITR D region chromosomal integration has been implicated in oncogenicity and is thought to be responsible for HCC (Nault et al., 2015). However, a recent study could not confirm the ITR's D region involvement in HCC as suggested earlier. Instead the study showed that a cluster of enhancer sequences upstream to right-hand ITR added in earlier recombinant AAV2 vector modifications were responsible for the oncogenic effects observed (Logan et al., 2017). These results highlighted the need for vector sequence analysis to identify redundant, but harmful enhancer sequences present in current AAV vectors for removal. Significantly these observations have only been seen in neonatal mice but not in non-human primates (Nathwani et al., 2011).

Notwithstanding, AAV vectors remain relevant, and have shown suitability to deliver therapeutic cargo in various studies (Chen et al., 2012, Chen et al., 2009, Giering et al., 2008, Kota et al., 2009, Maepa et al., 2017, Nathwani et al., 2007). Their relative lack of immunogenicity, long-term expression, and efficient transduction of both mitotic and post-mitotic are useful properties. The non-replicative nature of rAAVs allows for proper dose therapy regulation (Cideciyan et al., 2008, Maguire et al., 2008, Nathwani et al., 2011). In certain human trials, recombinant AAV serotype 2 (rAAV2) has been used successfully to restore blindness caused by deficiency in the *RPE65* gene (Cideciyan et al., 2008, Maguire et al., 2008) or nerve growth factor (NGF) in Alzheimer disease (AD) sufferers (Mandel, 2010). AD is a chronic neurodegenerative disorder characterised by degenerating cholinergic neurons. Further pre-clinical studies have seen recombinant AAV serotype 8 (rAAV8) mediated Factor IX (F-IX) restoration in non—human primates with inability to effect blood clotting due to F-IX deficiency (Nathwani et al., 2011). Different recombinant AAVs with clinically relevant features have since been developed.

#### 1.3.2.1. Types of rAAVs and their characteristics

Currently used rAAV constructs hold DNA that is either in a single stranded (ssAAV) or self-complementary (scAAV) form [reviewed in (Goncalves, 2005). Whereas ssAAV can package a 4.7 kb genome, the scAAV have half the packaging capacity (2.35 kb). Studies have shown that second strand synthesis is the rate-limiting step in AAV transgene expression (Ferrari et al., 1996, Russell et al., 1995, Qing et al.,

1997). Moreover, the interactions occurring at ITR D- sequence region with host binding proteins, single stranded D-sequence binding protein (ssD-BP) and FK506-binding protein 52 (FK506BP52) limits second-strand synthesis leading to poor or delayed AAV transgene expression from ssAAVs (Qing et al., 2001, Qing et al., 1998).

However, the de-phosphorylated versions of proteins ssD-BP and FKBP2 have been shown to lead to higher transgene expression (Qing et al., 2001, Qing et al., 1998). Since epidermal growth factor receptor tyrosine kinase (EGF-R PTK) is responsible for ssDP-BP phosphorylation, various studies have shown inhibition of PTK activity of EGF-R enhances transgene expression, but with accompanying toxic effects. So, to improve rAAV transduction and effect faster transgene expression kinetics, ready to express scAAV vectors are most commonly used where packaging capacity is not a limitation (Cai et al., 2016, Chen et al., 2009, Maepa et al., 2017, Nathwani et al., 2011)

Structurally, scAAV has two T-shaped loops at its ends, and one hairpin loop midway in the DNA genome that allows the molecule to fold and base pair with itself [**Figure 1.8,** (Koczot et al., 1973)].

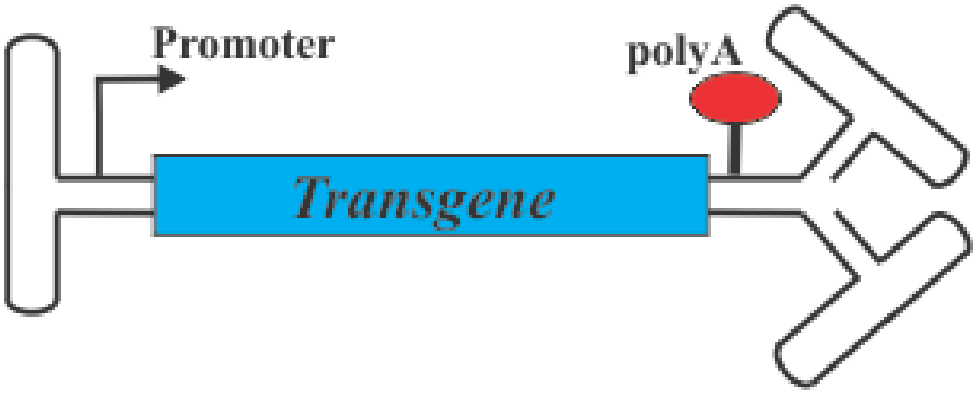


**Figure 1.8 Schematic representation of self-complementary recombinant AAV (scAAV) genome.** The genome has three T-hairpin structures, the one of the left that allows the single strand with palindromic ends to fold and form mature terminal ITR hairpin structures. In this double stranded conformation, the scAAV can readily express transgene material from a promoter, with polyA signal to terminate transcription.

In a proof of concept study, McCarty and team confirmed the transgene expression superiority of scAAVs over ssAAVs. Using AAVs expressing green fluorescent protein (GFP) as a reporter or erythropoietin to stimulate red cell production, they showed *in vitro* transgene expression of 5 to 140 times higher from scAAV as compared to ssAAV. The lesser GFP expression in ssAAV treated cells suggested transgene expression inefficiency as a result of host cell factors preventing second strand synthesis (McCarty et al., 2001).

Also, erythropoietin activity was significantly higher and observed earlier in scAAV compared to ssAAV treated mice. Moreover, the ssAAV vector never reached the same expression levels as that of scAAV. Collectively these results pointed to a higher and quicker gene expression by scAAVs that is independent of second-strand DNA synthesis. Notably, the attainment of higher gene expression by using scAAV is at the expense of transgene size. Despite scAAV small transgene capacity, it has

proved suitable in RNAi-based anti-viral therapy (Chen et al., 2012, Kota et al., 2009, Maepa et al., 2017).

#### 1.3.2.2. Application of AAVs for treatment of HBV infection

The fact that HBV infection appears to enhance AAV transduction of hepatocytes (Hosel et al., 2014) makes them more suitable for anti-HBV gene therapy. Hence, a persistent HBV replication inhibition in mice was demonstrated after scAAV, serotype 8 (scAAV8) mediated reprogramming of the RNAi pathway using pol III promoter driven shRNA to target HBV surface RNA transcripts (Grimm et al., 2006). However, the effect was short-lived as mice died from RNAi pathway oversaturation. Two years later the same group used the same viral vector to show a safe scAAV8 mediated anti-HBV shRNA which effected HBsAg level knockdown of above 95% and was sustained for over 3 months. In this case the shRNA transgene was driven from pol II promoter and no immune induction, liver toxicity or fatalities were reported (Giering et al., 2008)

HBV infection treatment with AAV2/8 mediated anti-HBV shRNA transfer in HBV transgenic mice resulted in HBV knockdown observed for 90 days before HBsAg rebounded to baseline levels 120 days post-injection (Chen et al., 2007). To prolong HBV gene silencing effect from about 5 months, two different AAV serotypes, AAV8 and AAV9 carrying anti-HBV shRNA were serially injected in HBV transgenic mice. Indeed, this extended HBV titre level knockdown of over 95% in relation to controls for about three more weeks (Chen et al., 2009). However, improved results have been seen recently with HBV inhibition extending to 10 months with a single injection of anti-HBV scAAV8 viral particles (VP). The study used 10 to 100 fold times less

dose than used in the Chen study and no signs of overt toxicity and harmful immune induction were observed (Maepa et al., 2017).

Despite the impressive efficiency and safety profile, rAAVs are not without their shortfalls. AAV capsid tropism towards certain cell types can be varied creating unintended off-target effects (Zincarelli et al., 2008). Also, some tissues are resistant to viral vector gene therapeutic transfer like human airway epithelial or neural stem cells, and the blood brain barrier (BBB) prevents access to central nervous system [CNS,(Excoffon et al., 2009, Gray et al., 2010, Jang et al., 2011)]. Most importantly, high prevalence of pre-existing immunity to rAAVs based on current serotypes such as AAV8, leads to short-lived transgene expression in humans (Calcedo et al., 2011, Calcedo et al., 2009, Manno et al., 2006, Nathwani et al., 2011). Most of these obstacles to gene transfer are being addressed through ongoing AAV capsid re-engineering or de novo construction in the context of rational design, directed evolution or in silico vector synthesis.

#### 1.3.2.3. AAV capsid re-engineering

Vector epitope rational design uses capsid's architectural analysis and knowledge of its extra- and intra-cellular navigation mechanism to introduce functionally enabling structural changes. Viral tropism modification have been done to target cancerous cells by enriching AAV2 surface with Ankyrin repeats protein that serve as ligands specific to overexpressed human epidermal receptor 2 (HER2) in tumour cells to facilitate vector internalisation (Munch et al., 2013). The liver infectivity and specificity of AAV2 was also enhanced by adding an AAV9 motif at corresponding AAV2 site responsible for galactose binding (Shen et al., 2013). Also, mutating antibody

docking site at AAV2 surface residues at different positions prevented murine IgG2a antibody docking on to AAV2 surface to effect neutralisation leading to significant transduction efficiency (Lochrie et al., 2006). Transduction improvements in these rationally designed vectors ranged from 10 to ~ 30-fold compared to wild-type AAV2 (Lochrie et al., 2006, Munch et al., 2013, Shen et al., 2013)

Intracellular trafficking of transgene cargo using rAAV2 is hindered by vector loss following phosphorylation at its tyrosine residue by epithelial growth factor tyrosine kinase. The phosphorylated rAAV2 is ubiquitinated, leading to its degradation due to proteasomes (Zhong et al., 2008a). Highly improved transduction was observed when AAV2 capsid tyrosine residue was mutated to phenylalanine to evade proteasomal degradation and cytotoxic T-lymphocyte recognition (Martino et al., 2013, Zhong et al., 2008b).

Directed evolution achieves vector improvement by enriching genetic diversity, and employing selection methods to concentrate beneficial mutations [reviewed in (Kotterman and Schaffer, 2014)]. Through directed evolution, a cap gene can be mutated by DNA shuffling, which combines capsid sequences from other serotypes (Kienle et al., 2012), or mutations introduced by amplifying capsid sequence using error-prone PCR (Asuri et al., 2012), or employing *in vitro* viral recombination methodology to produce chimeric AAV *cap* genes reflecting multiple serotype characteristics (Bowles et al., 2003). The mutated capsids are then exposed to selective pressure of neutralising antibodies through *in vitro* and *in vivo* experiments. This has led to enhanced hepatocyte transduction by AAV2 variants isolated after evading higher levels of neutralising antibodies (Lisowski et al., 2014, Perabo et al.,

2006). AAV variants mediated gene transfer directly to the difficult to reach photoreceptors after intravitreal injection. Vision improvement was observed in murine models of X-linked retinoschisis and congenital amaurosis (Dalkara et al., 2013). Recently, AAV2 variants derived from capsid shuffling were incubated with human serum containing neutralising antibodies (Li et al., 2016). Subsequently the vectors were later isolated from muscle demonstrating escape from neutralising antibody.

Capsid recombination, mutagenesis, and selection rounds of *in vitro* transduction of human airway epithelial cells or neural stem cells followed by adenovirus rescue produced AAV2 variants that were able to transduce the previously resistant human airway epithelial or neural stem cells (Excoffon et al., 2009, Jang et al., 2011). *In vivo* biopanning of mutant AAVs in mice resulted in AAV2 variants with specificity and high transduction efficiency of cardiomyocytes (Yang et al., 2009).

Other approaches to overcoming the challenge of pre-existing immunity to AAV capsids has been to administer transgene-carrying capsids with decoy (empty) capsids simultaneously (Mingozzi et al., 2013) or in silico construction of synthetic AAV vectors (Santiago-Ortiz et al., 2015, Zinn et al., 2015).

In silico construction is done by reconstructing ancestral genes encoding synthetic AAV capsid variants. The construction of ancestral proteins or capsids involves several steps. The gene descendants (in amino acid sequence form) are aligned, and ancestral proteins sequences are inferred by applying phylogenetic methods (maximum parsimony or likelihood). The resultant amino acid sequence is then converted to a DNA sequence. Then, the DNA sequence (ancestral gene) is cloned

into a high expressing plasmid, transfected into mammalian cells, and capsid proteins produced [reviewed in (Thornton, 2004)].

Santiago and team assessed transduction efficiencies by GFP expressing vectors between ancestral AAV variants (AL.C2C12, AL.IB3, AL.B16-F10, AL.GBM, AL.293T) and natural AAV serotypes, 1 – 9 (Santiago-Ortiz et al., 2015). The assessment was done across different cell lines, and found that all ancestral AAV vectors transduced cells more efficiently than AAV2, 4, 5, 8 & 9, with AAV1 and 6 showing similar efficiency. In another study, the resultant ancestral vector (Anc80L65) had enhanced infectious attributes, and could evade immune recognition. Anc80L65 lacks certain epitopes found on the current AAV capsids. As compared to rAAV8, Anc80L65 expressing GFP emitted more fluorescence in the muscle, liver and eye. During animal studies, out of 5 mammals pre-immunised against AAV8, Anc80L65 vector still mediated excellent transgene expression of chorionic gonadotropin in 3 rabbits, while rAAV8 was completely neutralised in all cases (Zinn et al., 2015).

In non-human primates Anc80L65 also proved to have superior transgene expression compared to rAAV8 (Zinn et al., 2015). What has not been attempted so far is assessment of the efficacy of ancestral AAVs when used to deliver sequences that inhibit HBV replication. Hence this study compared whether Anc80L65 performed comparably or better than AAV8 when used to deliver anti-HBV pri-miR-122/5 to cultured cells or hepatocytes *in vivo*.

## 1.4 Research Aims and Objectives

**Aim:** The aim of the study was to determine the efficacy of rAAV serotype 2, 8 and ANC80L65 as vehicles for delivery of anti-HBV pri-miR delivery.

**Objectives:**

To reach the aim, the following objectives were set:

I. To produce AAV vectors of different serotypes, namely AAV2, AAV8 and Anc80L65 of rAAV vector expressing luciferase

II. To determine luciferase gene expression in liver derived cell line and mice using a luminometer or bioluminescence imager.

III. To produce recombinant anti-HBV AAV vectors derived from different serotypes, namely rAAV2, rAAV8 and rAnc80L65.

IV. To assess HBV gene expression inhibition in a liver derived cell line using a dual luciferase and ELISA assays.

V. To assess suppression of HBV gene expression in HBV transgenic mice by ELISA assay.

VI. To measure levels of serum inflammatory markers and Alanine transferase (ALT) as a liver toxicity marker

# CHAPTER 2: METHODS

## 2.1 Bacterial Culturing

Culturing of XL-1 Blue *Escherichia coli* was performed in Luria Bertani (LB) or Luria Bertani agar (LA) media (Appendix A, 1 a) supplemented with 100 mg/mL Ampicillin (Appendix A, 3 a) or 50 mg/mL Kanamycin (Appendix A, 3 b). Cultures on solid media were incubated overnight in a 37 °C standing incubator. Liquid cultures were similarly incubated on a shaking incubator at 150 rpm.

## 2.2 Bacterial transformation

### 2.2.1 Preparation of chemically competent cells

To prepare chemically competent cells, XL-1 Blue *E. coli* cells were used to prepare bacterial pre-culture. This was done by inoculating 5 ml of LB with a single colony of *E. coli* for overnight incubation and shaking at 37 °C and 150 rpm, respectively.

After diluting the pre-culture 100 × with LB, it was placed in a 37 °C shaking incubator, shaking at 150 rpm until $OD_{600}$ read between 0.4 - 0.6. Centrifugation of culture at 2500 rpm for 15 minutes produced a pellet that was re-suspended in 10 mL transformation buffer (Appendix A, 1 a). The suspension was then incubated for 20 minutes on ice, and centrifuged again at 2500 rpm for 15 minutes to produce a pellet. After re-suspending the pellet in 1 mL Transformation buffer, 100 µl aliquots were made and kept for long term storage at -80 °C. Cells were thawed on ice before use.

### 2.2.2 Transformation of chemically competent cells

Ampicillin- or Kanamycin-resistant plasmid DNA was added to 100 µl of competent *E. coli* and mixed by tapping the micro-centrifuge tube gently. After incubating the mixture on ice for 10 minutes, it was heat shocked at 42 °C for 90 seconds, and placed in ice for 5 minutes. The mixture was spread onto pre-warmed Ampicillin or Kanamycin enriched LA plates with 40 µl of 20 mg/mL X-gal (5-bromo-4-chloro-3-indolyl-β-D-galactopyranoside (Appendix A, 3 c) and 8 µl of 100 mg/mL Isopropyl β-D-1-thiogalactopyranoside (IPTG, Appendix A, 3 d) spread on to it. Incubation at 37 °C overnight was done with plates facing down.

## 2.3 Large-scale plasmid DNA purification

All plasmid purifications were carried out using Maxi plasmid commercial kit according to the manufacturer's instructions (Qiagen$^{R}$, Hilden, Germany). Briefly, the bacterial culture was harvested by centrifugation and mixed serially with three different buffers (P1, P2 and P3) at 10 mL each to suspend the cells, gently release DNA, separate DNA-protein complexes, denature all DNA and renature plasmid DNA. Buffer P1 was added to suspend culture. The second buffer P2 was mixed with the suspension by gentle inversion 4 – 6 times and left for 5 minutes at room temperature. After adding P3, the mixture was vigorously inverted 4 – 6 times, and incubated on ice for 20 minutes. Centrifugation performed on cell lysate caused genomic DNA sedimentation, leaving plasmid DNA in solution. Anion-exchange resin based column and high-salt buffer treatment was used to purify and elute the plasmid DNA respectively. Then, isopropanol was added to desalt, concentrate and precipitate plasmid DNA by centrifugation. After washing the pellet with ethanol and

air-drying, plasmid DNA was dissolved in distilled water, quantified by spectrophotometry and stored at -20 °C.

## 2.4 Restriction digestion

Restriction enzymes from Thermo Scientific, Waltham, USA, were used for plasmid DNA digestion reactions. Twenty microlitres final volume samples consisted of 1 µg DNA, 1 unit of enzyme, 1 × buffer, and volume made up to 20 µl with distilled water. Samples were incubated at 37 °C overnight.

## 2.5 Quantitative Polymerase chain reaction (qPCR)

For AAV titration, quantitative PCR reactions were performed using Roche FastStart Essential DNA Green Master kit (Roche, Indianapolis, US) according to manufacturer's instructions. Forward and reverse primers [5'- CCCCTGTTCAAACATGTCCT-3', and 5'- ACTCAACATCCTCCCAGTGC-3',(Carmona et al., 2006)] were used for viral quantification, at the following set conditions for PCR cycles: Denaturation at 95 °C for 30 seconds, annealing at 62 °C for 1 minute, and an extension step at 72 °C for 1 minute/kb. The cycles were repeated 35 times and final extension step was done at 72 °C for 1 minute.

## 2.6 Gel electrophoresis

A 1% agarose (Lonza, Rockland, USA) gel was prepared in 1 × TAE buffer (Appendix A, 2 b) by melting the powder in a microwave. Once melted and cooled to ~ 50 °C, ethidium bromide (Sigma, St. Louis, USA) was then added to a final

concentration of 1 µg/ml. The gel was poured and allowed to stand on a casting tray (tray, comb, and dam) to solidify. When solid, the gel was submerged in an electrically charged 1 × TAE buffer filled chamber. Loading dye (6 × Loading dye, Fermentas, WI, USA) was added to the samples to 1 × and loaded on the gel. The gel was run at 100 V for 45 minutes to an hour and imaged used Gel doc (BIO-RAD, Johannesburg, South Africa).

## 2.7 Tissue culturing and freezing

Kidney derived HEK293T and liver derived Huh7 cells were used for viral propagation and infection assays respectively. Tissue cultures were grown in Dulbecco Modified Eagle Medium (DMEM,Life Technologies, CA, USA) supplemented with penicillin at 100 000 U/ml, streptomycin at 100 µg/ml and 10% Fetal Calf Serum (FCS, Appendix A, 2 c) and placed in a humidified incubator set at 37 °C and 5% $CO_2$.

To grow cells from frozen stock culture in a vial, cells were thawed in a 37 °C water bath, and diluted in 10 mL DMEM (Life Technologies, CA, USA). The cells were centrifuged for 3 min at 850 rpm to produce a pellet that was resuspended in 1 mL DMEM, and suspension transferred to a T25 flask (Sigma, SL, USA). Four millilitres DMEM was added in the flask before incubating in a 37 °C, 5% $CO_2$ humidified incubator overnight. After microscopic examination for healthy growth of culture, spent medium was aspirated, replaced with fresh 5 mL pre-warmed DMEM. The culture was re-incubated until between 70 – 80% confluency was reached before passaging.

Passaging of cells was done by aspirating spent medium, then cells washed once with pre-warmed phosphate buffered saline (PBS) containing 0.5 M EDTA (Appendix A, 4 b) to remove FCS. To detach cells from flask surface, 500 µl of 0.5 × trypsin was added and flask placed for 3 minutes in a 37 °C, 5% $CO_2$ humidified incubator. Upon removal from the incubator the flasks were tapped lightly on the sides to further detach cells. Trypsin was inactivated by adding 4.5 mL DMEM within a minute of removal from incubator. Cells were suspended by gentle pipetting up and down to remove clumped cells and then split into 1:2 into a T25 flask for Huh7 cells, or T75 for HEK293T cells and the media made up to 5 or 10 mL, respectively. Cells were then incubated until they reached ~ 80% confluency. Passaging into T150 flasks was done similarly with 20 mL final growth media. Seeding into 24 well dish was also done similarly with 500 µl final media per well. To freeze down cells from a T150 flask, cells were detached as above using 2 mL of 0.5 ×Trypsin and cells were pelleted and resuspended in 10 mL freezing media (Appendix A, 1 d). One millilitre aliquots were added to cryovial tubes and kept at -80 °C overnight and then transferred to liquid nitrogen for long-term storage.

## 2.8 Transfection assays

### 2.8.1. Transfections for viral production

To produce all recombinant AAV vectors, except for rAnc80L65, 319 µg of DNA mix consisting of a plasmid bearing the AAV ITRs and the transgene (pAAV-122/5 or pAAV-NLuc, **Table 2.1**), an Adenoviral gene bearing plasmid (pAd-helper, **Table 2.1**) as well as AAV *Cap* and *Rep* expressing plasmid (pAAV2 or pAAV8, **Table 2.1**) were transfected into HEK293T cells in a ratio of 0.25:1:2 respectively. For rAnc80L65 production an additional plasmid DNA expressing AAV2 AAP (pAAP2, **Table 2.1**)

was also included in the transfection mix. Hence 417.4 µg plasmid DNA mix consisting of [pAAV-122/5 or pAAV-NLuc], pAAP2 (**Table 2.1**) and Anc80L65 (**Table 2.1**) at a ratio of 0.25:1:1:2 was used respectively. Transfection was performed using Polyethyleneimine "Max" [PEI-max (Polyscience Inc, PA, USA)] according to the manufacturer's instructions. Briefly, PEI-max was mixed with DNA in a PEI-max:DNA ratio of 3:1 and diluted up to 8 mL with OPTIMEM (Life Technologies, NY, USA). The mixture was vortexed and incubated for 12-15 minutes at room temperature (RT) before distributed dropwise 2 mL per plate (150 $cm^2$) of four.

### 2.8.2. Transfection for knockdown assays

Huh7 cells were seeded at 40% confluency in a 24-well plate and grown until 70-90% confluency. Before transfection, pen/strep containing DMEM media was replaced with antibiotic free DMEM. Transfections were performed using Lipofectamine 3000 (Thermo Scientific, MA, USA) according to the manufacturer's instruction. Briefly, wells were cotransfected in triplicate with 100 µl transfection mixture consisting of Lipofectamine (Lipofectamine 3000, Thermo Scientific, MA, USA) and plasmids (pCH9-3091or psiCHECK-*HBx* and pBS-H1-GFP, **Table 2.1**) buffered in OPTIMEM. Three wells left untransfected served as controls. The mixture was prepared by adding 1.5 µl Lipofectamine 3000, 100 ng pCH9-3091 or psiCHECK-HBx and 100 ng pBS-H1-GFP and volume adjusted to 100 µl with OPTIMEM. After incubation for 12-15 minutes at RT, transfection mixture was then added dropwise onto the wells containing cells in 400 µl of media. Cells were then incubated for five hours in a 37 °C, 5% $CO_2$ humidified incubator.

## TABLE 2.1: Plasmids used

| Name | Description | Source or reference |
|---|---|---|
| **pAAV2** | A plasmid carrying AAV2 *cap* and *rep* ORFs. It carries ampicillin resistance ($Amp^R$) selection marker. | Generously provided by Prof. Dirk Grimm |
| **pAAV8** | A plasmid carrying AAV8 *cap* and *rep* ORFs. It carries ampicillin resistance ($Amp^R$) selection marker. | Generously provided by Prof. Dirk Grimm |
| **pAnc80L65** | A plasmid carrying Anc80L65 *cap* ORF and AAV2 *rep* ORF. It carries kanamycin selection marker ($Kan^R$). | (Zinn et al., 2015) |
| **pAAP2** | A plasmid expressing Assembly-activating protein (AAP) of AAV2. It carries ampicillin resistance ($Amp^R$) selection marker. | (Zinn et al., 2015) |
| **pBS-H1-GFP** | A plasmid expressing GFP from an RSV promoter. GFP cassette is flanged by ITR-2 and ITR-4 from AAV2 and AAV4 respectively. $Amp^R$. | Generously provided by Prof. Dirk Grimm |
| **pBS-mTTR** | pBS-H1-GFP plasmid with the GFP-RSV promoter cassette replaced with MTTR promoter sequence without any transgene. | (Bourhill, 2015) |
| **pAAV-122/5** | pBS-H1-GFP plasmid with the GFP-RSV promoter cassette replaced with pri-miR 122/5-MTTR promoter cassette. | Not published |
| **pNL1.1.CMV [NLuc/CMV]** | A plasmid expressing nano-luciferase (NLuc) under control of CMV promoter. | (Promega, WI, USA) |
| **pAAV-NLuc** | pBS-H1-GFP plasmid with the GFP-RSV promoter cassette replaced with NLuc-MTTR promoter cassette. | Unpublished. |
| **pCH-9/3901** | Plasmid bearing a greater than HBV genome length HBV sequence. | (Nassal, 1992) |
| **psiCHECK-*HBx*** | It bears an intact *HBx* target sequence downstream of *Renilla* luciferase reporter ORF and *Firefly* luciferase is constitutively produced from a separate expression cassette. | (Weinberg et al., 2007) |
| **p-Ad-helper** | A plasmid containing Adenovirus AAV helper genes | Generously provided by Prof. Dirk Grimm |

## 2.9 AAV Production, purification and titration

Recombinant AAV vector production was carried out according to previously reported methods (Lock et al., 2010, Zinn et al., 2015).

### 2.9.1. Viral vector harvesting

After HEK293T cell culturing (**Section 2.7**) and triple or quadruple plasmid transfection (**Section 2.8.1**), cells were left incubating for 120 hours to allow production and propagation of rAAV vectors. At time points 48, 72, 96, and 120 hours after transfection, spent media from four plates were collected and stored at 4 °C. At all time points, except the last, spent media was replaced with fresh 20 mL pen/strep enriched growth media (DMEM). At 120 hours after supernatant collection, 40 mL PBS (Sigma, MO, USA) was distributed in equal volumes of 10 mL in all plates. The cells were scraped off and collected into 50 mL centrifuge tubes. The harvesting of cells was done by centrifugation at 1500 rpm for 8 minutes, and supernatant discarded. Five millilitre lysate buffer (Appendix A, 2 e) was used to resuspend the pellet and the suspension was kept at -80 °C until cell lysis was performed. To completely lyse the harvested cells and release the viral particles, the cell suspension was put through 5 rounds of freeze-thaw cycles (5 × 37 °C, 5 × -196 °C), then sonication was performed for 80 seconds. To get rid of RNA and DNA complexes, the sample was treated with 50 units of Benzonase (Sigma, MO, USA) per mL of sample. Then the samples were kept at 37 °C removed only to vortex for 15 seconds at 10 minute intervals for over the period of an hour. To pellet cell debris, the samples were centrifuged for 15 minutes at 4 °C and 4000 rpm,

supernatant transferred to a new centrifuge tube and again centrifuged under same conditions. Supernatant containing virions was collected and kept for later use.

To precipitate virions from the supernatants collected, about 400 mL of media containing AAV were first filtered through 250 or 500 mL sterile cup [0.22 µm, (Millipore, MA, USA)] into sterile bottles. Then 12.5 mL of 5 × polyethylene glycol 8000 (Sigma, MO, USA) per 50 mL of filtrate was added and mixture stored at 4 °C for 24 hours. After centrifugation at 5000 rpm for 30 minutes supernatant was discarded and the pellet resuspended using 5 mL AAV containing supernatant previously collected from cell lysates. The suspension was then applied to the iodixanol gradient for viral purification.

### 2.9.2. AAV iodixanol gradient purification

Pasteur pipettes [230 mm, (Paul Marienfeld GmbH & Co KG, Laud-Kongshofen, Germany)] were used to gently transfer viral and iodixanol solution (Appendix A, 4 g) to the centrifuge tubes [16 × 76 mm, (Beckman Coulter Inc., CA, USA)]. The ~7 mL viral suspension was added first followed by 1.5 mL of each iodixanol solution at concentrations of 15%, 25%, 40% and 60%. Care was taken to avoid air bubbles that may be introduced as each iodixanol concentration layer was added. The centrifuge tubes were balanced, and sealed by melting before ultracentrifugation of samples with 70.1. Ti rotor (Beckman, CA, USA) at 50 000 rpm, 4 °C for 2 hours was performed.

To extract the pure virus containing fraction, the centrifuge tube was first punctured on top with a 20 × 1.5” gauge needle (Neomedic, Hertfordshire, UK) to release the pressure. Another 20 × 1.5” gauge needle attached to a 3 mL syringe (Neomedic, Hertfordshire, UK) was used to puncture the tube at the base of the 40% iodixanol fraction and extract recombinant viral particles.

### 2.9.3. rAAV genomic DNA extraction and viral titration

Viral genome isolation and purification was performed using Qiagen’s blood and body fluids commercial kit per manufacturer’s instructions (Qiagen$^{R}$, Hilden, Germany). Briefly, 50 µl pure viral sample was diluted 4 times and added to a microcentrifuge tube containing 20 µl Proteinase K. Two hundred microlitres of buffer AL were added to the sample and pulse vortexed for 15 seconds to mix. After incubation of the sample for 10 minutes at 56 °C and brief centrifugation, two hundred microlitres of ethanol were added and the mixture applied to a QIAmp Mini spin column. The spin column was centrifuged and washed with 500 µl of buffer AW1 with centrifugation at 8000 rpm for 1 minute. The spin column was washed again with 500 µl of buffer AW2 with centrifugation at 14 000 rpm for 3 minutes. Viral DNA was eluted with distilled water and titrated using qPCR (**Section 2.5**).

## TABLE 2.2: Recombinant AAV vectors used

| Name | Description | Source or reference |
|---|---|---|
| **rAAV2-EMPTY** | Recombinant AAV2 bearing the promoter sequence (mTTR) and no transgene. | This study |
| **rAAV8-EMPTY** | Recombinant AAV8 bearing only a promoter sequence (mTTR) and no transgene. | This study |
| **rAnc80L65-EMPTY** | Recombinant Anc80L65 bearing only a promoter sequence (mTTR) and no transgene. | This study |
| **rAAV2-122/5** | Recombinant AAV2 vector expressing anti- HBV pri-miR 122/5 gene from mTTR promoter | This study |
| **rAAV8-122/5** | Recombinant AAV8 vector expressing anti-HBV pri-miR 122/5 gene from mTTR promoter | This study |
| **rAAV2-31/5** | Recombinant AAV2 vector expressing anti-HBV pri-miR 31/5 gene from mTTR promoter | Maepa *et. al.* 2017 |
| **rAAV8-31/5** | Recombinant AAV8 vector expressing anti-HBV pri-miR 31/5 gene from mTTR promoter | Maepa *et. al*. 2017 |
| **rAnc80L65-122/5** | Recombinant Anc80L6 vector expressing anti- HBV pri-miR 122/5 gene from mTTR promoter | This study |
| **rAAV2-NLuc** | Recombinant AAV2 vector expressing nano-luciferase from mTTR promoter. | This study |
| **rAAV8-NLuc** | Recombinant AAV8 vector expressing nano-luciferase from mTTR promoter. | This study |
| **rAnc80L65-NLuc** | Recombinant Anc80L65 vector expressing Nano-luciferase from mTTR promoter. | This study |

## 2.10. Infection of cultured cells and HBV transgenic mice with rAAVs

### Nano-luciferase transgene expression

To assess transduction efficiency and transgene expression *in vitro,* Huh7 cells grown to ~ 70% confluency in 24-well plates were either not infected or infected at multiplicity of infection (MOI) of $10^5$ with empty control (rAAV2-EMPTY or rAnc80L65-EMPTY) or nano-luciferase expressing vectors [rAAV2-NLuc or rAnc80L65-NLuc (**Table 2. 2**). The cells were incubated in a humidifier set at 37 °C, 5% $CO_2$. Nano-luciferase is secreted by cells into the growth medium. Hence, 48 hours after infection, 100 µl supernatant was collected for luciferase activity assessment.

*In vivo* studies were carried out using HBV transgenic mice model. These mice have HBV genome integrated in to their genome and do not develop hepatitis B symptoms (Marion et al., 2003), hence modelling the chronic hepatitis B infection. To prepare for transduction efficiency and transgene expression assessment *in vivo*, three mice per group were injected via tail vein with $1 \times 10^{11}$ viral particles of rAAV8 or rAnc80L65 (**Table 2.2**) expressing nano-luciferase and bioluminescence measured at weeks, 2, 4, 8 and 12.

### Pri-miR expression and HBV replication inhibition assessment

To prepare for HBV replication inhibition assessment, Huh7 cells were transfected (**Section 2.8.2**) then infected with rAAVs. Five hours after transfection the transfection medium was removed and replaced with fresh growth medium (DMEM) transgene carrying rAAV [(rAAV2-122/5 or rAn80L65-122/5) or empty rAAV vectors

(rAAV2-EMPTY or rAnc80L65-EMPTY), **Table 2.2**] to a final volume 100 µl. Three wells were each infected at MOI of $1 \times 10^5$ or $10^6$ with transgene carrying or empty vectors or were not infected. Wells infected with empty vectors or not infected served as controls. For optimal transduction, the plates were incubated for 1 hour at 5% $CO_2$ and 37 °C with gentle rocking every ten minutes. Thereafter, fresh medium was topped up to 500 µl per well. HBV gene expression assessment was carried out at 48 and 72 hours.

To prepare for RNA isolation and anti-HBV sequence expression assessment, transgene carrying rAAV [(rAAV2-122/5 or rAn80L65-122/5) or empty rAAV vectors [(rAAV2-EMPTY or rAnc80L65-EMPTY), **Table 2.2**] were mixed in a tube with Huh7 cells suspended in 8 mL growth media. The mixture was then transferred to a 10 $cm^2$ tissue plate. All plates were incubated at 5% $CO_2$ and 37 °C for 48 hours before RNA isolation.

For *in vivo* HBV gene expression inhibition assays, five mice per group were infected with $1 \times 10^{11}$ viral particles of rAAV8-122/5 or rAnc80L65-122/5 via tail vein injection. The other five mice per group were similarly injected with rAAV8-EMPTY or rAnc80L65-EMPTY or SALINE and served as negative controls. Mice were bled by retro orbital puncture at week 2, 4, 8, 12, and 16. Serum samples were then used for assessment of HBV gene expression inhibition.

## 2.11. Determination of pri-miR expression and processing by Northern Blotting

### 2.11.1 RNA isolation from Huh7 cells

RNA isolation was performed using guanidinium thiocyanate-phenol-chloroform extraction method (Chomczynski et al., 1987). RNA was isolated from Huh7 cells previously infected with rAAVs or controls (**Section 2.10**). One millilitre Trizol (Sigma, MI, USA) was added to the plate to detach and lyse cells. The cell lysates were transferred to a microcentrifuge tube where the sample was pipetted up and down for efficient lysis before incubation for 5 minutes at RT. Two hundred microlitres of chloroform were then added to the lysate and mixed vigorously by shaking the microcentrifuge tube for 15 seconds and then allowed to stand at RT for 2 - 3 minutes. Centrifugation at 12 900 rpm for 12 minutes at 4 °C produced aqueous, and organic bi-layer. The top aqueous layer was transferred to a fresh tube. Five hundred microlitres of isopropanol were used to precipitate nucleic acid from the aqueous sample at RT. The precipitated solution was centrifuged at 12 900 rpm for 10 minutes at 4 °C and the resultant RNA pellet washed with 1 mL 75% ethanol diluted in DEPC water (Appendix A, 4 i). The RNA pellet was air dried, and re-suspended in RNAse free water and concentration reading taken using Nano-drop Spectrophotometer (Thermo Scientific, NC, USA). The RNA was stored at -70 °C for later use.

### 2.11.2. Radioactive labelling and purification of the probe and the RNA ladder

To target miR-122/5 script for visualisation a reaction mixture catalysing the transfer of radiolabelled Easytides® Adenosine 5’ Triphosphate, [γ-$^{32}$P] (ATP, γ-$^{32}$P) to 5’ OH of RNA was prepared. The reaction mixture consisted of T4 Polynucleotide Kinase

(PNK) 1 × buffer A, 2 µl of 10 µM probe (5' CCGTGTGCACTTCGCTTC 3'), 1 – 5 µl (ATP, γ-$^{32}$P) adjust to a final volume of 20 µl with distilled water. The volume of the probe added is dependent on the number of days from the start of decay date. To purify a labelled probe, size exclusion chromatography was used. A Sephadex column was prepared and used to purify the probe. It was prepared by inserting ~ ½ cm of compact filter fibre at the bottom of a 1 mL syringe. One millilitre of Sephadex (Pharmacia, Uppsala, Sweeden) was added to the syringe which was placed in a 15 mL centrifuge tube and centrifuged at 2000 rpm for 2 minutes. Thirty microlitres of water were added to the labelled probe, which was centrifuged through a Sephadex column at 2000 rpm for 2 minutes and collected in a 15 mL centrifuge tube.

To measure RNA band size for pri-miR detected RNA ladder labelling was done using Decade$^{TM}$ Marker System (Life Technologies, NY, USA). The decade marker was prepared in a nuclease free tube, by mixing the following components: 1 µl Decade marker RNA (100 ng), 6 µl nuclease free water, 1 µl 10 × Kinase reaction buffer A, 1 µl ATP, γ-$^{32}$P (≥3000 Ci/mmol), and 1 µl T4 Polynucleotide Kinase. The mixture was incubated at 37 °C for an hour. Before incubating for another 5 minutes at RT, eight microlitres nuclease-free water and 2 µl 10 × Cleavage reagents were added. Thereafter 20 × Gel Loading buffer was added before the mixture was heated at 95 °C for 5 minutes. The decade marker was stored at -20 °C for later use, wherein an appropriate volume was denatured at 95 °C for 5 minutes before loading on the gel.

### 2.11.3. Running a gel, blotting, UV crosslinking and hybridisation

To resolve the RNA, a 15 % gel was prepared and poured a day before use. The 60 mL solution consisted of Bis-acrylamide: acrylamide at 1: 19 (0.45 g and 8.55 g),

28.8 g Urea, and 6 mL 10 × TBE (Appendix 2 c) at pH 8. The solution was allowed to cool down to room temperature before gently mixing with 25 µl Tetraacetylethylenediamine [TEMED, Sigma, MO, USA)] and freshly made 250 µl of 1 % Ammonium per sulphate (Appendix A, 4 h). The solution was poured immediately into the gel casting apparatus and left overnight to solidify. Prior to loading samples, 500 mL of 0.5 × TBE was used to run the gel at 200V for 30 minutes. After loading the samples, the gel was run for 5 – 6 hours at the same voltage in a cold room maintained at 4 °C. To blot the gel onto a membrane, six pieces of thick filter paper were cut to dimensions of 15.5 cm × 15.2 cm. The Hybond$^{TM}$ positively charged nylon membrane was cut to dimensions for 15.5 cm × 15 cm. The filters and nylon membrane were all soaked in ethidium bromide (10 µL/1000 mL) enriched running buffer. Thereafter, a sandwich with 3 filter papers, membrane, then gel, then 3 filters papers were prepared and placed in a semi-dry blotter. Blotting was carried out with electric current set above 100 volts (V) and at 0.767 Amplitude (A).

UV crosslinking of the RNA to nylon membrane was carried out to fix RNA to the membrane using a UV cross linker machine at 200,000 $\mu$ J/cm$^2$ of energy. The ladder was cut out and exposed to imaging plates (IPs) nylon membrane baked at 80 °C for an hour. Thereafter, 10 mL rapid hybridisation buffer was heated to 42 °C in a hybridisation bottle before nylon membrane was put in the bottle to soak in buffer while temperature was maintained for 20 minutes. Before use, radiolabelled probes were heat denatured for 5 minutes at 95 °C and then put on ice. Next, probes were added to the hybridisation buffer soaked nylon membrane in the hybridisation bottle and kept overnight rotating at 42 °C.

### 2.11.4. Membrane washing and visualisation

After washing the membrane once with 50 mL 5 × SSC and 0.1% SDS (Appendix A, 4 c) at RT for 20 minutes then twice with 50 mL 1 × SSC and 0.1% SDS at 42 °C for 15 minutes, nylon membrane was covered with plastic, then exposed to the IPs while kept in the dark for 7 days before images were detected using a Phosphoimager FLA-700 (Fujifilm, Tokyo, Japan).

## 2.12 *In vitro* luciferase activity assay and *in vivo* bioluminescence imaging

To assess for transgene expression *in vitro* Huh7 cells were infected with rAAVs expressing nano-luciferase (**Section 2.10**) and luciferase assay conducted using Nano-Glo® Luciferase according to manufacturer's protocol (Promega, WI, USA). Briefly, the ratio of Luciferase Assay Reagent (LAR) to sample used was 1:1 and 10 µL final sample volume was used. Nano-Glo substrate® was diluted into 50 volumes of Nano-Glo buffer® to make required LAR. Luminescence readings were taken three minutes after adding LAR to sample using the Veritas Microplate luminometer (Turner Biosystems, CA, USA).

To assess the expression of nano-luciferase *in vivo* after mice were injected with a single dose of rAAVs expressing nano-luciferase (**Section 2.10**), mice were anesthetised and injected intraperitoneally with Nano-Glo® Luciferase Assay substrate. Five minutes later, bioluminescence imaging using IVIS Kinetic Bioluminescence imager (PerkinElmer, MA, USA) was performed.

## 2.13 Determination of HBV gene silencing by Dual luciferase assay

For *in vitro* gene silencing, Huh7 cells were transfected with plasmids (**Section 2.8.2**) and infected with rAAVs (**Section 2.10**). Dual luciferase assay was performed using Dual-Luciferase® Reporter 1000 Assay System (Promega, WI, USA) according to manufacturer's protocol. Briefly, after 48 hours post rAAV infection, supernatant was removed and cells lysed using 100 µl of 1 × Lysis buffer per well. Cell lysates harvested, and 24-well plate placed on the shaker and agitated for 15 minutes. Ten microlitres of each sample was transferred to luminometer microplate and luminescence measured by Veritas Microplate luminometer (Turner Biosystems, CA, USA) dispensing 50 µl of Luciferase Assay Buffer II into each well followed by STOP and GLO substrate.

## 2.14 Determination of HBV gene silencing by ELISA

For *in vitro* gene silencing determination by ELISA, Huh7 cells were transfected with plasmids (**Section 2.8.2**) and then infected with rAAVs (**Section 2.10**). At 48 and 72 hours post infection, 100 µl supernatant per well was collected. Knockdown of HBV antigen secretion was assessed by measuring the secretion of HBV surface antigen (HBsAg) in the culture supernatants using Monolisa® Ag HBs Plus immunoassay kit (Bio-Rad, CA, USA) according to manufacturer's protocol. Briefly, 50 µl of conjugate working solution (R6+ R7) was added to each sample collected (100 µl of supernatant per well) in a microplate well. The plate was covered with adhesive film and incubated for ~ 90 minutes.

After removing the adhesive film, 5 × washing cycles using 375 µl washing solution were carried out. One hundred microlitres of chromogen development solution (R8 + R9) were added to sample wells and the reaction allowed to develop in the dark for ~ 30 minutes before adding a STOPPING solution. After 4 minutes, optical density at 490/655 nm was measured using a plate reader (BioRad, IN, USA). For *in vivo* gene silencing assessment, blood samples were collected by retro-orbital puncture at time points: 0 (pre-injection), 2, 4, 8, 12, and 16 weeks post-injection and 2:100 diluted serum HBsAg measured using Monolisa® Ag HBs Plus immunoassay kit (Bio-Rad, CA, USA) as described above.

## 2.15 Inflammatory and toxicity tests

### 2.15.1 Cytometric bead array

Five mice per group received intravenous injections of $1\times10^{11}$ rAAV viral particles or saline. Six hours after injections, blood samples were collected by retro-orbital puncture. Induction of inflammatory immune response was assessed by measuring the serum concentration of inflammation markers: interleukin 6 (IL-6), interleukin 10 (IL-10), monocyte chemoattractant protein-1 (MCP-1), interferon gamma (IFN-γ), tumour necrosis alpha (TNF-α) and interleukin 12p70 (IL-12p70) using a cytometric bead array mouse inflammation kit (BD Biosciences, CA) according to the manufacturer's instructions. Fifty microlitres of serially diluted standards and undiluted serum samples were added in to sample tubes containing 50 µl of mouse inflammation capture bead mix. Then 1 mL of Wash buffer was added to each assay tube and centrifuged at 1660 rpm for 5 minutes to pellet the capture beads. Careful aspiration and discarding of supernatant was carried out to avoid disturbing the capture bead pellet. To resuspend the bead pellet, 300 µl of Wash buffer were added

to each assay tube. CBA reactions were processed by Fortessa FSR flow cytometer using a BD FACSDiva software and data analysed using FCAP Array software 3.0 (BD Biosciences, CA).

### 2.15.2 Serum alanine transferase activity assay

To assess liver toxicity, serum alanine transferase (ALT) was measured. Seven mice per group were injected intravenously with saline or with single dose of $1\times 10^{11}$ rAAV viral particles [rAAV8-122/5 or rAnc80L65-122/5 or rAAV8-EMPTY or rAnc80L65-EMPTY] (**Table 2.2**). Blood was collected from mice by retro-orbital puncture before, and at 1, 2, 4, 6 and 8 weeks after injection. Serum ALT activity was assessed using a kinetic assay on an automated photometric analyser (Roche Diagnostics, Rotkreuz, Switzerland) by the South African National Health Laboratory Services.

# CHAPTER 3: RESULTS

The current study breaks new ground by investigating the suitability of an ancestral AAV vector (Anc80L65) to deliver RNAi-based therapeutics to chronically infected hepatocytes in terms of efficacy and safety. It also sought to corroborate findings from previous studies on Anc80L65 transduction efficiency. The results section describes data from rAAV production, assessment of Anc80L65 transduction efficiency, HBV knockdown assessment and assessment of Anc80L65 safety.

## 3.1 Characterisation of plasmids for rAAV vector production

To assess the integrity of the plasmids used for AAV production, restriction analysis was performed. All plasmids pAAV-122/5, pAAV-NLuc, pAAV2, pAAV8, pAnc80L65, pAd-helper were digested with multiple cutter restriction enzymes showed expected number of bands and base pair sizes, (**Figure 3.1**). Digestion of pAAV-122/5 with either *Bgl*II and SacI or *Pst*I yielded the following base pair sizes, 3041, 1039, 653, 174, 91 or 3052, 930, 508, 254, 163 and 91, respectively. Restricting pAAV-NLuc with either *Bgl*II and SacI or *Pst*I enzymes yielded the following base pair sizes, 3041, 1000, 661, 432, 174 or 3952, 1323, 508, 262, and 163, respectively. The inverted terminal repeats are essential for AAV genome packaging and the presence of 163 or 174 base pair sizes after restriction enzyme analysis of pAAV-122/5 and pAAV-NLuc plasmids indicate presence of ITR2 or ITR4 respectively (**Figure 3.1 a, b**). Capsid plasmids pAAV2 or pAAV8 or pAnc80L65 were restricted with *Pst*I or *BamH*I or *Dra*I enzymes, yielding base pair sizes, 3175, 2300, 1462, 223, 153 or 4192, 2778, 352 or 3846, 3851, 19 (off the gel), respectively, (**Figure 3.1 b, c, d**).

Partial digestion of pAAV8 by *BamH*I resulted in an extra top band [lane 3], therefore showing four bands instead of expected three (**Figure 3.1 b**). Helper plasmid pAd-helper restricted with *Dra*I enzyme yielded base pair sizes 892, 832, 700 and 59, (**Figure 3.1 d**).

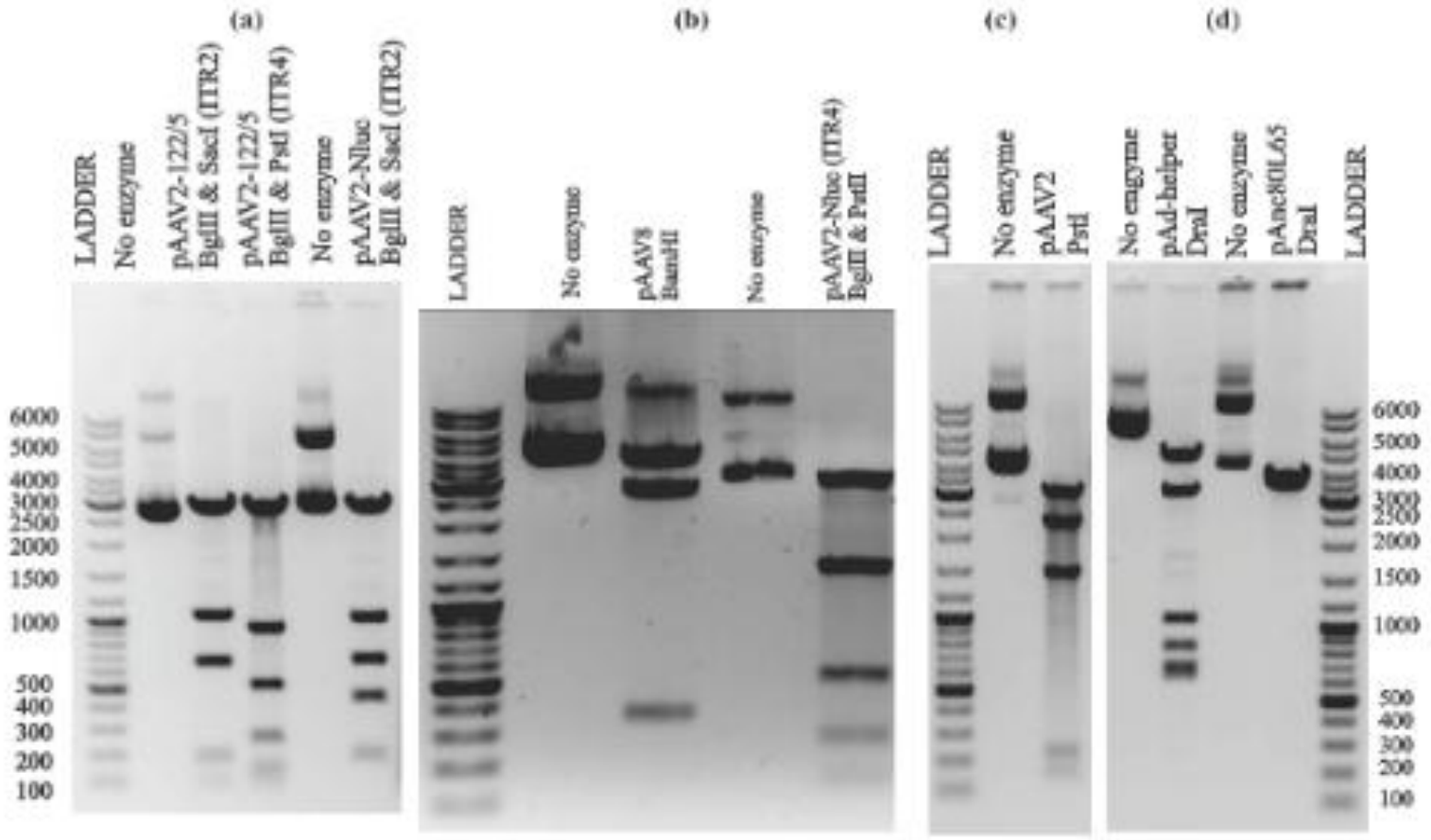


**Figure 3.1 Plasmid characterisation in preparation for large-scale viral AAV vector production.** (a) – (d) Gel electrophoresis images depicting undigested or digested plasmid DNA by various restriction enzymes. Plasmid names and enzymes are indicated at top of gel, with ladder band sizes either on the sides of far left or right lanes. No enzyme denotes undigested DNA.

## 3.2 Large-scale production of recombinant Adeno-associated viral vectors (rAAV)

To produce rAAV2 and rAAV8 vectors in quantities enough for *in vitro* and *in vivo* studies, a triple transfection of HEK293T cells with plasmids (pAAV-122/5 or pAAV-NLuc, pAd-helper, pAAV2 or pAAV8) was performed. To produce enough Anc80L65 vectors, a quadruple transfection with pAAV-122/5 or pAAV-NLuc, pAd-helper, pAnc80L65 and a plasmid expressing AAV2 assembly activating protein (pAAP2) was included to enhance packaging efficiency (Zinn et al., 2015).

Vectors of serotype AAV2, AAV8 and Anc80L65 expressing anti-HBV sequence (miR-122/5), or reporter gene nano-luciferase (NLuc) from a liver specific promoter, mouse transthyretin (mTTR) were successfully produced in large scale **(Table 3.1)**. AAV2 and AAV8 vectors served as positive controls for *in vitro* and *in vivo* experiments respectively. The recombinant AAV vectors with no transgene were also produced in large-scale as controls. The viral titres for different rAAV vectors (rAnc80L65, rAAV8 and rAAV2) expressing a transgene varied with rAAV8 recording higher titres followed by rAAV2 vectors. Titres of the rAAV2 and rAAV8 empty vectors were consistently lower followed by NLuc expressing vectors. As expected, the addition of pAAP2 in production protocol caused an increase in Anc80L65 production titres **(Table 3.1)**. The amounts of VPs produced for all vectors were sufficient for purpose of this study (**Table 3.1**)

# TABLE 3.1: Recombinant AAV vector titres determined by qPCR

| **First Batch** | | | |
|---|---|---|---|
| **rAAV vectors** | **Averages (VPs/mL)** | **Volume extracted (mL)** | **Total VPs** |
| rAAV2-122/5 | 3,14E+12 | 1.000 | 3,14E+12 |
| rAAV2-NLuc | 2,06E+12 | 1.050 | 2,163E+12 |
| rAAV2-EMPTY | 1,93E+12 | 1.100 | 2,123E+12 |
| | | | |
| rAAV8-122/5 | 1,78E+13 | 1.100 | 1,958E+13 |
| rAAV8-NLuc | 1,39E+13 | 1.000 | 1,39E+13 |
| rAAV8-EMPTY | 1,03E+13 | 1.100 | 1,133E+13 |
| | | | |
| rAnc80L65-122/5 | 1,67E+11 | 0.850 | 1,4195E+11 |
| rAnc80L65-NLuc | 3,75E+09 | 0.900 | 3,375E+09 |
| rAnc80L65-EMPTY | 4,28E+09 | 0.850 | 3,6438E+09 |

| **rAnc80L65 second batch with pAAP2 included** | | | |
|---|---|---|---|
| **rAAV vectors** | **Averages (VP/mL)** | **Volume extracted (mL)** | **Total VPs** |
| rAnc80L65-122/5 | 1,867E+12 | 1.000 | 1,867E+12 |
| rAnc80L65-NLuc | 4,825E+12 | 1.000 | 4,825E+12 |
| rAnc80L65-EMPTY | 1,152E+12 | 1.000 | 1,152E+12 |

**VPs: viral particles**

**Total VPs = VPs/mL × total volume (mL) extracted**

## 3.3 AAV transduction efficiency *in vitro* and *in vivo*

To assess the efficiency of AAV vectors to transduce liver-derived cells in culture, Huh7 cells were infected with rAAV expressing luciferase (rAAV2-NLuc or rAnc80L65-NLuc) or control empty vectors (rAAV2-EMPTY or rAnc80L65-EMPTY) at multiplicity of infection (MOI) of $10^5$. After 48 hours, luciferase assays were performed. The luciferase expression of ~1.4 times higher was observed in cells treated with rAnc80L65-NLuc compared to rAAV2-NLuc. As expected, luciferase activity from cells infected with rAAV2-EMPTY or rAnc80L65-EMPTY controls was not detected (**Figure 3.2**). These results suggested that Anc80L65 can transduce liver cells more efficiently. Furthermore, to assess whether the effects observed in cell culture could be replicated *in vivo* as well as to assess long term luciferase expression, four groups of three mice were injected with $1 \times 10^{11}$ per mouse of rAAV2-NLuc or rAnc80L65-NLuc or respective control empty vectors. Bioluminescence measurements were then performed over 12 weeks.

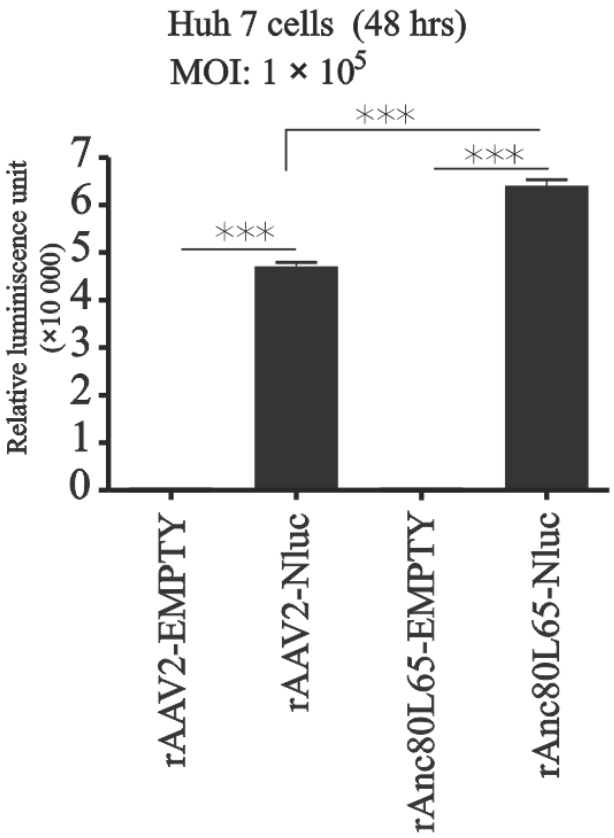


**Figure 3.2 Culture transduction by rAnc80L65 and rAAV2.** Luminescence reading from Huh7 cells infected with nano-luciferase expressing rAAVs at MOI of $10^5$ was taken after 48 hours, n = 3. *P*-values ≤ 0.0001 (***) were regarded as statistically significant. Results obtained were normalised to the negative control, and comparisons made relative to controls.

The bioluminescence imaging of live animals revealed high levels of NLuc expression in the liver from both rAAV2-NLuc and rAnc80L65-NLuc during the 12-week observation. However, there was no statistical difference of NLuc expression between the two vectors. As expected, bioluminescence was not detected in mice treated with empty vector controls. Transgene expression from both rAnc80L65-NLuc and rAAV8-NLuc viral vectors was constant over an 8 week period, decreasing significantly at 12 weeks post injection (**Figure 3.3, 3.4**). The similar pattern of transgene expression by rAnc80L65-NLuc and rAAV8-NLuc pointed to similar

transduction efficiency by both vectors in mice. This is therefore contradictory to the enhanced *in vitro* transduction efficiency by rAnc80L65-NLuc (**Figure 3.2**).

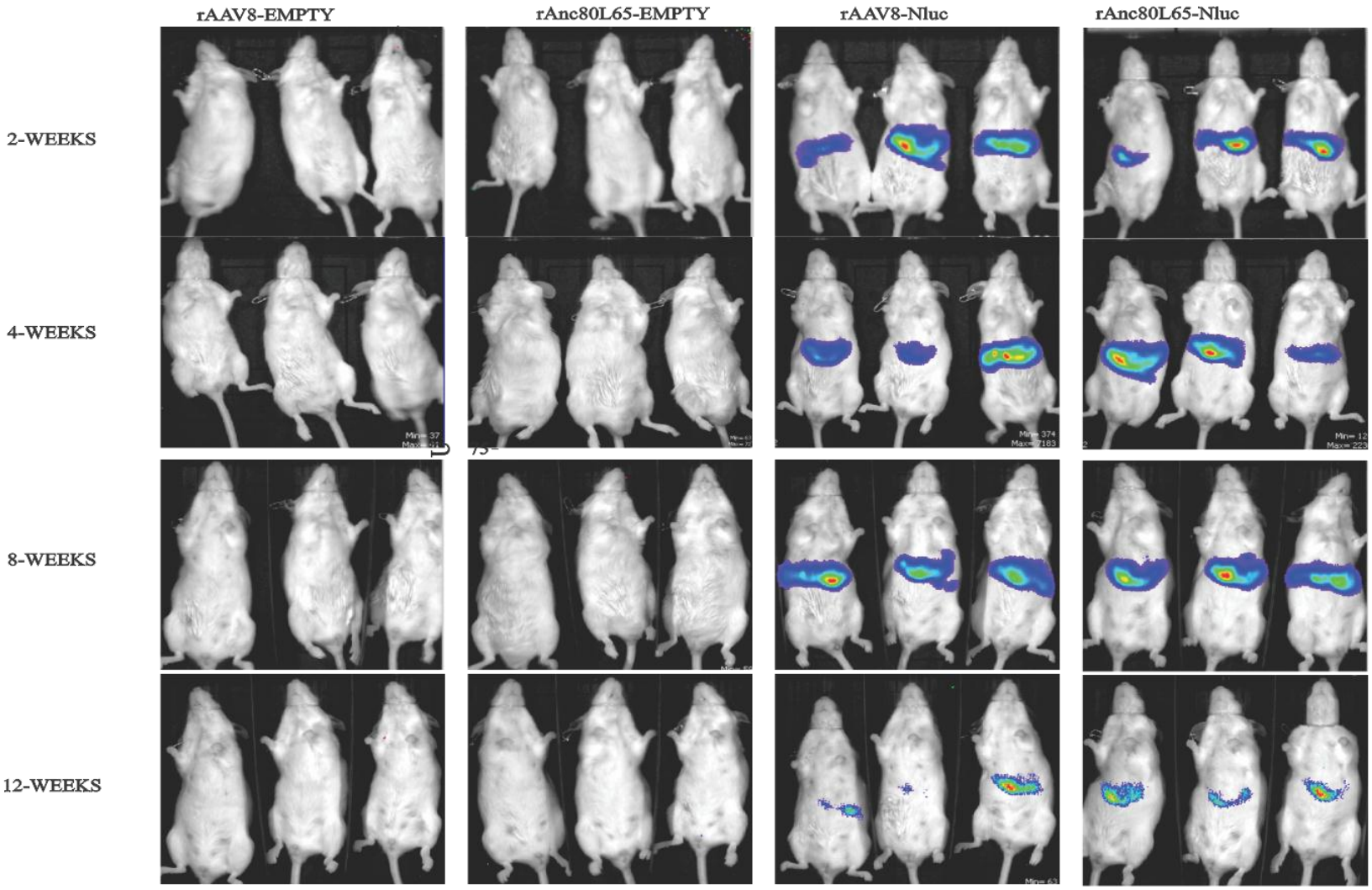


**Figure 3.3 Hepatic NLuc expression from rAnc80L65 in mice.** Luminescence emission was recorded using a bioluminescence imager after 60 seconds of exposure of mice that received nano-luciferase expressing rAAVs or empty control vectors over 12 weeks post infection.

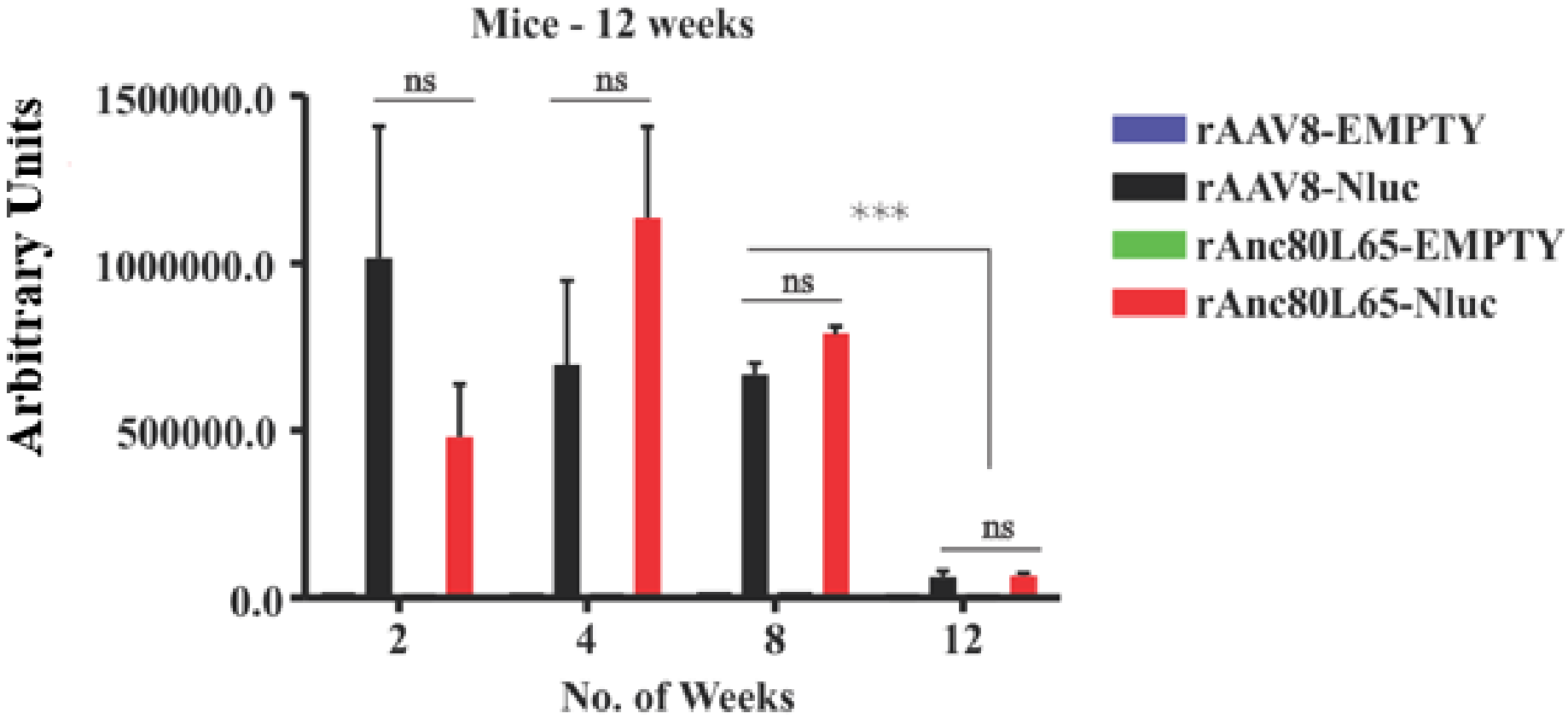


**Figure 3.4 Bioluminescence quantification in mice that received NLuc expressing rAAVs.** Photon counts from mice were calculated using bioluminescence imager software for week 2, 4, 8 and 12. The +-SEM was derived from, n = 3 samples per group. *P*-values ≥ 0.05 (not significant, ns) was regarded as statistically insignificant, *P*-values ≤ 0.0001 (***) were regarded as statistically significant.

The steady transgene expression by rAnc80L65-NLuc over an 8 week period confirmed earlier findings that in silico constructed Anc80L65 was capable of efficiently transducing liver cells and expressing transgenes (Zinn et al., 2015).

Next, we sought to evaluate whether rAAV8 or rAnc80L65 expressing anti-HBV primary microRNA could inhibit HBV replication.

## 3.4 Assessment of anti-HBV pri-miR expression and HBV gene expression inhibition *in vitro*.

To assess AAV mediated pri-miR-122/5 expression and processing in liver derived cells, Northern blot was performed. RNA samples used in the blot were extracted from Huh7 cells infected with rAAV2-122/5 or rAnc80L65-122/5 or empty control (rAnc80L65-EMPTY). The radioactively probe against guide 5 was used to detect RNA species produced. RNA isolated from pri-miR 122/5 expressing adenoviral vector [HD Ad HB pri-miR 122/5, (Mowa et al., 2012)] infected Huh 7 cells was included as a positive control. The RNA bands on the gel were of expected size of ~ 22 nucleotides, which correspond to the size of the predicted mature miR. The absence of larger bands denotes complete processing of pri or pre-miR to mature miR. Both rAnc80L65-122/5 and rAAV2-122/5 exhibited anti-HBV sequence expression, though a signal from rAnc80L65-122/5 infected cells was much weaker. No radioactive signal was detected from RNA isolated from empty vector infected cells (**Figure 3.5**). The blot results shows that both rAnc80L65-122/5 and rAAV2-122/5 vectors can transduce cells and express pri-miR122/5, which then enters the endogenous RNAi pathway to be processed in to mature miRs.

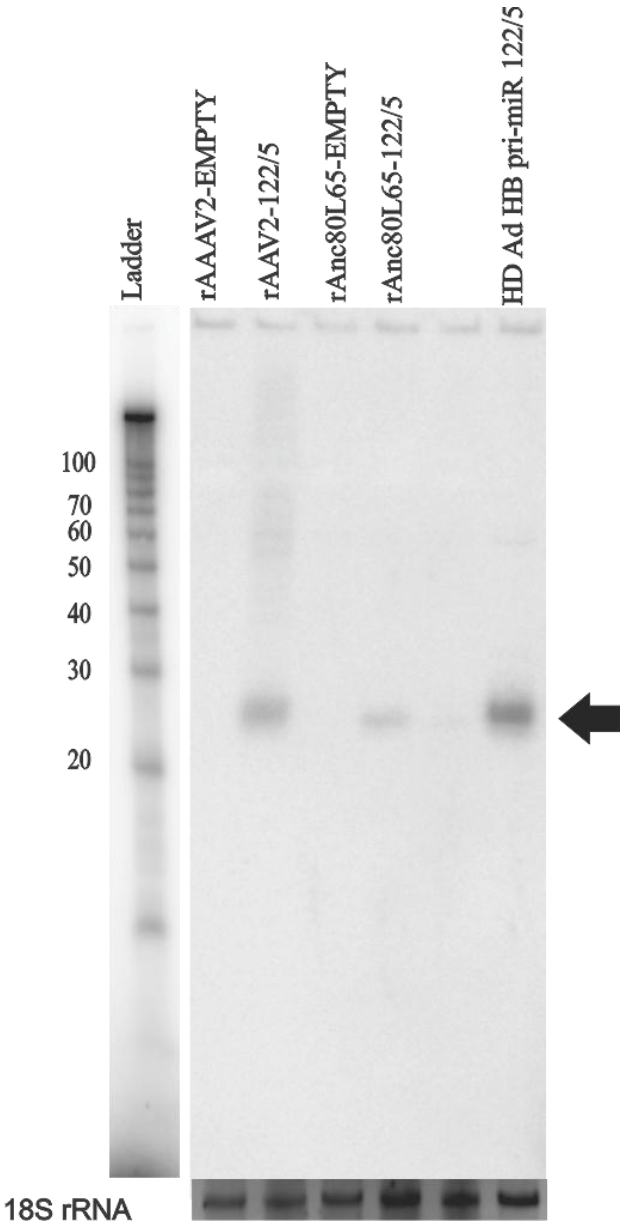


**Figure 3.5 Pri-miR expression and processing in rAAV infected Huh7 cells**. RNA samples isolated from Huh 7 cells infected with rAnc80L65-122/5 or rAAV2-122/5 or empty control (rAnc80L65EMPTY or rAAV2EMPTY ) or positive control (HD Ad HB pri-miR 122/5) vectors were ran on an PAGE gel and detected by radioactively labelled (ATP, γ-$^{32}$P) 5' OH RNA oligonucleotides complementary to miR-122/5 sequence. The arrow points to the mature miR bands, and 18SrRNA was used as input loading control

Because of the ease with which a luciferase assay can be performed, the ability of rAAV vectors encoding anti-HBV miR-122/5 to target HBV *X* gene was assessed by first transfecting liver derived Huh7 cell line with a dual reporter plasmid psiCHECK.*HBx* (Ely et al., 2009). The psiCHECK.*HBx* plasmid has *Firefly* luciferase

and downstream of *Renilla* luciferase contains an intact *HBx* ORF, which includes the target of miR-122/5. Luminiscence produced by *Firefly* luciferase was used to relativise *Renilla* luciferase activity. Following transfection, cells were infected with empty control (rAAV2-EMPTY or rAnc80L65-EMPTY) or miR-122/5 expressing rAAV2-122/5 or rAnc80L65-122/5 vectors at MOI $1 \times 10^5$. After 48 hours, lysates were used for luciferase assay. Unexpectedly and despite positive miR-122/5 expression detected by Northern blots (**Figure 3.5**)**,** both viral vectors encoding anti-HBV miR sequences did not effect HBV gene silencing in relation to controls (**Figure 3.6**)**.** We speculated that the luciferase assay was not sensitive enough to detect the minimal HBV knockdown differences in relation to empty vector controls at the dose used. Hence we opted to assess HBV knockdown using ELISA, at a higher MOI of $1 \times 10^6$.

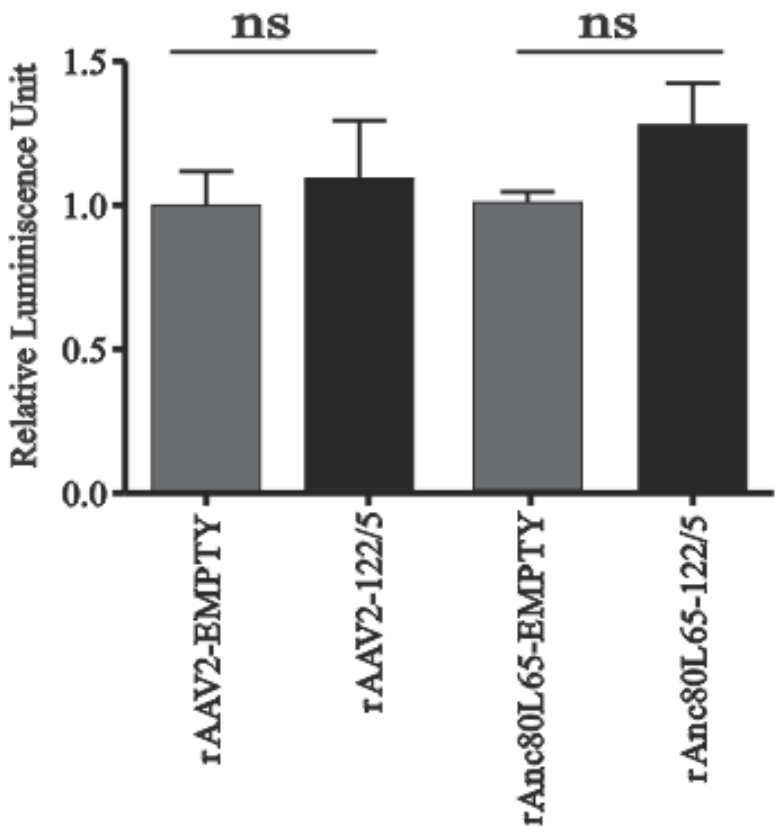


**Figure 3.6 Assessment of HBV gene silencing by luciferase assay.** Huh7 cells were transfected with a dual reporter plasmid psiCHECK.*HBx*. Later cells were infected with empty control (rAAV2-EMPTY or rAnc80L65-EMPTY) or miR-122/5 expressing rAAV2-122/5 or rAnc80L65-122/5 vectors at an MOI 1 × $10^5$. The quantification data shown was normalised to respective empty control of each transgene carrying vector at 48 hours post infection with rAAV vectors. *P*-values ≥ 0.05 (not significant, ns) were regarded as statistically insignificant. The +-SEM was derived from n = 3 samples per group.

ELISA essay was performed with supernatants from Huh 7 cells transfected with pcH9/3901 target plasmid and infected with AAVs at an MOI of 1 × $10^5$ or $10^6$. Gene silencing effects of rAAV vectors were then assed at 48 and 72 hours. Cells treated at a higher dose of rAAV2-122/5 showed a significant knockdown of ~55 and 25% at 48 and 72 hours respectively, which was dose dependent (**Figure 3.7 a, b**). This (was expected as AAV2 serotype is renowned for transducing cells efficiently *in vitro*.

Higher rAnc80L65-122/5 dose produced a moderate but significant HBV surface antigen (HBsAg) level knockdown of about 25 % after 48 hours (**Figure 3.7 a**).

However, after 72 hours, the knockdown effect produced was completely abolished. At a lower dose, no gene silencing effect was observed for rAnc80L65-122/5 after both 48 and 72 hours in relation to empty controls (**Figure 3.7 a, b**)**,** a result also observed previously with luciferase knockdown assay (**Figure 3.6**). These results also corroborate the poor transgene expression after Northern blot analysis following use of rAnc80L65-122/5 to transduce cultured (**Figure 3.5**). Both the knockdown assays and Northern blotting suggests a poor *in vitro* cell transduction by Anc80L65. However, this does not agree with the NLuc expression from Anc80L65 experiments (**Figure 3. 2**), which could be a result of the differences between assays. AAV8 serotype is also known for poorly transducing cells *in vitro,* while it is quite efficient *in vivo* (Chen et al., 2009, Maepa et al., 2017, Zincarelli et al., 2008). We speculated that AAV8's close phylogenetic relationship to Anc80L65 (Zinn et al., 2015) might explain rAnc80L65-122/5 poor transduction efficiency *in vitro*. Collectively these results suggested that rAnc80L65-122/5 could transduce cells, express the gene of interest and transiently effect HBV gene expression inhibition in a dose dependent manner in culture. However, the effect was lower than that observed with rAAV2.

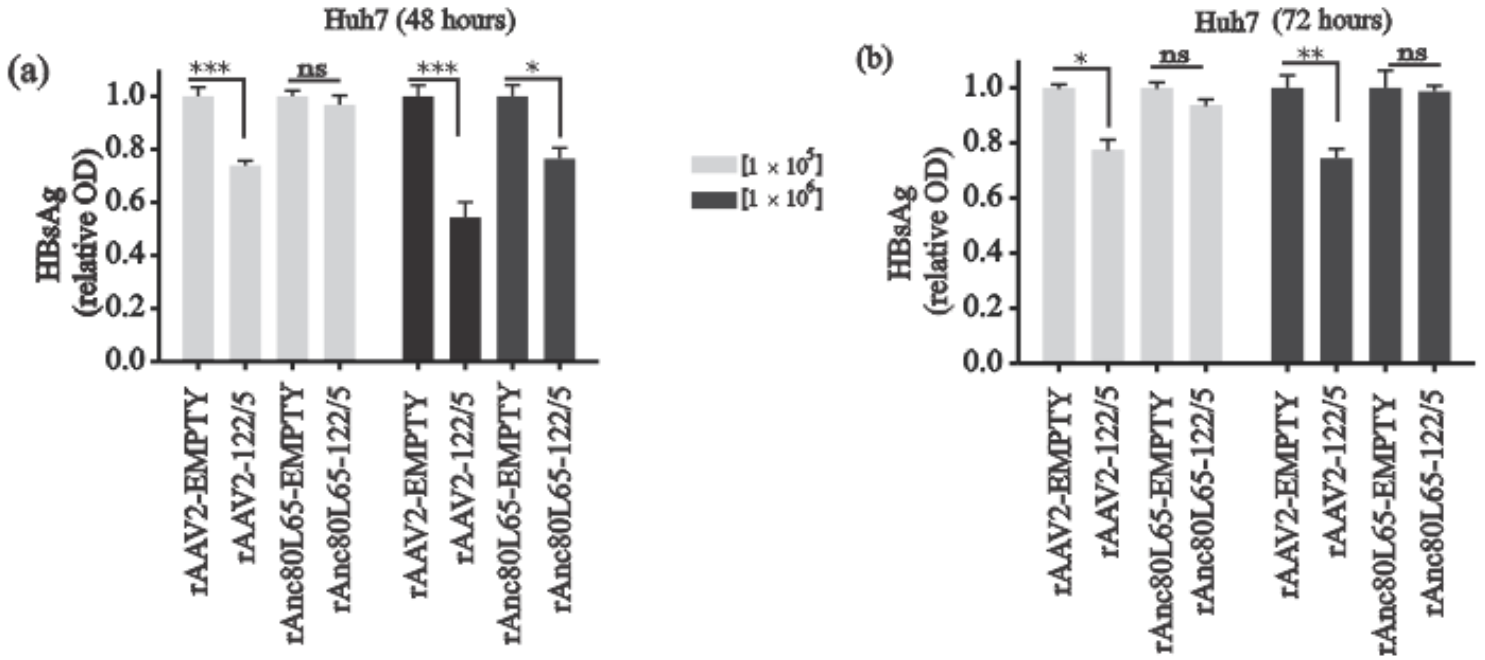


**Figure 3.7 HBV gene knockdown from Huh7 cells infected with rAAV vectors.** Samples were treated with HBV replication compented plasmid (pcH9/3901) then rAAV vectors encoding anti-HBV rAAV2-122/5 or rAnc80L65-122/5) transgene or no transgene (rAAV2-EMPTY or rAnc80L65-EMPTY), and ELISA was performed at timepoints of 48, and 72 hours. Data shown is relative to respective viral vector empty control. The +-SEM was derived from n = 3 samples per group. *P*-values ≤ 0.05 (*), ≤ 0.001 (**) and ≤ 0.0001 (***) were regarded as statistically significant. P-values ≥ 0.05 (not significant, ns) were regarded as statistically insignificant.

## 3.5 Assessment inhibition of HBV replication *in vivo*

To assess suppression of HBV replication *in vivo* gene expression suppression by five groups of five HBV transgenic mice were injected with rAAV vectors or saline. The rAAV vectors injected either expressed anti-HBV miR-122/5 transgene (rAAV8-122/5 or rAnc80L65-122/5), or were empty vectors (rAAV8-EMPTY or rAnc80L65-122/5). In relation to empty vector controls, both rAAVs encoding anti-HBV sequence effected a sustained, and significant HBsAg knockdown with about 50 % knockdown observed as early as the first week after treatment. This improved to about 70 % at four weeks post injection. HBV gene silencing was sustained over the 16 weeks observation period (**Figure 3.8**). Interestingly, unlike the case in cultured cells where rAAV2 was better than Anc80L65 (**Figure 3.7**), the efficacy of both anti-HBV rAAVs *in vivo* was indistinguishable from each other. This suggests that both rAnc80L65-122/5 and rAAV8-122/5 were equally competent at liver tissue transduction and transgene expression. Collectively these results show for the first time that the ancestral AAV vector can efficiently transduce mouse hepatocytes and inhibit HBV replication. Next, we aimed to assess the safely of the AAVs used in this study.

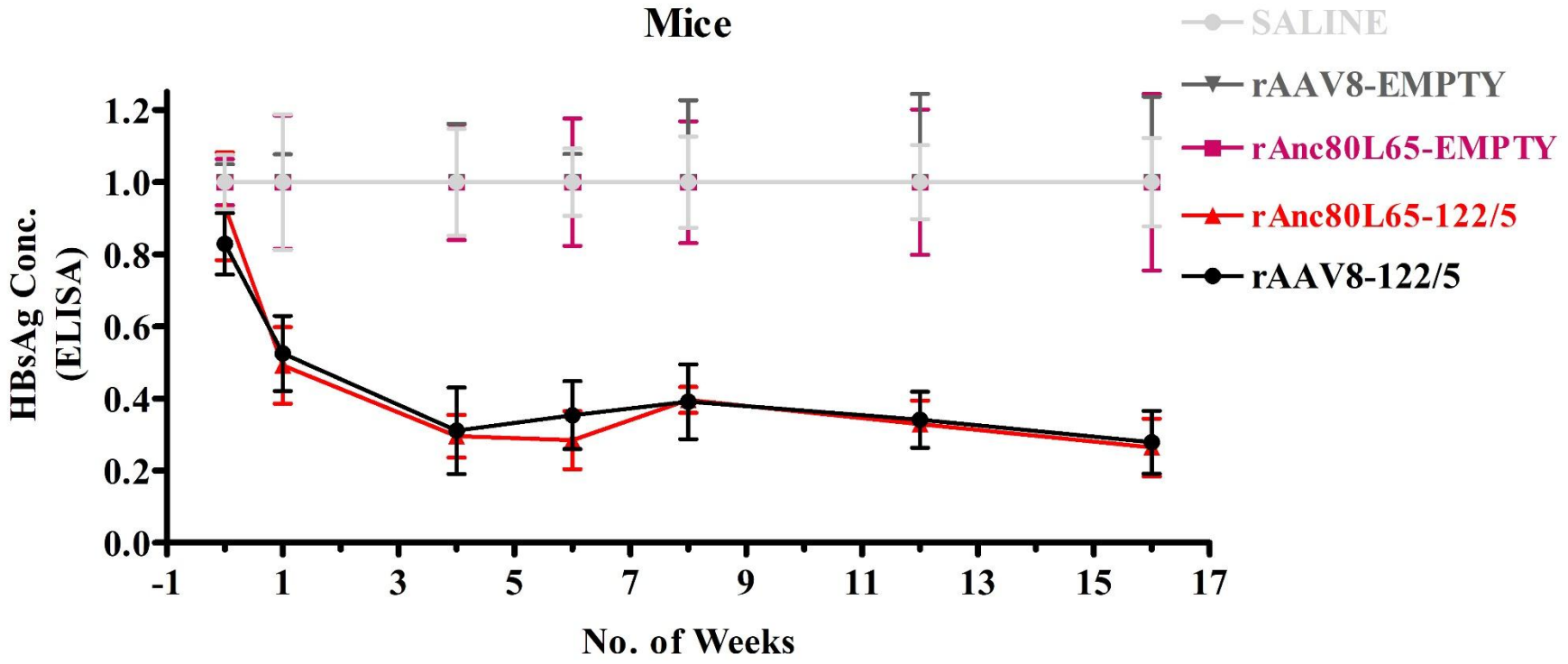


**Figure 3.8 HBV gene silencing in mice infected with rAAV vectors.** Serum samples were obtained from mice treated with rAAV vectors and HBsAg levels assessed weekly for the 1st month and monthly up to four months by ELISA. The +-SEM was derived from n = 5 mice per group. *P*-values ≤ 0.05 (*) were regarded as statistically significant. Data shown here are relative to empty viral vector.

## 3.6 Assessment of rAAV vector inflammatory and toxic effects

RNAi activators and viral infections have been implicated in stimulating inflammatory response leading to cytokine production in mammalian systems (Osterlund et al., 2005, Sioud, 2005). To assess the safety of rAAVs used here, we first determined the inflammatory response to AAVs in mice by quantifying serum IL-12p70, IFN-γ, MCP-1, TNF, IL-10 and IL-6 cytokine levels using cytometric bead array. Mice treated with rAAV vectors revealed IL-12p70, IFN-γ, TNF, IL-10 and IL-6 levels that were not statistical different to mice treated with saline (**Figure 3.9 a, b, c, e, f**) There was a MCP-1 cytokine induction from viral vectors rAAV8-122/5, rAnc80L65-122/5 and rAnc80L65-EMPTY when compared to saline, but rAAV8-EMPTY was an exception (**Figure 3.9 d**). This suggests that anti-HBV RNAi sequence and Anc80L65 capsids are immunogenic. Poly (I:C) is a synthetic double stranded RNA that can elicit immune response, and was used as a positive control to indicate immune stimulation. As expected all cytokine levels were elevated in Poly (I:C) treated mice with MCP-1, TNF, IL-10 and IL-6 significantly higher (**Figure 3.9 b, d, e, f**).

The liver is an important organ for metabolic reactions and Alanine Aminotransferase (ALT) is an intracellular enzyme involved in amino acid metabolism. Liver tissue destruction following inflammatory response or other hepatocellular stress results in enzyme release into the circulation leading to increased ALT levels in the blood. The elevated ALT blood concentration is therefore associated with liver damage. Furthermore, the oversaturation of the RNAi pathway by polymerase III driven anti-HBV RNAi activators delivered by self-complementary AAV8 (sc-AAV8) has previously resulted in liver toxicity with raised ALT and fatalities in mice (Grimm et

al., 2006). Hence we sought to assess whether rAAVs carrying pri-miR122/5 induced liver damage to compromise the health of animals. Serum ALT activity assay over 2 months and changes in animal weights over four months were monitored. The ALT assay revealed results within the normal range (<100 U/L) in all mice treated with rAAV vectors carrying RNAi activators and controls (**Figure 3.10**). This result suggested absence of liver damage arising from rAAVs mediated anti-HBV miR-122/5 delivery or expression. Moreover, the weights of animals remained stable after anti-HBV miR-122/5 administration and similar to weights of animals infected with either empty controls or saline (**Figure 3.11**). Thus, the MCP-1 induced expression did not result in overt physiological stress in the mice as result of infection with rAAV vectors. Only 3 mice died for reasons unrelated to the study, the remainder showed signs of good health, were consuming food normally and were physically active throughout the period of study.

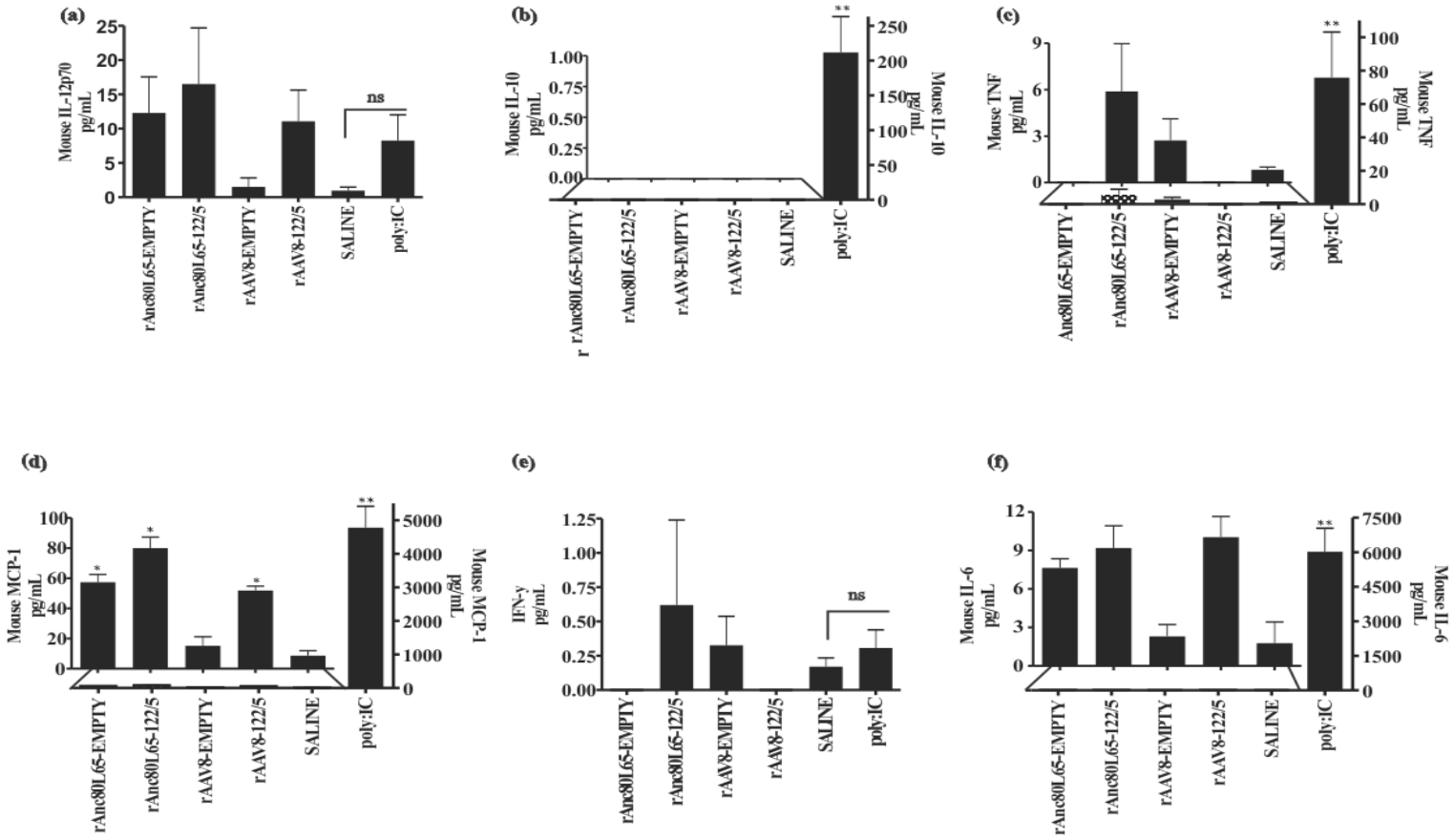


**Figure 3.9 Evaluation of cytokine expression induction in HBV transgenic mice post intravenous administration of rAAVs.** (a)-(f) Concentration of IL-12p70 (a), IL-10 γ (b), TNF (c), MCP-1 (d), IFN- (e), IL-6 (f). The quantification of cytokines was carried out 6 hours after injection of mice with either rAAV indicated or saline or poly (I:C) by cytometric bead array. Data showed comparison between mice injected with rAAV vectors and saline. Poly (I:C) served as a positive control. The +-SEM was derived from n=3 mice per group. *P*-values ≤ 0.05 (*) or ≤ 0.001 (**) were regarded as statistically significant. *P*-values ≥ 0.05 (ns) were regarded as statistically insignificant.

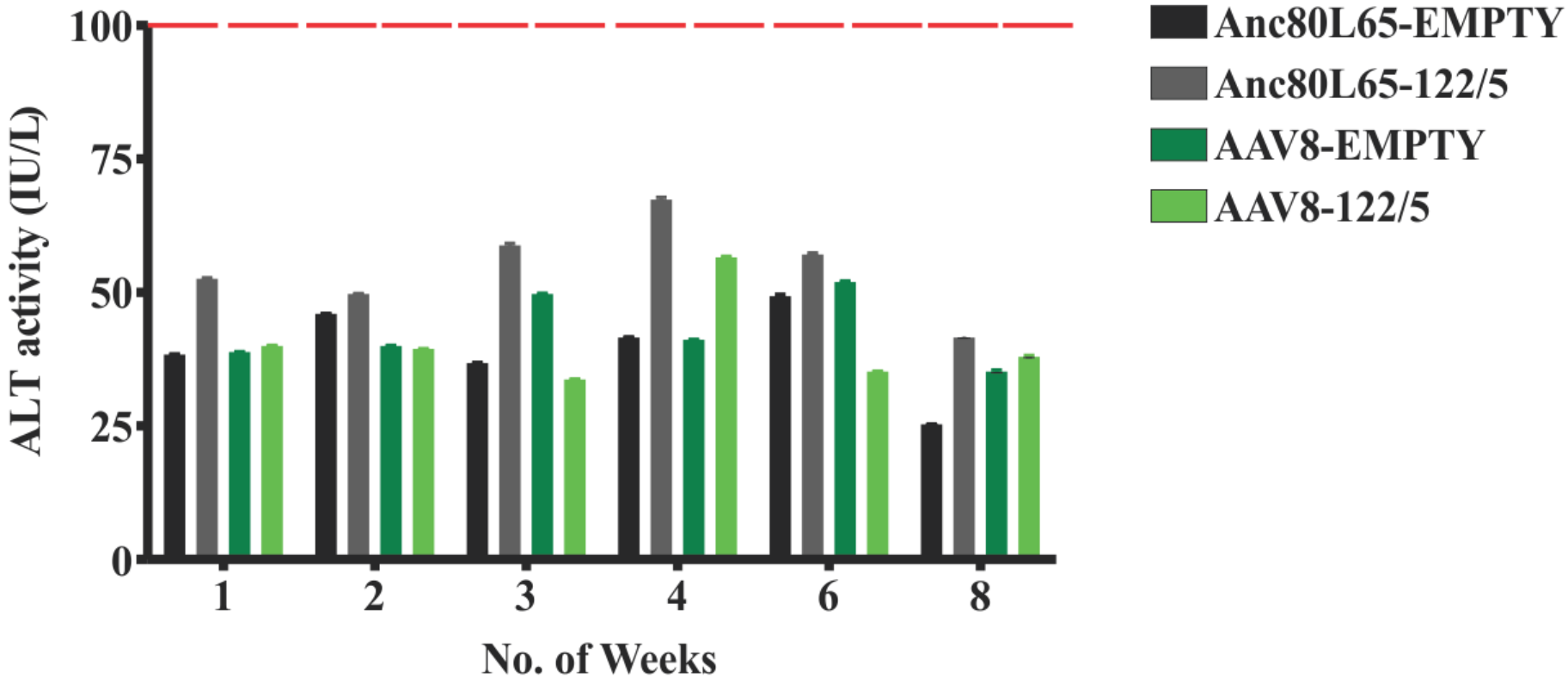


**Figure 3.10 ALT activity assessed from mice serum samples.** Serum collected from mice treated with saline or empty rAAV control (rAAV8-EMPTY or rAnc80L65-EMPTY) or anti-HBV miR-122/5 expressing rAAVs (rAAV8-122/5 or rAnc80L65-122/5 at weeks 1, 2, 3, 4, 6 and 8 were send for ALT activity analysis. Dotted line indicate cut-off for ALT levels indicating healthy liver

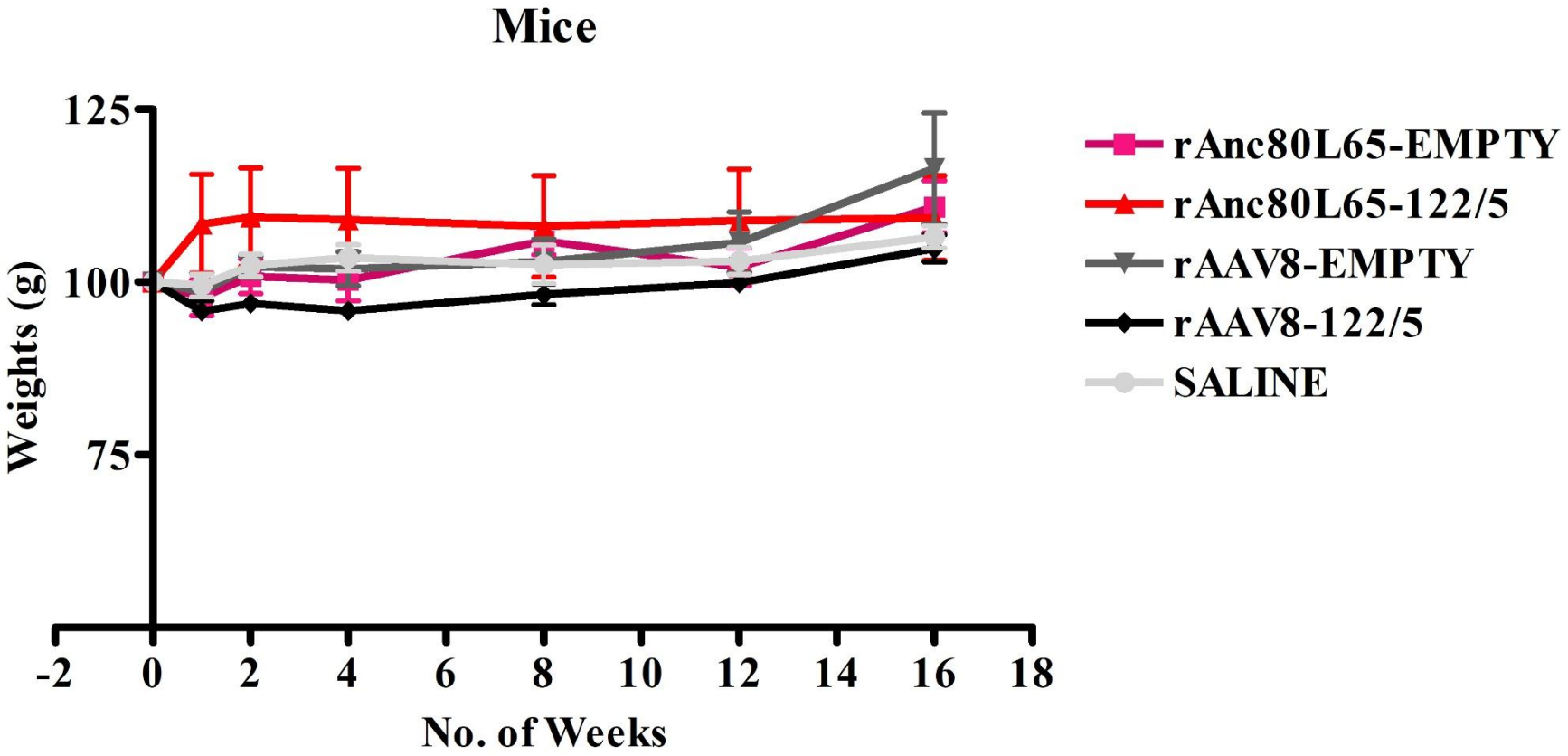


**Figure 3.11 Assessment of changes in weights of mice post rAAV administration.** Normalised weights attained from groups of mice before and after receiving treatment with either empty control (rAAV8-EMPTY or rAnc80L65-EMPTY) or anti-HBV miR-122/5 (rAAV8-122/5 or rAnc80L65-122/5) expressing vectors for a period of 16 weeks are shown. +-SEM indicated by the error bars were derived from values from groups comprising 5 mice each. Data were normalised to the baseline and mice injected with rAAV vectors compared with injected with saline.

# CHAPTER 4: DISCUSSION

Chronic hepatitis B viral infection remains a global challenge despite the presence of an effective anti-HBV vaccine, and use of currently licenced anti-HBV drugs. These drugs require life-long administration, treatment withdrawal and schedule non-adherence are associated with HBV rebounding and drug resistance. Alternative therapeutic approaches are being explored and perfected to treat this infection more effectively. Reprogramming of the RNA interference strategy has been applied previously as a strategy to inhibit HBV replication (Carmona et al., 2006, Chen et al., 2012, Chen et al., 2007, Ely et al., 2009, Ely et al., 2008, McCaffrey et al., 2003). This strategy adopted by current study exploits for therapeutic benefit HBV's genomic arrangement that makes it vulnerable to viral replication cycle interruption by targeting its conserved open reading frames.

Despite demonstrated RNAi efficiency to inhibit HBV replication, an ideal delivery system of RNAi-based treatment to chronically infected hepatocytes remains elusive. AAVs have shown impressive bio-safety profile and efficiency (Cideciyan et al., 2008, Maguire et al., 2008, Mandel, 2010, Nathwani et al., 2011, Rafii et al., 2014). However, the findings that rAAVs elicits immune response, and AAV2- and AAV8-specific antibodies have a high human seroprevalence of 60 and 30% respectively in the African population poses a challenge to achieving effective gene transfer and sustained therapeutic effect (Manno et al, 2006, Calcedo et al., 2009, Calcedo et al., 2011, Nathwani et al., 2011). Recently, AAV ancestral lineage mapping to gain insight on the vector's structural determinants defining its biology and mode of action has led to in silico construction of a synthetic AAV (Anc80L65) capsid possessing

ancient genetic sequence. We therefore postulated that as a result of the ancestral origin of the Anc80L65 capsid, the extant human population was unlikely to have developed Anc80L65 capsid-specific antibodies. Hence, we sought to corroborate earlier findings that the Anc80L65 vector transduced hepatic cells efficiently with a view to investigating its efficacy and safety to deliver anti-HBV RNAi-based therapy to chronically infected hepatocytes.

## 4.1 Large scale recombinant AAV vector production

To conduct the study on the efficacy and safety of AAV vectors to deliver anti-HBV therapy and following the confirmation of AAV production plasmids integrity, the AAV vector production was carried out in mammalian HEK293T cells. This yielded sufficient but varied rAAV titres from different capsids. Titres of the rAAV2 and rAAV8 empty vectors were consistently lower followed by NLuc expressing vectors. Self-complementary AAV vectors package genome size of ~ 2.05 - 2.45 kb optimally and smaller than 2.05 kb or larger than 2.5 kb less efficiently (Dong et al., 1996, Hermonat et al., 1997, Wu et al., 2010). The rAAV2-EMPTY, rAAV2 or rAAV8 expressing NLuc and rAAV2 or rAAV8 expressing miR 122/5 have a genome size of 1.635, 2.068 kb and 2,378respectively. Hence miR 122/5 expressing vectors generally gave the highest titres followed by Nluc expressing vectors and EMPTY vectors gave the lowest titres. Interestingly the rAnc80L65 vectors did not abide to this norm, suggesting a different packaging dynamics for this ancestral capsid (**Table 3.1**). The addition of activating assembly protein (AAP2) sequence in the production protocol improved Anc80L65 viral vector titres ten to hundred fold. The activating assembly protein (AAP2) aids in protein folding to stabilise VP1- 3 capsid

unit allowing for rapid capsid assembly in most serotypes except AAV4 and AAV5 which are AAP sequence independent (Grosse et al., 2017). Titres of ≥ $1 \times 10^{12}$ VPs/mL produced in all viral vector types are optimal and commonly reported (Chen et al., 2009, Markakis et al., 2010, Zincarelli et al., 2008).

## 4.2 Anc80L65 transduces the liver efficiently and mediate significant transgene expression.

The transduction efficiency by the AAV vectors was carried out in liver-derived (Huh7) cells and mice using luciferase assay. The significant transgene expression by Anc80L65 vector over the highly efficient *in vitro* cell transducing AAV2 vector seen *in vitro* confirmed superior transduction efficiency over Anc80L65 as reported earlier (Zinn et al., 2015). However, in animal studies, viral vectors AAV8 and Anc80L65 expressing NLuc revealed a similar expression profile pointing to a similar transduction efficiency, which was a departure from earlier findings (Zinn et al., 2015). Also, the use of a liver-expression promoter (mTTR) led to transgene expression that was localised in the hepatocytes, which are sites of viral hepatitis B infection. The reduction of luciferase expression in animals over time from both viral AAV vectors was expected, as this has been observed previously (Qiao et al., 2011), and studies routinely restrict their luciferase expression observations from rAAV vectors to periods ranging from about a month up to just over three months (Prasad et al., 2011, Zincarelli et al., 2008).

Despite the excellent transgene expression of NLuc observed *in vitro*, we speculate that luciferase as foreign protein is immunogenic *in vivo*, resulting in transduced cells being actively cleared by the immune response, leading to a decrease over time in

transgene expression. However, the two month high level NLuc expression allowed confirmation of an earlier finding that in silico constructed Anc80L65 was capable of transducing liver cells (Zinn et al., 2015). The fact that Anc80L65 vector transduced cells efficiently like rAAV8 enabled further Anc80L65 vector assessment for its ability to deliver and mediate expression and processing of RNAi activators against HBV. *In vitro* Anti-HBV pri-miR expression from rAAV2 and rAnc80L65 was confirmed by Northern blot. Both viral vectors showed positive pri-miR expression although rAnc80L65 resulted in fainter guide band, suggesting poor transgene expression (**Figure 3.5**). Whereas, this contradicted with our earlier finding showing significantly higher luciferase expression by Anc80L65 compared to rAAV2 (**Figure 3.2**)**,** animal studies showed relatively equal transgene expression efficiency between a competent AAV8 hepatocyte transducer and Anc80L65.

## 4.3 rAnc80L65 can mediate a significant and sustained HBV gene silencing

The HBV gene expression knockdown was assessed *in vitro* by transducing dual luciferase reporter plasmid transfected cells with rAnc80L65-122/5 and rAAV2-122/5 vectors and performing luciferase assay. We observed no HBV gene expression silencing effects in relation to controls (**Figure 3.6**). Having established the excellent transduction profile for Anc80L65 *in vitro* (**Figure 3.2**) we reasoned that increasing the vector dose will lead to high transgene expression and using highly sensitive ELISA assay might assist in detecting differences in HBsAg changes. Indeed, at the increased MOI of $1 \times 10^6$, we observed statistically significant but modest ~ 25% gene expression knockdown by rAnc80L65 vector compared to ~50% from positive rAAV2 vector control after 48 hours (**Figure 3.7a**). As expected from previous

experience with viral vector mediated HBV inhibition in cultured cells, after 72 hours of cell growth, HBsAg level reduction was completely reversed [unpublished data, (**Figure 3.7b**)]. The AAV8 vector has liver tropism and transduces hepatic cells *in vivo* efficiently (Zincarelli et al., 2008) and less so *in vitro*. Hence, Anc80L65 phylogenetically close relatedness to AAV8 most likely account for its poor transduction efficiency (Zinn et al., 2015).

HBV replication inhibition assessment *in vivo* was carried out by injecting Anc80L65-122/5 and rAAV2-122/5 vectors in HBV transgenic mice to target viral mRNA scripts and effect HBV gene expression silencing. While HBV gene knockdown was modest, initially at 50% in the first week post-injection and increasing to about 70% in four weeks, Anc80L65 demonstrated equal competent to AAV8 at efficiently transducing hepatocytes and transgene expression (**Figure 3.8**). Naturally, AAV gene expression is delayed by single stranded DNA conversion to double stranded DNA conformation which is a rate limiting step in transgene expression kinetics (Ferrari et al., 1996). In our case the delay in expression was mitigated by use of ready to express self-complementary DNA bearing rAAV, hence in the first week statistically significant gene knockdown was seen as has been reported by others (Chen et al., 2009, Maepa et al., 2017). Previously, AAV8/AAV9 mediated RNAi activation has yielded much more improved and ~95%, HBsAg knockdown for periods up to 10 months (Chen et al., 2009, Maepa et al., 2017). The modest HBV knockdown levels observed using miR-122/5 anti-HBV RNAi activator mimic were not surprising and have been observed previously (Mowa et al., 2012). The RNAi mimic used in the study is derived from a naturally occurring, and highly expressed miR-122 in the liver. It has been shown previously, that HBx protein in

HBV infected hepatocytes downregulates miR-122 expression, and this might explain the relatively low HBsAg level reduction observed in our study (Bandopadhyay et al., 2016, Yu et al., 2016).

## 4.4 rAnc80L65 does not induce detrimental inflammatory effects or liver toxicity

RNAi activators and viral infections have been implicated in stimulating cytokine production in mammalian systems leading to inflammatory response (Osterlund et al., 2005, Sioud, 2005). Both interferon and interleukin cytokines form a repertoire of immune signalling peptides modulating the host immune system response upon microbial infection. Interferons-α/β and lL-12 produced by immune cells like monocytes/macrophages upon viral infection activate natural killer and Type 1 T helper cells. This induce IFN-γ production and promote cell-mediated immune response characterised by pro-inflammatory and anti-viral activities [as reviewed, (Meng and Lu, 2017)].

Foreign double stranded RNAs, similar to those used in current study, have previously been shown to induce pro-inflammatory IL-6, MCP-1 and TNF cytokine production (Matsukura et al., 2006, Sioud, 2005). IL-6 is a cytotoxic B- and T-cell differentiation factor, while TNF is cytotoxic for tumour cells and mediates inflammatory response (Wiley et al., 2011). MCP-1, a chemokine, enhances immune cells (monocytes/macrophages) pro-inflammatory properties and tumoricidal activities against certain cancer cells [as reviewed (Mukaida et al., 1998)]. In regulating high cytokine production, IL-10 cytokines produced from macrophages,

Type 2 T helper cells and B-cells act to reduce IFN- γ, TNF and IL-6 cytokines (Wiley et al., 2011). Immune activation by rAAVs was assessed by evaluating the levels of IL-12p70, IFN-γ, MCP-1, TNF, IL-10 and IL-6 in animals injected with rAAV vectors carrying transgene or no transgene and compared to saline injected mice. We observed immune induction stimulated by one cytokine MCP-1 out of six evaluated without harmful effect (**Figure 9**). Previous studies have showed that harmful inflammatory response in hepatocytes translates to liver tissue injury with resultant release of intracellular enzymes specifically Alanine transaminase [ALT, (Bala et al., 2012, Kerner et al., 2005, Zylberberg et al., 1999)]. In addition, oversaturation of the RNAi pathway by polymerase III driven anti-HBV pre-miR mimics delivered by self-complementary AAV8 (scAAV8) has previously resulted in liver toxicity characterised by elevated ALT levels and eventual fatalities in mice (Grimm et al., 2006). This study evaluated ALT levels in mice injected with scAAVs expressing pri-miR mimic from a pol II promoter. ALT levels were found to be within the normal range of below 100 IU/L over 8 weeks, ruling out presence of inflammation or RNAi oversaturation mediated liver injury.

Moreover, data relating to weights collected from mice injected with rAAV vectors or saline were indistinguishable from each other and revealed that mice were growing normally and healthy. Similar findings were observed where in rAAV vector mediated anti HBV RNAi or human factor IX gene therapeutics were delivered to mice and rhesus macaques, respectively (Maepa et al., 2017, Nathwani et al., 2011). Mice remained physically active throughout our study, with only three dying of causes unrelated to the study.

# CONCLUSION

Collectively, these results show Anc80L65 to be a safe and efficient delivery vector of anti-HBV RNAi based therapeutics to hepatocytes. Moreover, sustained viral hepatitis B inhibition shown by Anc80L65 is advantageous when using RNAi-based therapy to treat chronic viral hepatitis infection as it achieves long-term maintenance of anti-HBV effect. Of relevance is that serial AAV mediated therapy delivery using alternate AAV vectors have previously been shown to extend transgene expression (Chen et al., 2009). The finding that Anc80L65 vector is as competent as AAV8 means the existence of Anc80L65 vector increases the AAV vector repertoire creating more options for delivering more expressed therapeutic nucleic acids to the liver. This is especially important in the era of high seroprevalence of AAV capsid specific antibodies in the human population which remain a hurdle to effective therapeutic gene transfer.

## Future studies

Using Anc80L65 and more potent HBV gene expression silencing sequences like miR-31/5 or miR-31/5/8/9 previously reported to effect ~ 95% HBV gene knockdown (Maepa et al., 2017) can improve HBV inhibition seen in this study.

With previous findings of high seroprevalence of AAV2 capsid-specific antibodies, and to a lesser extent AAV8-capsid specific antibody, future studies will evaluate if the ancestral capsid can evade immune detection by AAV2 and AAV8 capsid specific human antibodies to achieve efficient gene transfer.

# CHAPTER 5: REFERENCES


ARBUTHNOT, P., CARMONA, S. & ELY, A. 2005. Exploiting the RNA interference pathway to counter hepatitis B virus replication. *Liver Int,* 25**,** 9-15.

ASOKAN, A., HAMRA, J. B., GOVINDASAMY, L., AGBANDJE-MCKENNA, M. & SAMULSKI, R. J. 2006. Adeno-associated virus type 2 contains an integrin alpha5beta1 binding domain essential for viral cell entry. *J Virol,* 80**,** 8961-9.

BALA, S., PETRASEK, J., MUNDKUR, S., CATALANO, D., LEVIN, I., WARD, J., ALAO, H., KODYS, K. & SZABO, G. 2012. Circulating microRNAs in exosomes indicate hepatocyte injury and inflammation in alcoholic, drug-induced, and inflammatory liver diseases. *Hepatology,* 56**,** 1946-57.

BANDOPADHYAY, M., SARKAR, N., DATTA, S., DAS, D., PAL, A., PANIGRAHI, R., BANERJEE, A., PANDA, C. K., DAS, C., CHAKRABARTI, S. & CHAKRAVARTY, R. 2016. Hepatitis B virus X protein mediated suppression of miRNA-122 expression enhances hepatoblastoma cell proliferation through cyclin G1-p53 axis. *Infect Agent Cancer,* 11**,** 40.

BEATON, A., PALUMBO, P. & BERNS, K. I. 1989. Expression from the adeno-associated virus p5 and p19 promoters is negatively regulated in trans by the rep protein. *J Virol,* 63**,** 4450-4.

BECERRA, S. P., KOCZOT, F., FABISCH, P. & ROSE, J. A. 1988. Synthesis of adeno-associated virus structural proteins requires both alternative mRNA splicing and alternative initiations from a single transcript. *J Virol,* 62**,** 2745-54.

BELL, C. L., GURDA, B. L., VAN VLIET, K., AGBANDJE-MCKENNA, M. & WILSON, J. M. 2012. Identification of the galactose binding domain of the adeno-associated virus serotype 9 capsid. *J Virol,* 86**,** 7326-33.

BERNS, K. I. & LINDEN, R. M. 1995. The cryptic life style of adeno-associated virus. *Bioessays,* 17**,** 237-45.

BERNS, K. I. & PARRISH, C. 2007. *In Fields Virology,* New York, Lippincott Williams & Wilkins.

BLEKER, S., SONNTAG, F. & KLEINSCHMIDT, J. A. 2005. Mutational analysis of narrow pores at the fivefold symmetry axes of adeno-associated virus type 2 capsids reveals a dual role in genome packaging and activation of phospholipase A2 activity. *J Virol,* 79**,** 2528-40.

BLOOM, K., ELY, A., MUSSOLINO, C., CATHOMEN, T. & ARBUTHNOT, P. 2013. Inactivation of hepatitis B virus replication in cultured cells and in vivo with engineered transcription activator-like effector nucleases. *Mol Ther,* 21**,** 1889-97.

BOHNSACK, M. T., CZAPLINSKI, K. & GORLICH, D. 2004. Exportin 5 is a RanGTP-dependent dsRNA-binding protein that mediates nuclear export of pre-miRNAs. *RNA,* 10**,** 185-91.

BOURHILL, T. 2015. *Successful disabling of the 5' UTR of HCV using adeno-associated viral vectors to deliver artificial primary microrna mimics* . Masters Dissertation, University of the Witwatersrand.

BOWLES, D. E., RABINOWITZ, J. E. & SAMULSKI, R. J. 2003. Marker rescue of adeno-associated virus (AAV) capsid mutants: a novel approach for chimeric AAV production. *J Virol,* 77**,** 423-32.

BULLER, R. M. & ROSE, J. A. 1978. Characterization of adenovirus-associated virus-induced polypeptides in KB cells. *J Virol,* 25**,** 331-8.

BUTZ, K., RISTRIANI, T., HENGSTERMANN, A., DENK, C., SCHEFFNER, M. & HOPPE-SEYLER, F. 2003. siRNA targeting of the viral E6 oncogene efficiently kills human papillomavirus-positive cancer cells. *Oncogene,* 22**,** 5938-45.

CAI, S., YU, T., JIANG, Y., ZHANG, Y., LV, F. & PENG, J. 2016. Comparison of entecavir monotherapy and de novo lamivudine and adefovir combination therapy in HBeAg-positive chronic hepatitis B with high viral load: 48-week result. *Clin Exp Med,* 16**,** 429-36.

CALCEDO, R., MORIZONO, H., WANG, L., MCCARTER, R., HE, J., JONES, D., BATSHAW, M. L. & WILSON, J. M. 2011. Adeno-associated virus antibody profiles in newborns, children, and adolescents. *Clin Vaccine Immunol,* 18**,** 1586-8.

CALCEDO, R., VANDENBERGHE, L. H., GAO, G., LIN, J. & WILSON, J. M. 2009. Worldwide epidemiology of neutralizing antibodies to adeno-associated viruses. *J Infect Dis,* 199**,** 381-90.

CARMONA, S., ELY, A., CROWTHER, C., MOOLLA, N., SALAZAR, F. H., MARION, P. L., FERRY, N., WEINBERG, M. S. & ARBUTHNOT, P. 2006. Effective inhibition of HBV replication in vivo by anti-HBx short hairpin RNAs. *Mol Ther,* 13**,** 411-21.

CASSINOTTI, P., WEITZAND, M. & TRATSCHIN, J. D. 1988. Organization of the adeno-associated virus (AAV) capsid gene: mapping of a minor spliced mRNA coding for virus capsid protein. *Virology,* 167**,** 176-84.

CHEN, C. C., CHANG, C. M., SUN, C. P., YU, C. P., WU, P. Y., JENG, K. S., HU, C. P., CHEN, P. J., WU, J. C., SHIH, C. H., GERSHWIN, M. E. & TAO, M. H. 2012. Use of RNA interference to modulate liver adenoma development in a murine model transgenic for hepatitis B virus. *Gene Ther,* 19**,** 25-33.

CHEN, C. C., KO, T. M., MA, H. I., WU, H. L., XIAO, X., LI, J., CHANG, C. M., WU, P. Y., CHEN, C. H., HAN, J. M., YU, C. P., JENG, K. S., HU, C. P. & TAO, M. H. 2007. Long-term inhibition of hepatitis B virus in transgenic mice by double-stranded adeno-associated virus 8-delivered short hairpin RNA. *Gene Ther,* 14**,** 11-9.

CHEN, C. C., SUN, C. P., MA, H. I., FANG, C. C., WU, P. Y., XIAO, X. & TAO, M. H. 2009. Comparative study of anti-hepatitis B virus RNA interference by double-stranded adeno-associated virus serotypes 7, 8, and 9. *Mol Ther,* 17**,** 352-9.

CHOMCZYNSKI, P., FAU - SACCHI, N. & SACCHI, N. 1987. Single-step method of RNA isolation by acid guanidinium thiocyanate-phenol-chloroform extraction.

CIDECIYAN, A. V., ALEMAN TS FAU - BOYE, S. L., BOYE SL FAU - SCHWARTZ, S. B., SCHWARTZ SB FAU - KAUSHAL, S., KAUSHAL S FAU - ROMAN, A. J., ROMAN AJ FAU - PANG, J.-J., PANG JJ FAU - SUMAROKA, A., SUMAROKA A FAU - WINDSOR, E. A. M., WINDSOR EA FAU - WILSON, J. M., WILSON JM FAU - FLOTTE, T. R., FLOTTE TR FAU - FISHMAN, G. A., FISHMAN GA FAU - HEON, E., HEON E FAU - STONE, E. M., STONE EM FAU - BYRNE, B. J., BYRNE BJ FAU - JACOBSON, S. G., JACOBSON SG FAU - HAUSWIRTH, W. W. & HAUSWIRTH, W. W. 2008. Human gene therapy for RPE65 isomerase deficiency activates the retinoid cycle of vision but with slow rod kinetics.

DALKARA, D., BYRNE, L. C., KLIMCZAK, R. R., VISEL, M., YIN, L., MERIGAN, W. H., FLANNERY, J. G. & SCHAFFER, D. V. 2013. In vivo-directed evolution of a new adeno-associated virus for therapeutic outer retinal gene delivery from the vitreous. *Sci Transl Med,* 5**,** 189ra76.

DAYA, S. & BERNS, K. I. 2008. Gene therapy using adeno-associated virus vectors. *Clin Microbiol Rev,* 21**,** 583-93.

DEWANGAN, H. K., PANDEY, T., MAURYA, L. & SINGH, S. 2018. Rational design and evaluation of HBsAg polymeric nanoparticles as antigen delivery carriers. *Int J Biol Macromol,* 111**,** 804-812.
DIMATTIA, M. A., NAM, H. J., VAN VLIET, K., MITCHELL, M., BENNETT, A., GURDA, B. L., MCKENNA, R., OLSON, N. H., SINKOVITS, R. S., POTTER, M., BYRNE, B. J., ASLANIDI, G., ZOLOTUKHIN, S., MUZYCZKA, N., BAKER, T. S. & AGBANDJE-MCKENNA, M. 2012. Structural insight into the unique properties of adeno-associated virus serotype 9. *J Virol,* 86**,** 6947-58.
DONG, J. Y., FAN, P. D. & FRIZZELL, R. A. 1996. Quantitative analysis of the packaging capacity of recombinant adeno-associated virus. *Hum Gene Ther,* 7**,** 2101-12.
DREYER, T., NICHOLSON, S., ELY, A., ARBUTHNOT, P. & BLOOM, K. 2016. Improved antiviral efficacy using TALEN-mediated homology directed recombination to introduce artificial primary miRNAs into DNA of hepatitis B virus. *Biochem Biophys Res Commun,* 478**,** 1563-8.
DROUIN, L. M. & AGBANDJE-MCKENNA, M. 2013. Adeno-associated virus structural biology as a tool in vector development. *Future Virol,* 8**,** 1183-1199.
DYALL, J. & BERNS, K. I. 1998. Site-specific integration of adeno-associated virus into an episome with the target locus via a deletion-substitution mechanism. *J Virol,* 72**,** 6195-8.
DYALL, J., SZABO, P. & BERNS, K. I. 1999. Adeno-associated virus (AAV) site-specific integration: formation of AAV-AAVS1 junctions in an in vitro system. *Proc Natl Acad Sci U S A,* 96**,** 12849-54.
ELBASHIR, S. M., HARBORTH, J., LENDECKEL, W., YALCIN, A., WEBER, K. & TUSCHL, T. 2001a. Duplexes of 21-nucleotide RNAs mediate RNA interference in cultured mammalian cells. *Nature,* 411**,** 494-8.
ELBASHIR, S. M., LENDECKEL, W. & TUSCHL, T. 2001b. RNA interference is mediated by 21- and 22-nucleotide RNAs. *Genes Dev,* 15**,** 188-200.
ELY, A., NAIDOO, T. & ARBUTHNOT, P. 2009. Efficient silencing of gene expression with modular trimeric Pol II expression cassettes comprising microRNA shuttles. *Nucleic Acids Res,* 37**,** e91.
ELY, A., NAIDOO, T., MUFAMADI, S., CROWTHER, C. & ARBUTHNOT, P. 2008. Expressed anti-HBV primary microRNA shuttles inhibit viral replication efficiently in vitro and in vivo. *Mol Ther,* 16**,** 1105-12.
ESCRIOU, V., CIOLINA C FAU - LACROIX, F., LACROIX F FAU - BYK, G., BYK G FAU - SCHERMAN, D., SCHERMAN D FAU - WILS, P. & WILS, P. 1998. Cationic lipid-mediated gene transfer: effect of serum on cellular uptake and intracellular fate of lipopolyamine/DNA complexes.
EXCOFFON, K. J., KOERBER, J. T., DICKEY, D. D., MURTHA, M., KESHAVJEE, S., KASPAR, B. K., ZABNER, J. & SCHAFFER, D. V. 2009. Directed evolution of adeno-associated virus to an infectious respiratory virus. *Proc Natl Acad Sci U S A,* 106**,** 3865-70.
FDA, U. 2017. *FDA approval brings first gene therapy to the United States* [Online]. Online: US Food and Drug Administration (FDA). Available: https://www.fda.gov/NewsEvents/Newsroom/PressAnnouncements/ucm574058.htm [Accessed 09/12 2017].
FERRARI, F. K., SAMULSKI, T., SHENK, T. & SAMULSKI, R. J. 1996. Second-strand synthesis is a rate-limiting step for efficient transduction by recombinant adeno-associated virus vectors. *J Virol,* 70**,** 3227-34.
FERREIRA, V., PETRY, H. & SALMON, F. 2014. Immune Responses to AAV-Vectors, the Glybera Example from Bench to Bedside. *Front Immunol,* 5**,** 82.

FISICARO, P., BARILI, V., MONTANINI, B., ACERBI, G., FERRACIN, M., GUERRIERI, F., SALERNO, D., BONI, C., MASSARI, M., CAVALLO, M. C., GROSSI, G., GIUBERTI, T., LAMPERTICO, P., MISSALE, G., LEVRERO, M., OTTONELLO, S. & FERRARI, C. 2017. Targeting mitochondrial dysfunction can restore antiviral activity of exhausted HBV-specific CD8 T cells in chronic hepatitis B. *Nat Med,* 23**,** 327-336.

GAJ, T., GERSBACH, C. A. & BARBAS, C. F., 3RD 2013. ZFN, TALEN, and CRISPR/Cas-based methods for genome engineering. *Trends Biotechnol,* 31**,** 397-405.

GANEM, D. & PRINCE, A. M. 2004. Hepatitis B virus infection--natural history and clinical consequences. *N Engl J Med,* 350**,** 1118-29.

GEBBING, M., BERGMANN, T., SCHULZ, E. & EHRHARDT, A. 2015. Gene therapeutic approaches to inhibit hepatitis B virus replication. *World J Hepatol,* 7**,** 150-64.

GIERING, J. C., GRIMM, D., STORM, T. A. & KAY, M. A. 2008. Expression of shRNA from a tissue-specific pol II promoter is an effective and safe RNAi therapeutic. *Mol Ther,* 16**,** 1630-6.

GILADI, H., KETZINEL-GILAD, M., RIVKIN, L., FELIG, Y., NUSSBAUM, O. & GALUN, E. 2003. Small interfering RNA inhibits hepatitis B virus replication in mice. *Mol Ther,* 8**,** 769-76.

GIROD, A., WOBUS, C. E., ZADORI, Z., RIED, M., LEIKE, K., TIJSSEN, P., KLEINSCHMIDT, J. A. & HALLEK, M. 2002. The VP1 capsid protein of adeno-associated virus type 2 is carrying a phospholipase A2 domain required for virus infectivity. *J Gen Virol,* 83**,** 973-8.

GLEBE, D. & BREMER, C. M. 2013. The molecular virology of hepatitis B virus. *Semin Liver Dis,* 33**,** 103-12.

GONCALVES, M. A. 2005. Adeno-associated virus: from defective virus to effective vector. *Virol J,* 2**,** 43.

GRAY, S. J., BLAKE, B. L., CRISWELL, H. E., NICOLSON, S. C., SAMULSKI, R. J., MCCOWN, T. J. & LI, W. 2010. Directed evolution of a novel adeno-associated virus (AAV) vector that crosses the seizure-compromised blood-brain barrier (BBB). *Mol Ther,* 18**,** 570-8.

GRIEGER, J. C., SNOWDY, S. & SAMULSKI, R. J. 2006. Separate basic region motifs within the adeno-associated virus capsid proteins are essential for infectivity and assembly. *J Virol,* 80**,** 5199-210.

GRIMM, D. & KAY, M. A. 2003. From virus evolution to vector revolution: use of naturally occurring serotypes of adeno-associated virus (AAV) as novel vectors for human gene therapy. *Curr Gene Ther,* 3**,** 281-304.

GRIMM, D., STREETZ, K. L., JOPLING, C. L., STORM, T. A., PANDEY, K., DAVIS, C. R., MARION, P., SALAZAR, F. & KAY, M. A. 2006. Fatality in mice due to oversaturation of cellular microRNA/short hairpin RNA pathways. *Nature,* 441**,** 537-41.

GRIMM, D., ZHOU, S., NAKAI, H., THOMAS, C. E., STORM, T. A., FUESS, S., MATSUSHITA, T., ALLEN, J., SUROSKY, R., LOCHRIE, M., MEUSE, L., MCCLELLAND, A., COLOSI, P. & KAY, M. A. 2003. Preclinical in vivo evaluation of pseudotyped adeno-associated virus vectors for liver gene therapy. *Blood,* 102**,** 2412-9.

GROSSE, S., PENAUD-BUDLOO, M., HERRMANN, A. K., BORNER, K., FAKHIRI, J., LAKETA, V., KRAMER, C., WIEDTKE, E., GUNKEL, M., MENARD, L., AYUSO, E. & GRIMM, D. 2017. Relevance of Assembly-Activating Protein for

Adeno-associated Virus Vector Production and Capsid Protein Stability in Mammalian and Insect Cells. *J Virol,* 91.
HAMILTON, A. J. & BAULCOMBE, D. C. 1999. A species of small antisense RNA in posttranscriptional gene silencing in plants. *Science,* 286**,** 950-2.
HAN, J., LEE, Y., YEOM, K. H., KIM, Y. K., JIN, H. & KIM, V. N. 2004. The Drosha-DGCR8 complex in primary microRNA processing. *Genes Dev,* 18**,** 3016-27.
HERMONAT, P. L., QUIRK, J. G., BISHOP, B. M. & HAN, L. 1997. The packaging capacity of adeno-associated virus (AAV) and the potential for wild-type-plus AAV gene therapy vectors. *FEBS Lett,* 407**,** 78-84.
HOLT, N., WANG, J., KIM, K., FRIEDMAN, G., WANG, X., TAUPIN, V., CROOKS, G. M., KOHN, D. B., GREGORY, P. D., HOLMES, M. C. & CANNON, P. M. 2010. Human hematopoietic stem/progenitor cells modified by zinc-finger nucleases targeted to CCR5 control HIV-1 in vivo. *Nat Biotechnol,* 28**,** 839-47.
HOSEL, M., LUCIFORA, J., MICHLER, T., HOLZ, G., GRUFFAZ, M., STAHNKE, S., ZOULIM, F., DURANTEL, D., HEIKENWALDER, M., NIERHOFF, D., MILLET, R., SALVETTI, A., PROTZER, U. & BUNING, H. 2014. Hepatitis B virus infection enhances susceptibility toward adeno-associated viral vector transduction in vitro and in vivo. *Hepatology,* 59**,** 2110-20.
HUSER, D., GOGOL-DORING, A., CHEN, W. & HEILBRONN, R. 2014. Adeno-associated virus type 2 wild-type and vector-mediated genomic integration profiles of human diploid fibroblasts analyzed by third-generation PacBio DNA sequencing.
HUSER, D., GOGOL-DORING A FAU - LUTTER, T., LUTTER T FAU - WEGER, S., WEGER S FAU - WINTER, K., WINTER K FAU - HAMMER, E.-M., HAMMER EM FAU - CATHOMEN, T., CATHOMEN T FAU - REINERT, K., REINERT K FAU - HEILBRONN, R. & HEILBRONN, R. 2010. Integration preferences of wildtype AAV-2 for consensus rep-binding sites at numerous loci in the human genome.
HUTVAGNER, G. & ZAMORE, P. D. 2002. A microRNA in a multiple-turnover RNAi enzyme complex. *Science,* 297**,** 2056-60.
IVACIK, D., ELY, A., FERRY, N. & ARBUTHNOT, P. 2015. Sustained inhibition of hepatitis B virus replication in vivo using RNAi-activating lentiviruses. *Gene Ther,* 22**,** 163-71.
JANG, J. H., KOERBER, J. T., KIM, J. S., ASURI, P., VAZIN, T., BARTEL, M., KEUNG, A., KWON, I., PARK, K. I. & SCHAFFER, D. V. 2011. An evolved adeno-associated viral variant enhances gene delivery and gene targeting in neural stem cells. *Mol Ther,* 19**,** 667-75.
JIN, L., ZENG, X., LIU, M., DENG, Y. & HE, N. 2014. Current progress in gene delivery technology based on chemical methods and nano-carriers. *Theranostics,* 4**,** 240-55.
JING, X. J., KALMAN-MALTESE V FAU - CAO, X., CAO X FAU - YANG, Q., YANG Q FAU - TREMPE, J. P. & TREMPE, J. P. 2001. Inhibition of adenovirus cytotoxicity, replication, and E2a gene expression by adeno-associated virus.
KAMINSKY, P. M., KEISER, N. W., YAN, Z., LEI-BUTTERS, D. C. & ENGELHARDT, J. F. 2012. Directing integrin-linked endocytosis of recombinant AAV enhances productive FAK-dependent transduction. *Mol Ther,* 20**,** 972-83.
KERN, A., SCHMIDT, K., LEDER, C., MULLER, O. J., WOBUS, C. E., BETTINGER, K., VON DER LIETH, C. W., KING, J. A. & KLEINSCHMIDT, J. A. 2003. Identification of a heparin-binding motif on adeno-associated virus type 2 capsids. *J Virol,* 77**,** 11072-81.
KERNER, A., AVIZOHAR, O., SELLA, R., BARTHA, P., ZINDER, O., MARKIEWICZ, W., LEVY, Y., BROOK, G. J. & ARONSON, D. 2005. Association between elevated

liver enzymes and C-reactive protein: possible hepatic contribution to systemic inflammation in the metabolic syndrome. *Arterioscler Thromb Vasc Biol,* 25**,** 193-7.
KETTING, R. F., FISCHER, S. E., BERNSTEIN, E., SIJEN, T., HANNON, G. J. & PLASTERK, R. H. 2001. Dicer functions in RNA interference and in synthesis of small RNA involved in developmental timing in C. elegans. *Genes Dev,* 15**,** 2654-9.
KHAN, I., SAEED, K. & KHAN, I. 2017. Nanoparticles: Properties, Applications and Toxicities. *Arabian Journal of Chemistry*.
KIENLE, E., SENIS, E., BORNER, K., NIOPEK, D., WIEDTKE, E., GROSSE, S. & GRIMM, D. 2012. Engineering and evolution of synthetic adeno-associated virus (AAV) gene therapy vectors via DNA family shuffling. *J Vis Exp*.
KIM, H. & KIM, J. S. 2014. A guide to genome engineering with programmable nucleases. *Nat Rev Genet,* 15**,** 321-34.
KNIGHT, S. W. & BASS, B. L. 2001. A role for the RNase III enzyme DCR-1 in RNA interference and germ line development in Caenorhabditis elegans. *Science,* 293**,** 2269-71.
KOCZOT, F. J., CARTER, B. J., GARON, C. F. & ROSE, J. A. 1973. Self-complementarity of terminal sequences within plus or minus strands of adenovirus-associated virus DNA. *Proc Natl Acad Sci U S A,* 70**,** 215-9.
KOTA, J., CHIVUKULA, R. R., O'DONNELL, K. A., WENTZEL, E. A., MONTGOMERY, C. L., HWANG, H. W., CHANG, T. C., VIVEKANANDAN, P., TORBENSON, M., CLARK, K. R., MENDELL, J. R. & MENDELL, J. T. 2009. Therapeutic microRNA delivery suppresses tumorigenesis in a murine liver cancer model. *Cell,* 137**,** 1005-17.
KOTIN, R. M., SINISCALCO, M., SAMULSKI, R. J., ZHU, X. D., HUNTER, L., LAUGHLIN, C. A., MCLAUGHLIN, S., MUZYCZKA, N., ROCCHI, M. & BERNS, K. I. 1990. Site-specific integration by adeno-associated virus. *Proc Natl Acad Sci U S A,* 87**,** 2211-5.
KOTTERMAN, M. A. & SCHAFFER, D. V. 2014. Engineering adeno-associated viruses for clinical gene therapy. *Nat Rev Genet,* 15**,** 445-51.
KRONENBERG, S., KLEINSCHMIDT, J. A. & BOTTCHER, B. 2001. Electron cryo-microscopy and image reconstruction of adeno-associated virus type 2 empty capsids. *EMBO Rep,* 2**,** 997-1002.
KWON, H. & LOK, A. S. 2011. Hepatitis B therapy. *Nat Rev Gastroenterol Hepatol,* 8**,** 275-84.
KYOSTIO, S. R., WONDERLING, R. S. & OWENS, R. A. 1995. Negative regulation of the adeno-associated virus (AAV) P5 promoter involves both the P5 rep binding site and the consensus ATP-binding motif of the AAV Rep68 protein. *J Virol,* 69**,** 6787-96.
LANDERS, T. A., GREENBERG, H. B. & ROBINSON, W. S. 1977. Structure of hepatitis B Dane particle DNA and nature of the endogenous DNA polymerase reaction. *J Virol,* 23**,** 368-76.
LI, C., WU, S., ALBRIGHT, B., HIRSCH, M., LI, W., TSENG, Y. S., AGBANDJE-MCKENNA, M., MCPHEE, S., ASOKAN, A. & SAMULSKI, R. J. 2016. Development of Patient-specific AAV Vectors After Neutralizing Antibody Selection for Enhanced Muscle Gene Transfer. *Mol Ther,* 24**,** 53-65.
LIEN, J. M., ALDRICH, C. E. & MASON, W. S. 1986. Evidence that a capped oligoribonucleotide is the primer for duck hepatitis B virus plus-strand DNA synthesis. *J Virol,* 57**,** 229-36.
LINDEN, R. M., WARD, P., GIRAUD, C., WINOCOUR, E. & BERNS, K. I. 1996a. Site-specific integration by adeno-associated virus. *Proc Natl Acad Sci U S A,* 93**,** 11288-94.

LINDEN, R. M., WINOCOUR, E. & BERNS, K. I. 1996b. The recombination signals for adeno-associated virus site-specific integration. *Proc Natl Acad Sci U S A,* 93**,** 7966-72.

LISOWSKI, L., DANE, A. P., CHU, K., ZHANG, Y., CUNNINGHAM, S. C., WILSON, E. M., NYGAARD, S., GROMPE, M., ALEXANDER, I. E. & KAY, M. A. 2014. Selection and evaluation of clinically relevant AAV variants in a xenograft liver model. *Nature,* 506**,** 382-6.

LOCHRIE, M. A., TATSUNO, G. P., CHRISTIE, B., MCDONNELL, J. W., ZHOU, S., SUROSKY, R., PIERCE, G. F. & COLOSI, P. 2006. Mutations on the external surfaces of adeno-associated virus type 2 capsids that affect transduction and neutralization. *J Virol,* 80**,** 821-34.

LOCK, M., ALVIRA, M., VANDENBERGHE, L. H., SAMANTA, A., TOELEN, J., DEBYSER, Z. & WILSON, J. M. 2010. Rapid, simple, and versatile manufacturing of recombinant adeno-associated viral vectors at scale. *Hum Gene Ther,* 21**,** 1259-71.

LOGAN, G. J., DANE, A. P., HALLWIRTH, C. V., SMYTH, C. M., WILKIE, E. E., AMAYA, A. K., ZHU, E., KHANDEKAR, N., GINN, S. L., LIAO, S. H. Y., CUNNINGHAM, S. C., SASAKI, N., CABANES-CREUS, M., TAM, P. P. L., RUSSELL, D. W., LISOWSKI, L. & ALEXANDER, I. E. 2017. Identification of liver-specific enhancer-promoter activity in the 3' untranslated region of the wild-type AAV2 genome. *Nat Genet,* 49**,** 1267-1273.

MA, G., SHIMADA, H., HIROSHIMA, K., TADA, Y., SUZUKI, N. & TAGAWA, M. 2009. Gene medicine for cancer treatment: commercially available medicine and accumulated clinical data in China. *Drug Des Devel Ther,* 2**,** 115-22.

MAEPA, M. B., ELY, A., GRAYSON, W. & ARBUTHNOT, P. 2017. Sustained Inhibition of HBV Replication In Vivo after Systemic Injection of AAVs Encoding Artificial Antiviral Primary MicroRNAs. *Mol Ther Nucleic Acids,* 7**,** 190-199.

MAGUIRE, A. M., SIMONELLI, F., PIERCE, E. A., PUGH, E. N., JR., MINGOZZI, F., BENNICELLI, J., BANFI, S., MARSHALL, K. A., TESTA, F., SURACE, E. M., ROSSI, S., LYUBARSKY, A., ARRUDA, V. R., KONKLE, B., STONE, E., SUN, J., JACOBS, J., DELL'OSSO, L., HERTLE, R., MA, J. X., REDMOND, T. M., ZHU, X., HAUCK, B., ZELENAIA, O., SHINDLER, K. S., MAGUIRE, M. G., WRIGHT, J. F., VOLPE, N. J., MCDONNELL, J. W., AURICCHIO, A., HIGH, K. A. & BENNETT, J. 2008. Safety and efficacy of gene transfer for Leber's congenital amaurosis. *N Engl J Med,* 358**,** 2240-8.

MANDEL, R. J. 2010. CERE-110, an adeno-associated virus-based gene delivery vector expressing human nerve growth factor for the treatment of Alzheimer's disease.

MANNO, C. S., PIERCE, G. F., ARRUDA, V. R., GLADER, B., RAGNI, M., RASKO, J. J., OZELO, M. C., HOOTS, K., BLATT, P., KONKLE, B., DAKE, M., KAYE, R., RAZAVI, M., ZAJKO, A., ZEHNDER, J., RUSTAGI, P. K., NAKAI, H., CHEW, A., LEONARD, D., WRIGHT, J. F., LESSARD, R. R., SOMMER, J. M., TIGGES, M., SABATINO, D., LUK, A., JIANG, H., MINGOZZI, F., COUTO, L., ERTL, H. C., HIGH, K. A. & KAY, M. A. 2006. Successful transduction of liver in hemophilia by AAV-Factor IX and limitations imposed by the host immune response. *Nat Med,* 12**,** 342-7.

MANZOOR, S., SAALIM, M., IMRAN, M., RESHAM, S. & ASHRAF, J. 2015. Hepatitis B virus therapy: What's the future holding for us? *World J Gastroenterol,* 21**,** 12558-75.

MARIMANI, M. D., ELY, A., BUFF, M. C., BERNHARDT, S., ENGELS, J. W., SCHERMAN, D., ESCRIOU, V. & ARBUTHNOT, P. 2015. Inhibition of replication of hepatitis B virus in transgenic mice following administration of hepatotropic

lipoplexes containing guanidinopropyl-modified siRNAs. *J Control Release,* 209**,** 198-206.

MARION, P., SALAZAR, F. H., LIITTSCHWAGER, K. & BORDIER, B. B. (eds.) 2003. *A transgenic mouse lineage useful for testing antivirals targeting*
*hepatitis B virus,* Amsterdam, The Netherlands: Elsevier Science.

MARKAKIS, E. A., VIVES, K. P., BOBER, J., LEICHTLE, S., LERANTH, C., BEECHAM, J., ELSWORTH, J. D., ROTH, R. H., SAMULSKI, R. J. & REDMOND, D. E., JR. 2010. Comparative transduction efficiency of AAV vector serotypes 1-6 in the substantia nigra and striatum of the primate brain. *Mol Ther,* 18**,** 588-93.

MARTINO, A. T., BASNER-TSCHAKARJAN, E., MARKUSIC, D. M., FINN, J. D., HINDERER, C., ZHOU, S., OSTROV, D. A., SRIVASTAVA, A., ERTL, H. C., TERHORST, C., HIGH, K. A., MINGOZZI, F. & HERZOG, R. W. 2013. Engineered AAV vector minimizes in vivo targeting of transduced hepatocytes by capsid-specific CD8+ T cells. *Blood,* 121**,** 2224-33.

MATSUKURA, S., KOKUBU, F., KUROKAWA, M., KAWAGUCHI, M., IEKI, K., KUGA, H., ODAKA, M., SUZUKI, S., WATANABE, S., TAKEUCHI, H., KASAMA, T. & ADACHI, M. 2006. Synthetic double-stranded RNA induces multiple genes related to inflammation through Toll-like receptor 3 depending on NF-kappaB and/or IRF-3 in airway epithelial cells. *Clin Exp Allergy,* 36**,** 1049-62.

MCCAFFREY, A. P., NAKAI, H., PANDEY, K., HUANG, Z., SALAZAR, F. H., XU, H., WIELAND, S. F., MARION, P. L. & KAY, M. A. 2003. Inhibition of hepatitis B virus in mice by RNA interference. *Nat Biotechnol,* 21**,** 639-44.

MCCARTY, D. M., MONAHAN, P. E. & SAMULSKI, R. J. 2001. Self-complementary recombinant adeno-associated virus (scAAV) vectors promote efficient transduction independently of DNA synthesis. *Gene Ther,* 8**,** 1248-54.

MENESES, P., BERNS, K. I. & WINOCOUR, E. 2000. DNA sequence motifs which direct adeno-associated virus site-specific integration in a model system. *J Virol,* 74**,** 6213-6.

MENG, Z. & LU, M. 2017. RNA Interference-Induced Innate Immunity, Off-Target Effect, or Immune Adjuvant? *Front Immunol,* 8**,** 331.

MINGOZZI, F., ANGUELA, X. M., PAVANI, G., CHEN, Y., DAVIDSON, R. J., HUI, D. J., YAZICIOGLU, M., ELKOUBY, L., HINDERER, C. J., FAELLA, A., HOWARD, C., TAI, A., PODSAKOFF, G. M., ZHOU, S., BASNER-TSCHAKARJAN, E., WRIGHT, J. F. & HIGH, K. A. 2013. Overcoming preexisting humoral immunity to AAV using capsid decoys. *Sci Transl Med,* 5**,** 194ra92.

MINGOZZI, F., MAUS, M. V., HUI, D. J., SABATINO, D. E., MURPHY, S. L., RASKO, J. E., RAGNI, M. V., MANNO, C. S., SOMMER, J., JIANG, H., PIERCE, G. F., ERTL, H. C. & HIGH, K. A. 2007. CD8(+) T-cell responses to adeno-associated virus capsid in humans. *Nat Med,* 13**,** 419-22.

MOLNAR-KIMBER, K. L., SUMMERS, J. W. & MASON, W. S. 1984. Mapping of the cohesive overlap of duck hepatitis B virus DNA and of the site of initiation of reverse transcription. *J Virol,* 51**,** 181-91.

MOWA, M. B., CROWTHER, C., ELY, A. & ARBUTHNOT, P. 2012. Efficient silencing of hepatitis B virus by helper-dependent adenovirus vector-mediated delivery of artificial antiviral primary micro RNAs. *Microrna,* 1**,** 19-25.

MOWA, M. B., CROWTHER, C., ELY, A. & ARBUTHNOT, P. 2014. Inhibition of hepatitis B virus replication by helper dependent adenoviral vectors expressing artificial anti-HBV pri-miRs from a liver-specific promoter. *Biomed Res Int,* 2014**,** 718743.

MUKAIDA, N., HARADA, A. & MATSUSHIMA, K. 1998. Interleukin-8 (IL-8) and monocyte chemotactic and activating factor (MCAF/MCP-1), chemokines essentially involved in inflammatory and immune reactions. *Cytokine Growth Factor Rev,* 9**,** 9-23.

MUNCH, R. C., JANICKI, H., VOLKER, I., RASBACH, A., HALLEK, M., BUNING, H. & BUCHHOLZ, C. J. 2013. Displaying high-affinity ligands on adeno-associated viral vectors enables tumor cell-specific and safe gene transfer. *Mol Ther,* 21**,** 109-18.

NAGHAVI, M., WANG, H., LOZANO, R., DAVIS, A., LIANG, X. & ZHOU, M. 2015. Global, regional, and national age-sex specific all-cause and cause-specific mortality for 240 causes of death, 1990-2013: a systematic analysis for the Global Burden of Disease Study 2013. *Lancet,* 385**,** 117-71.

NAKAI, H., MONTINI E FAU - FUESS, S., FUESS S FAU - STORM, T. A., STORM TA FAU - GROMPE, M., GROMPE M FAU - KAY, M. A. & KAY, M. A. 2003. AAV serotype 2 vectors preferentially integrate into active genes in mice.

NAKAI, H., WU X FAU - FUESS, S., FUESS S FAU - STORM, T. A., STORM TA FAU - MUNROE, D., MUNROE D FAU - MONTINI, E., MONTINI E FAU - BURGESS, S. M., BURGESS SM FAU - GROMPE, M., GROMPE M FAU - KAY, M. A. & KAY, M. A. 2005. Large-scale molecular characterization of adeno-associated virus vector integration in mouse liver.

NAKAI, H., YANT SR FAU - STORM, T. A., STORM TA FAU - FUESS, S., FUESS S FAU - MEUSE, L., MEUSE L FAU - KAY, M. A. & KAY, M. A. 2001. Extrachromosomal recombinant adeno-associated virus vector genomes are primarily responsible for stable liver transduction in vivo.

NASH, K., CHEN, W. & MUZYCZKA, N. 2008. Complete in vitro reconstitution of adeno-associated virus DNA replication requires the minichromosome maintenance complex proteins. *J Virol,* 82**,** 1458-64.

NASSAL, M. 1992. The arginine-rich domain of the hepatitis B virus core protein is required for pregenome encapsidation and productive viral positive-strand DNA synthesis but not for virus assembly. *J Virol,* 66**,** 4107-16.

NASSAL, M. 2015. HBV cccDNA: viral persistence reservoir and key obstacle for a cure of chronic hepatitis B. *Gut,* 64**,** 1972-84.

NATHWANI, A. C., GRAY, J. T., MCINTOSH, J., NG, C. Y., ZHOU, J., SPENCE, Y., COCHRANE, M., GRAY, E., TUDDENHAM, E. G. & DAVIDOFF, A. M. 2007. Safe and efficient transduction of the liver after peripheral vein infusion of self-complementary AAV vector results in stable therapeutic expression of human FIX in nonhuman primates. *Blood,* 109**,** 1414-21.

NATHWANI, A. C., TUDDENHAM, E. G., RANGARAJAN, S., ROSALES, C., MCINTOSH, J., LINCH, D. C., CHOWDARY, P., RIDDELL, A., PIE, A. J., HARRINGTON, C., O'BEIRNE, J., SMITH, K., PASI, J., GLADER, B., RUSTAGI, P., NG, C. Y., KAY, M. A., ZHOU, J., SPENCE, Y., MORTON, C. L., ALLAY, J., COLEMAN, J., SLEEP, S., CUNNINGHAM, J. M., SRIVASTAVA, D., BASNER-TSCHAKARJAN, E., MINGOZZI, F., HIGH, K. A., GRAY, J. T., REISS, U. M., NIENHUIS, A. W. & DAVIDOFF, A. M. 2011. Adenovirus-associated virus vector-mediated gene transfer in hemophilia B. *N Engl J Med,* 365**,** 2357-65.

NAULT, J. C., DATTA, S., IMBEAUD, S., FRANCONI, A., MALLET, M., COUCHY, G., LETOUZE, E., PILATI, C., VERRET, B., BLANC, J. F., BALABAUD, C., CALDERARO, J., LAURENT, A., LETEXIER, M., BIOULAC-SAGE, P., CALVO, F. & ZUCMAN-ROSSI, J. 2015. Recurrent AAV2-related insertional mutagenesis in human hepatocellular carcinomas. *Nat Genet,* 47**,** 1187-93.

NELSON, C. E., HAKIM, C. H., OUSTEROUT, D. G., THAKORE, P. I., MOREB, E. A., CASTELLANOS RIVERA, R. M., MADHAVAN, S., PAN, X., RAN, F. A., YAN, W. X., ASOKAN, A., ZHANG, F., DUAN, D. & GERSBACH, C. A. 2016. In vivo genome editing improves muscle function in a mouse model of Duchenne muscular dystrophy. *Science,* 351**,** 403-7.

NI, T. H., MCDONALD, W. F., ZOLOTUKHIN, I., MELENDY, T., WAGA, S., STILLMAN, B. & MUZYCZKA, N. 1998. Cellular proteins required for adeno-associated virus DNA replication in the absence of adenovirus coinfection. *J Virol,* 72**,** 2777-87.

NOVINA, C. D., MURRAY, M. F., DYKXHOORN, D. M., BERESFORD, P. J., RIESS, J., LEE, S. K., COLLMAN, R. G., LIEBERMAN, J., SHANKAR, P. & SHARP, P. A. 2002. siRNA-directed inhibition of HIV-1 infection. *Nat Med,* 8**,** 681-6.

OSTERLUND, P., VECKMAN V FAU - SIREN, J., SIREN J FAU - KLUCHER, K. M., KLUCHER KM FAU - HISCOTT, J., HISCOTT J FAU - MATIKAINEN, S., MATIKAINEN S FAU - JULKUNEN, I. & JULKUNEN, I. 2005. Gene expression and antiviral activity of alpha/beta interferons and interleukin-29 in virus-infected human myeloid dendritic cells.

PERABO, L., ENDELL, J., KING, S., LUX, K., GOLDNAU, D., HALLEK, M. & BUNING, H. 2006. Combinatorial engineering of a gene therapy vector: directed evolution of adeno-associated virus. *J Gene Med,* 8**,** 155-62.

PHILPOTT, N. J., GIRAUD-WALI, C., DUPUIS, C., GOMOS, J., HAMILTON, H., BERNS, K. I. & FALCK-PEDERSEN, E. 2002a. Efficient integration of recombinant adeno-associated virus DNA vectors requires a p5-rep sequence in cis. *J Virol,* 76**,** 5411-21.

PHILPOTT, N. J., GOMOS, J., BERNS, K. I. & FALCK-PEDERSEN, E. 2002b. A p5 integration efficiency element mediates Rep-dependent integration into AAVS1 at chromosome 19. *Proc Natl Acad Sci U S A,* 99**,** 12381-5.

PILLAY, S., MEYER, N. L., PUSCHNIK, A. S., DAVULCU, O., DIEP, J., ISHIKAWA, Y., JAE, L. T., WOSEN, J. E., NAGAMINE, C. M., CHAPMAN, M. S. & CARETTE, J. E. 2016. An essential receptor for adeno-associated virus infection. *Nature,* 530**,** 108-12.

POLING, B. C., TSAI, K., KANG, D., REN, L., KENNEDY, E. M. & CULLEN, B. R. 2017. A lentiviral vector bearing a reverse intron demonstrates superior expression of both proteins and microRNAs. *RNA Biol***,** 1-10.

POPA-WAGNER, R., SONNTAG, F., SCHMIDT, K., KING, J. & KLEINSCHMIDT, J. A. 2012. Nuclear translocation of adeno-associated virus type 2 capsid proteins for virion assembly. *J Gen Virol,* 93**,** 1887-98.

PRASAD, K. M., XU, Y., YANG, Z., ACTON, S. T. & FRENCH, B. A. 2011. Robust cardiomyocyte-specific gene expression following systemic injection of AAV: in vivo gene delivery follows a Poisson distribution. *Gene Ther,* 18**,** 43-52.

QIAO, C., YUAN, Z., LI, J., HE, B., ZHENG, H., MAYER, C., LI, J. & XIAO, X. 2011. Liver-specific microRNA-122 target sequences incorporated in AAV vectors efficiently inhibits transgene expression in the liver. *Gene Ther,* 18**,** 403-10.

QING, K., HANSEN J FAU - WEIGEL-KELLEY, K. A., WEIGEL-KELLEY KA FAU - TAN, M., TAN M FAU - ZHOU, S., ZHOU S FAU - SRIVASTAVA, A. & SRIVASTAVA, A. 2001. Adeno-associated virus type 2-mediated gene transfer: role of cellular FKBP52 protein in transgene expression.

QING, K., KHUNTIRAT B FAU - MAH, C., MAH C FAU - KUBE, D. M., KUBE DM FAU - WANG, X. S., WANG XS FAU - PONNAZHAGAN, S., PONNAZHAGAN S FAU - ZHOU, S., ZHOU S FAU - DWARKI, V. J., DWARKI VJ FAU - YODER,

M. C., YODER MC FAU - SRIVASTAVA, A. & SRIVASTAVA, A. 1998. Adeno-associated virus type 2-mediated gene transfer: correlation of tyrosine phosphorylation of the cellular single-stranded D sequence-binding protein with transgene expression in human cells in vitro and murine tissues in vivo.

QING, K., WANG XS FAU - KUBE, D. M., KUBE DM FAU - PONNAZHAGAN, S., PONNAZHAGAN S FAU - BAJPAI, A., BAJPAI A FAU - SRIVASTAVA, A. & SRIVASTAVA, A. 1997. Role of tyrosine phosphorylation of a cellular protein in adeno-associated virus 2-mediated transgene expression.

RAFII, M. S., BAUMANN, T. L., BAKAY, R. A., OSTROVE, J. M., SIFFERT, J., FLEISHER, A. S., HERZOG, C. D., BARBA, D., PAY, M., SALMON, D. P., CHU, Y., KORDOWER, J. H., BISHOP, K., KEATOR, D., POTKIN, S. & BARTUS, R. T. 2014. A phase1 study of stereotactic gene delivery of AAV2-NGF for Alzheimer's disease.

ROSSMANITH, W., CHABICOVSKY, M., HERKNER, K. & SCHULTE-HERMANN, R. 2002. Cellular gene dose and kinetics of gene expression in mouse livers transfected by high-volume tail-vein injection of naked DNA. *DNA Cell Biol,* 21**,** 847-53.

RUFFING, M., ZENTGRAF, H. & KLEINSCHMIDT, J. A. 1992. Assembly of viruslike particles by recombinant structural proteins of adeno-associated virus type 2 in insect cells. *J Virol,* 66**,** 6922-30.

RUIZ-OPAZO, N., CHAKRABORTY, P. R. & SHAFRITZ, D. A. 1982. Evidence for supercoiled hepatitis B virus DNA in chimpanzee liver and serum Dane particles: possible implications in persistent HBV infection. *Cell,* 29**,** 129-36.

RUSSELL, D. W., ALEXANDER IE FAU - MILLER, A. D. & MILLER, A. D. 1995. DNA synthesis and topoisomerase inhibitors increase transduction by adeno-associated virus vectors.

SAMULSKI, R. J., BERNS, K. I., TAN, M. & MUZYCZKA, N. 1982. Cloning of adeno-associated virus into pBR322: rescue of intact virus from the recombinant plasmid in human cells. *Proc Natl Acad Sci U S A,* 79**,** 2077-81.

SAMULSKI, R. J. & MUZYCZKA, N. 2014. AAV-Mediated Gene Therapy for Research and Therapeutic Purposes. *Annu Rev Virol,* 1**,** 427-51.

SAMULSKI, R. J., ZHU, X., XIAO, X., BROOK, J. D., HOUSMAN, D. E., EPSTEIN, N. & HUNTER, L. A. 1991. Targeted integration of adeno-associated virus (AAV) into human chromosome 19. *EMBO J,* 10**,** 3941-50.

SANLIOGLU, S., BENSON, P. K., YANG, J., ATKINSON, E. M., REYNOLDS, T. & ENGELHARDT, J. F. 2000. Endocytosis and nuclear trafficking of adeno-associated virus type 2 are controlled by rac1 and phosphatidylinositol-3 kinase activation. *J Virol,* 74**,** 9184-96.

SANTIAGO-ORTIZ, J., OJALA, D. S., WESTESSON, O., WEINSTEIN, J. R., WONG, S. Y., STEINSAPIR, A., KUMAR, S., HOLMES, I. & SCHAFFER, D. V. 2015. AAV ancestral reconstruction library enables selection of broadly infectious viral variants. *Gene Ther,* 22**,** 934-46.

SATHER, B. D., ROMANO IBARRA, G. S., SOMMER, K., CURINGA, G., HALE, M., KHAN, I. F., SINGH, S., SONG, Y., GWIAZDA, K., SAHNI, J., JARJOUR, J., ASTRAKHAN, A., WAGNER, T. A., SCHARENBERG, A. M. & RAWLINGS, D. J. 2015. Efficient modification of CCR5 in primary human hematopoietic cells using a megaTAL nuclease and AAV donor template. *Sci Transl Med,* 7**,** 307ra156.

SCOTT, T., MOYO, B., NICHOLSON, S., MAEPA, M. B., WATASHI, K., ELY, A., WEINBERG, M. S. & ARBUTHNOT, P. 2017. ssAAVs containing cassettes encoding SaCas9 and guides targeting hepatitis B virus inactivate replication of the virus in cultured cells. *Sci Rep,* 7**,** 7401.

SEEGER, C. & MASON, W. S. 2000. Hepatitis B virus biology. *Microbiol Mol Biol Rev,* 64**,** 51-68.
SHEN, S., HOROWITZ, E. D., TROUPES, A. N., BROWN, S. M., PULICHERLA, N., SAMULSKI, R. J., AGBANDJE-MCKENNA, M. & ASOKAN, A. 2013. Engraftment of a galactose receptor footprint onto adeno-associated viral capsids improves transduction efficiency. *J Biol Chem,* 288**,** 28814-23.
SHIN, D., KIM, S. I., KIM, M. & PARK, M. 2006. Efficient inhibition of hepatitis B virus replication by small interfering RNAs targeted to the viral X gene in mice. *Virus Res,* 119**,** 146-53.
SHLOMAI, A. & SHAUL, Y. 2003. Inhibition of hepatitis B virus expression and replication by RNA interference. *Hepatology,* 37**,** 764-70.
SIOUD, M. 2005. Induction of inflammatory cytokines and interferon responses by double-stranded and single-stranded siRNAs is sequence-dependent and requires endosomal localization.
SONG, J. J., SMITH, S. K., HANNON, G. J. & JOSHUA-TOR, L. 2004. Crystal structure of Argonaute and its implications for RISC slicer activity. *Science,* 305**,** 1434-7.
SONNTAG, F., SCHMIDT, K. & KLEINSCHMIDT, J. A. 2010. A viral assembly factor promotes AAV2 capsid formation in the nucleolus. *Proc Natl Acad Sci U S A,* 107**,** 10220-5.
SRIVASTAVA, A., LUSBY, E. W. & BERNS, K. I. 1983. Nucleotide sequence and organization of the adeno-associated virus 2 genome. *J Virol,* 45**,** 555-64.
SUMMERFORD, C., BARTLETT, J. S. & SAMULSKI, R. J. 1999. AlphaVbeta5 integrin: a co-receptor for adeno-associated virus type 2 infection. *Nat Med,* 5**,** 78-82.
SUMMERFORD, C. & SAMULSKI, R. J. 1998. Membrane-associated heparan sulfate proteoglycan is a receptor for adeno-associated virus type 2 virions. *J Virol,* 72**,** 1438-45.
SUROSKY, R. T., URABE, M., GODWIN, S. G., MCQUISTON, S. A., KURTZMAN, G. J., OZAWA, K. & NATSOULIS, G. 1997. Adeno-associated virus Rep proteins target DNA sequences to a unique locus in the human genome. *J Virol,* 71**,** 7951-9.
THORNTON, J. W. 2004. Resurrecting ancient genes: experimental analysis of extinct molecules. *Nat Rev Genet,* 5**,** 366-75.
TOMPKINS, S. M., LO, C. Y., TUMPEY, T. M. & EPSTEIN, S. L. 2004. Protection against lethal influenza virus challenge by RNA interference in vivo. *Proc Natl Acad Sci U S A,* 101**,** 8682-6.
TREMPE, J. P. & CARTER, B. J. 1988. Alternate mRNA splicing is required for synthesis of adeno-associated virus VP1 capsid protein. *J Virol,* 62**,** 3356-63.
UPRICHARD, S. L., BOYD, B., ALTHAGE, A. & CHISARI, F. V. 2005. Clearance of hepatitis B virus from the liver of transgenic mice by short hairpin RNAs. *Proc Natl Acad Sci U S A,* 102**,** 773-8.
VANDENBERGHE, L. H., WANG, L., SOMANATHAN, S., ZHI, Y., FIGUEREDO, J., CALCEDO, R., SANMIGUEL, J., DESAI, R. A., CHEN, C. S., JOHNSTON, J., GRANT, R. L., GAO, G. & WILSON, J. M. 2006. Heparin binding directs activation of T cells against adeno-associated virus serotype 2 capsid. *Nat Med,* 12**,** 967-71.
VON KNEBEL DOEBERITZ, M., RITTMULLER, C., ZUR HAUSEN, H. & DURST, M. 1992. Inhibition of tumorigenicity of cervical cancer cells in nude mice by HPV E6-E7 anti-sense RNA. *Int J Cancer,* 51**,** 831-4.
WANG, G., ZHAO, N., BERKHOUT, B. & DAS, A. T. 2016. A Combinatorial CRISPR-Cas9 Attack on HIV-1 DNA Extinguishes All Infectious Provirus in Infected T Cell Cultures. *Cell Rep,* 17**,** 2819-2826.

WANG, L., BELL, P., LIN, J., CALCEDO, R., TARANTAL, A. F. & WILSON, J. M. 2011. AAV8-mediated hepatic gene transfer in infant rhesus monkeys (Macaca mulatta). *Mol Ther,* 19**,** 2012-20.

WANG, Z., MA, H. I., LI, J., SUN, L., ZHANG, J. & XIAO, X. 2003. Rapid and highly efficient transduction by double-stranded adeno-associated virus vectors in vitro and in vivo. *Gene Ther,* 10**,** 2105-11.

WARD, P., DEAN, F. B., O'DONNELL, M. E. & BERNS, K. I. 1998. Role of the adenovirus DNA-binding protein in in vitro adeno-associated virus DNA replication. *J Virol,* 72**,** 420-7.

WATER, F. M. V. D., BOERMAN, O. C., WOUTERSE, A. C., PETERS, J. G. P., RUSSEL, F. G. M. & MASEREEUW, R. 2006. INTRAVENOUSLY ADMINISTERED SHORT INTERFERING RNA ACCUMULATES IN THE KIDNEY AND SELECTIVELY SUPPRESSES GENE FUNCTION IN RENAL PROXIMAL TUBULES. *Drug Metabolism and Disposition,* 34**,** 1393-1397.

WEINBERG, M. S., ELY, A., BARICHIEVY, S., CROWTHER, C., MUFAMADI, S., CARMONA, S. & ARBUTHNOT, P. 2007. Specific inhibition of HBV replication in vitro and in vivo with expressed long hairpin RNA. *Mol Ther,* 15**,** 534-41.

WILEY, J. M., SHERWOOD, L. M. & WOLVERTON, C. J. 2011. *Prescottt's Microbiology,* New York, McGraw-Hill.

WU, P., XIAO, W., CONLON, T., HUGHES, J., AGBANDJE-MCKENNA, M., FERKOL, T., FLOTTE, T. & MUZYCZKA, N. 2000. Mutational analysis of the adeno-associated virus type 2 (AAV2) capsid gene and construction of AAV2 vectors with altered tropism. *J Virol,* 74**,** 8635-47.

WU, Z., YANG, H. & COLOSI, P. 2010. Effect of Genome Size on AAV Vector Packaging. *Molecular Therapy,* 18**,** 80-86.

XIAOFEI, E., STADLER, B. M., DEBATIS, M., WANG, S., LU, S. & KOWALIK, T. F. 2012. RNA interference-mediated targeting of human cytomegalovirus immediate-early or early gene products inhibits viral replication with differential effects on cellular functions. *J Virol,* 86**,** 5660-73.

XIE, Q., BU, W., BHATIA, S., HARE, J., SOMASUNDARAM, T., AZZI, A. & CHAPMAN, M. S. 2002. The atomic structure of adeno-associated virus (AAV-2), a vector for human gene therapy. *Proc Natl Acad Sci U S A,* 99**,** 10405-10.

YAKOBSON, B., HRYNKO, T. A., PEAK, M. J. & WINOCOUR, E. 1989. Replication of adeno-associated virus in cells irradiated with UV light at 254 nm. *J Virol,* 63**,** 1023-30.

YAKOBSON, B., KOCH, T. & WINOCOUR, E. 1987. Replication of adeno-associated virus in synchronized cells without the addition of a helper virus. *J Virol,* 61**,** 972-81.

YAN, H., ZHONG, G., XU, G., HE, W., JING, Z., GAO, Z., HUANG, Y., QI, Y., PENG, B., WANG, H., FU, L., SONG, M., CHEN, P., GAO, W., REN, B., SUN, Y., CAI, T., FENG, X., SUI, J. & LI, W. 2012. Sodium taurocholate cotransporting polypeptide is a functional receptor for human hepatitis B and D virus. *Elife,* 1**,** e00049.

YANG, L., JIANG, J., DROUIN, L. M., AGBANDJE-MCKENNA, M., CHEN, C., QIAO, C., PU, D., HU, X., WANG, D. Z., LI, J. & XIAO, X. 2009. A myocardium tropic adeno-associated virus (AAV) evolved by DNA shuffling and in vivo selection. *Proc Natl Acad Sci U S A,* 106**,** 3946-51.

YEKTA, S., SHIH, I. H. & BARTEL, D. P. 2004. MicroRNA-directed cleavage of HOXB8 mRNA. *Science,* 304**,** 594-6.

YI, R., QIN, Y., MACARA, I. G. & CULLEN, B. R. 2003. Exportin-5 mediates the nuclear export of pre-microRNAs and short hairpin RNAs. *Genes Dev,* 17**,** 3011-6.

YU, G., CHEN, X., CHEN, S., YE, W., HOU, K. & LIANG, M. 2016. MiR-19a, miR-122 and miR-223 are differentially regulated by hepatitis B virus X protein and involve in cell proliferation in hepatoma cells. *J Transl Med,* 14**,** 122.

YUAN, J., WANG, J., CRAIN, K., FEARNS, C., KIM, K. A., HUA, K. L., GREGORY, P. D., HOLMES, M. C. & TORBETT, B. E. 2012. Zinc-finger nuclease editing of human cxcr4 promotes HIV-1 CD4(+) T cell resistance and enrichment. *Mol Ther,* 20**,** 849-59.

ZELPHATI, O., UYECHI LS FAU - BARRON, L. G., BARRON LG FAU - SZOKA, F. C., JR. & SZOKA, F. C., JR. 1998. Effect of serum components on the physico-chemical properties of cationic lipid/oligonucleotide complexes and on their interactions with cells.

ZENG, Y., YI, R. & CULLEN, B. R. 2005. Recognition and cleavage of primary microRNA precursors by the nuclear processing enzyme Drosha. *EMBO J,* 24**,** 138-48.

ZHANG, S. 2018. *You May Already Be Immune to CRISPR* [Online]. Online. Available: https://www.theatlantic.com/science/archive/2018/01/crispr-humans-immune-system/549974/ [Accessed March 27 2018].

ZHONG, L., LI, B., JAYANDHARAN, G., MAH, C. S., GOVINDASAMY, L., AGBANDJE-MCKENNA, M., HERZOG, R. W., WEIGEL-VAN AKEN, K. A., HOBBS, J. A., ZOLOTUKHIN, S., MUZYCZKA, N. & SRIVASTAVA, A. 2008a. Tyrosine-phosphorylation of AAV2 vectors and its consequences on viral intracellular trafficking and transgene expression. *Virology,* 381**,** 194-202.

ZHONG, L., LI, B., MAH, C. S., GOVINDASAMY, L., AGBANDJE-MCKENNA, M., COOPER, M., HERZOG, R. W., ZOLOTUKHIN, I., WARRINGTON, K. H., JR., WEIGEL-VAN AKEN, K. A., HOBBS, J. A., ZOLOTUKHIN, S., MUZYCZKA, N. & SRIVASTAVA, A. 2008b. Next generation of adeno-associated virus 2 vectors: point mutations in tyrosines lead to high-efficiency transduction at lower doses. *Proc Natl Acad Sci U S A,* 105**,** 7827-32.

ZINCARELLI, C., SOLTYS, S., RENGO, G. & RABINOWITZ, J. E. 2008. Analysis of AAV serotypes 1-9 mediated gene expression and tropism in mice after systemic injection. *Mol Ther,* 16**,** 1073-80.

ZINN, E., PACOURET, S., KHAYCHUK, V., TURUNEN, H. T., CARVALHO, L. S., ANDRES-MATEOS, E., SHAH, S., SHELKE, R., MAURER, A. C., PLOVIE, E., XIAO, R. & VANDENBERGHE, L. H. 2015. In Silico Reconstruction of the Viral Evolutionary Lineage Yields a Potent Gene Therapy Vector. *Cell Rep,* 12**,** 1056-68.

ZYLBERBERG, H., RIMANIOL, A. C., POL, S., MASSON, A., DE GROOTE, D., BERTHELOT, P., BACH, J. F., BRECHOT, C. & ZAVALA, F. 1999. Soluble tumor necrosis factor receptors in chronic hepatitis C: a correlation with histological fibrosis and activity. *J Hepatol,* 30**,** 185-91.

# APPENDICES

## APPENDIX A

## Buffers, Media, Reagents, and Solutions

### 1. Buffers

#### *(a) Transformation Buffer*

To make transformation buffer the following were put together: 100mM $CaCl_2$, 10 mM PIPES-HCl and 15% Glycerol. The pH was adjusted to 7.0 with NaOH, and the solution autoclaved for 20 minutes at 121 °C and 1 $kg/cm^2$, and stored at -20 $^{\circ}$C.

#### *(b) Tris Acetate EDTA (TAE) Buffer*

Fifty times TAE buffer consisted of: 1.6 M Tris base, 0.8 M Na Acetate.3.$H_2O$, and 40 mM EDTA-$Na_2$.2$H_2O$. The pH was adjusted to 7.2 with acetic acid, and the water was added to 1 litre.

#### *(c) Tris Boris EDTA (TBE) Buffer*

Ten times TBE buffer was prepared by dissolving 52 g Tris and 27.5 g Boric acid in 450 mL distilled water. Twenty millilitre of 0.5 M $Na_2$EDTA at pH8 was added, and final volume adjusted to 500 mL with distilled water, and stored at RT.

**(d) *TE Buffer***

A solution of 1 mL of TE buffer was prepared by adding [1 mM EDTA (pH8), Appendix A, 4 b], [10 mM Tris-HCl, Appendix A, 4 a] to a final volume adjusted to 1 L with distilled water and kept at RT.

***(e) Viral Lysate Buffer (100 mL)***

Lysate buffer was prepared by making a solution of 0.15 M NaCl, [50 mM Tris-HCl (pH 8.5)] and up to 100 mL of distilled water.

.

## 2. Media

***(a) Luria-Bertani (LB)***

Ten grams of Tryptone, 5 g Yeast Extract (Oxoid, UK) and 2.5 g NaCl were dissolved in 1 L of distilled water. LB medium was autoclaved for 20 minutes at 121 $^{o}$C and 1kg/cm$^{2}$, and kept at room temperature.

***(b) Luria-Agar (LA) plate***

Bacterial plates were prepared as follows: Agar (Oxoid, UK) was added into LB medium to a final concentration of 1% (w/v). The mixture was sterilized by autoclaving for 20 minutes at 121 $^{\circ}$C and 1 kg/cm2 then cooled to 50 $^{\circ}$C. Ampicillin was added to a final concentration of 100 µg/ml of LB agar solution. To prepare LB agar plates, solution was poured to Petri dishes and agar allowed to solidify at room temperature. Plates were stored at 4 °C.

***(c) Fetal calf serum (FCS)***

Fetal calf serum (FCS, Highveld Biological, South Africa) was heat inactivated before use at 60 °C for 30 minutes.

***(d) Freezing media***

Media solution consisting of 5.6 mL DMEM, 3.4 mL FCS, and 1 mL DMSO was filter sterilised using a 0.2 µM + 20 mL syringe.

## 3. Reagents

***(a) 1000 × Ampicillin***

A solution of Ampicillin (Roche, Germany) was prepared by dissolving 1 g in 10 mL of 50 % ethanol, and was stored at -20 °C.

***(b) 1000 × Kanamycin***

A solution of Kanamycin (Sigma, St. Louis, USA) was prepared by dissolving 0.5 g in 10 mL of sterile water and was stored at -20 °C.

***(c) 5-bromo-4-chroro-3-indolyl-β-D-galactopyranoside (X-gal) stock solution***

To prepare X-gal solution, 200 mg of X-gal were dissolved in 10 mL dimethyl formamide. The light sensitive solution was covered with aluminium foil and stored at -20 °C.

***(d)* Isopropyl β-D-1-thiogalactopyranoside (IPTG)**

To prepare IPTG solution, 200 mg of IPTG was dissolved in 10 mL of distilled water, and filter sterilized with a 0,22 µm syringe filter. One millilitre aliquots were made and kept at -20 °C.

## 4. Solutions

### *(a) 1 L, 1 M Tris-HCl (pH 8.0 or pH 8.5)*

Tris-HCl (molecular weight = 157.60 g) was dissolved in 800 mL distilled water and pH adjusted to 8 or 8.5 using HCl, and water volume added up to 1 L.

### *(b) 500 mL 1 M EDTA stock solution*

One molar, 500 mL EDTA solution was prepared by dissolving 186.12 g of EDTA [EDTA.$Na_2$2$H_2O$ (molecular weight = 372.24 g)] in 400 mL distilled water and adjusting pH to 8 using approximately 10 g of NaOH pellets.

### *(c) 1 % SDS stock solution*

1 gram of SDS stock was dissolved in distilled water added up to 100 mL.

### *(d) PBS-MK solution*

A 250 mL solution of 1 × PBS, 1 mM $MgCl_2$, and 2.5 KCl was prepared and filter sterilised.

### *(e) PBS-MK-NACl solution*

A 250 mL solution of PBS-MK and 1M Nacl was prepared and filter sterilised.

### *(f) Phenol red solution*

A 0.5 % solution was prepared by dissolving 0.5 g of phenol red to 100 mL of distilled water.

### *(g) Iodixanol solution*

To prepare forty five millilitres of 60% iodixanol solution, 112 µl phenol red (2.5 µl/mL) was added to 45 mL Optiprep$^{TM}$ (Sigma, St. Louis, USA) also referred to as iodixanol. The solution was yellow in colour. Forty percent iodixanol solution was prepared by adding 15 mL PBS-MK (Appendix A, 4 d) to 30 mL Optiprep$^{TM}$, making a clear solution. Twenty five percent iodixanol solution consisted of 20 mL Optiprep$^{TM}$, 28 mL PBS-MK, and 120 µl phenol red, making a red coloured solution. Fifteen percent iodixanol solution consisted of 12 mL Optiprep$^{TM}$ and 36 mL PBS-MK-NaCl (Appendix A, 4 e), a clear solution.

### *(h) 1% Ammonium persulphate solution*

One gram of Ammonium persulphate was dissolved in distilled water adjusted to 100 mL.

### *(i) Dethylpyrocarbonate water solution*

One millilitre of 0.1% [Diethylpyrocarbonate, DEPC (Sigma, MO, USA) was mixed with up to 1000 ml distilled water, and set at RT for 1 hour. It was autoclaved for the same duration, and allowed to coo prior to use.